

Appln No.: 09/601,644
Amendment Dated: April 9, 2007
Reply to Office Action of November 20, 2006

REMARKS/ARGUMENTS

This is in response to the Office Action mailed November 20, 2006 for the above-captioned application. Reconsideration and further examination are respectfully requested.

The withdrawal of the restriction requirement with respect to claims 18, 32, 33 and 37-41 is noted with appreciation. The Examiner's statement concerning the application of the PCT Unity of invention rules to claims 17, 18, 24 and 25, however, is not understood. The Examiner states that the claims are drawn to different categories of invention, namely a method of making a cytotoxic mutant protein, and a method of using the cytotoxic mutant protein, and that "the withdrawn method claims are patentably distinct from the method of claim 1, because they do not contain a further invention, by virtue of being drawn to different categories of claims." This statement is not understood. PCT Rules specifically provide that claims in different categories routinely do share unity of invention. For example, one such combination is "in addition to an independent claim for a given product, an independent claim for a process specially adapted for the manufacture of the said product, and an independent claim for a use of the said product." The claims in this instance are the method of making and the method of using. Further, the Examiner has seemingly argued that there is no additional invention, so it is not clear how it could be argued that there is a lack of unity. Thus, further consideration is requested.

Claims 15 and 27 have been amended in view of the Examiner's objections. Claim 20 is presently withdrawn. Claims 28 and 29 are dependent on claim 27.

Claims 1-7, 9-16, 18, 20, 27-29, 32, 33, 37-41 and 43 are rejected under 35 USC § 112, first paragraph, for failure to comply with written description requirement. Applicants again traverse this rejection. The Examiner asserts that the specification does not provide description "for any heteromeric ribosome inactivating protein because the specification does not provide nucleic acid sequences for ribosome inactivating proteins." (Office Action, Page 13) This argument is plainly inconsistent with the holding in *Capon v Eschar* that recitation of sequences that are known in the art and used as part of the invention is not required for written description. Here, the invention is not the sequences of ribosome inactivating proteins (RIP) *per se*, but the use of such proteins in a certain way. Moreover, no knowledge of the sequence of the protein is required to use it in the claimed method, provided that cDNA for the protein is available.

The specification in Seq. ID No. 2 shows the amino acid sequences for Sequence for the B subunit of ShT and SLT-1 (these two being identical) and the modification of these sequences is illustrated by way of example. However, other ribosome inactivating proteins were extensively known and characterized at the time the application was filed, as reflected in the exemplary documents in Exhibit A hereto (Frankel et. al, 1995; Kreitman, 1999). Thus, this basis for the lack of written description rejection is plainly in error.

Appln No.: 09/601,644
Amendment Dated: April 9, 2007
Reply to Office Action of November 20, 2006

The second reason asserted for maintaining the written description rejections is that the specification does not disclose cell lines that are insensitive to particular toxins other than CAMA-1. Applicants point out that the method of this invention is applicable to any cells, not just certain cell lines. The purpose of the invention is the development of new targeting or binding moieties that will target a specific cell type, by observation of the induction of toxicity where no toxicity is observed with the wild-type toxin. The person skilled in the art would recognize that selection of cell type and toxin is a matter of testing the cell type to be investigated against different wild-type toxins, finding one with little or no sensitivity, and then performing the method. Indeed, the method is a mere academic exercise if one selects the cell type based on its sensitivity to toxins instead of being of interest for some other reason (i.e., as a therapeutic target). No creation of a cell line is required, just the existence of cells that are of interest. No knowledge of the receptors on that cell line is required. Thus, this basis for the rejection is also in error and should be withdrawn.

It is further noted that the Examiner argues that possession of one combination of RIP and insensitive cell line does not convey possession of for mutants of other RIPs which have specificity for other receptors. (Office Action, page 15) This is not what is claimed, however. What is claimed is a method for finding these combinations, and of this method the inventors clearly had possession.

The Examiner has also rejected the claims under 35 USC § 112, first paragraph for lack of enablement. On Page 11 of the Official Action (not the section relating to enablement), the examiner states that "in regard to the newly examined claims ... the specification does not provide guidance and direction for detecting or treating disease *in vivo*." Then, on Page 19, the examiner stated that "the specification does not provide guidance and directions for detecting or treating any disease."

The Examiner's statement concerning these claims is incomplete because it does not say why a person skilled in the art would have difficulty practicing the claimed invention of these claims based on the teaching in the specification. Indeed, the comment appears to imply that the Examiner's argument is based on enablement of a certain use of the products made the various methods. However, since there is no question concerning *in vitro* or *ex vivo* use, this argument is not relevant since to claim a method of making a compound, or a compound *per se*, an inventor need only provide some use for the compounds. Here that is done (See, e.g., Example 6, and Page 25).

It is also noted that in the response to arguments, the Examiner argues that "the nature of the receptor is relevant to enablement of the claimed invention" because without knowing what the receptor specificity to start with, one cannot know that the new receptor now targeted is

Appln No.: 09/601,644
Amendment Dated: April 9, 2007
Reply to Office Action of November 20, 2006

different. (Page 14). Applicants submit that this argument is erroneous. Since the toxicity of the mutant protein depends on binding to the cell, and since the target cells initially are insensitive, the receptor binding specificity must have changed. The user of the invention does not need to know what receptor is targeted however to use the invention. To clarify this point, however, Applicants have amended claim 1 to specify that the change in binding specificity is reflected in the observation of toxicity.

The Examiner also argues that with respect to claims to making probes and medicaments, that the specification does not provide guidance and direction for detecting or treating of disease *in vivo*. The present invention provides methods of making a probe or a medicament, and does not claim the probe or medicament for the detection or treatment of disease. The Examiner has not provided any reasons why the making and using of a probe would require undue experimentation. At most the Examiner has implied that use of an probe for *in vivo* detection might require undue experimentation but he has not said why this would be the case. With respect to medicaments, he argues that the claims "read upon vectors for gene therapy" which he argues are unpredictable. Since the claim relates to methods of making medicaments that do not necessarily require the use of "gene therapy" to work, the Examiner has not shown how the claims to a method of making the medicaments lack enablement.

With respect to claims for making medicaments, the Examiner further argues that the claims read on making vectors for gene therapy which is an unpredictable art. The article cited for this proposition states that one of the problems of gene therapy is targeting. The present invention offers a solution to that problem. Furthermore, the statement of challenges to be met for optimization is not a statement of inoperability, and it is absurd to take the position that no gene therapy can be patented until all of the various factors are fully optimized.

This application is believed to now be in form for allowance. Reconsideration and allowance are therefore urged.

Respectfully submitted.



Marina T. Larson, Ph.D
Attorney/Agent for Applicant(s)
Reg. No. 32038
(970) 262 1800

Attachment

Immunotoxins in cancer therapy

Robert J Kreitman

Immunotoxins are composed of a protein toxin connected to a binding ligand such as an antibody or growth factor. These molecules bind to surface antigens (which internalize) and kill cells by catalytic inhibition of protein synthesis within the cell cytosol. Immunotoxins have recently been tested clinically in hematologic malignancies and solid tumors and have demonstrated potent clinical efficacy in patients with malignant diseases that are refractory to surgery, radiation therapy and chemotherapy — the traditional modalities of cancer treatment. This therapy is thus evolving into a separate modality of cancer treatment, capable of rationally targeting cells on the basis of surface markers. Efforts are underway to obviate impediments to clinical efficacy, including immunogenicity and toxicity to normal tissues. Immunotoxins are now being developed to new antigens for the treatment of cancer.

Addresses

Laboratory of Molecular Biology, Division of Cancer Biology, National Cancer Institute, National Institutes of Health, 37/4B27, 9000 Rockville Pike, 4255 Bethesda, MD 20892, USA; e-mail: kreitmar@mail.nih.gov

Current Opinion in Immunology 1999, 11:570–578

0952-7915/99/\$ — see front matter © 1999 Elsevier Science Ltd. All rights reserved.

Abbreviations

CR	complete remission
CSF	cerebrospinal fluid
CTCL	cutaneous T cell lymphoma
dgA	deglycosylated ricin A chain
DT	diphtheria toxin
EGFR	epidermal growth factor receptor
FDA	Food and Drugs Administration
GVHD	graft-versus-host disease
HD	Hodgkin's disease
HUVEC	human umbilical vein endothelial cell
IFN- γ	interferon γ
IL-2R	IL-2 receptor
MAb	monoclonal antibody
PE	<i>Pseudomonas</i> exotoxin
PR	partial response
RTA	ricin A chain
TfR	transferrin receptor
TGF- α	transforming growth factor α
TNF- α	tumor necrosis factor α
VLS	vascular leak syndrome

Introduction

It has been estimated that — in the year 1999 — 1,228,000 people in the US will be diagnosed with invasive cancer and 564,800 people are expected to die of it [1]. Treatment of cancer classically consisted of surgery, radiation therapy and chemotherapy — the latter having had the sole task of treating widespread disease that usually afflicts the dying cancer patient. The success of chemotherapy requires the malignant cells to be sensitive by virtue of intracellular metabolic processes or growth rates that are different from those of normal cells.

A different modality for cancer treatment

Human cancer is becoming more definable by surface proteins displayed on the malignant cell surface. Targeting cells selectively via these surface proteins is inherently different from surgery, radiation and chemotherapy and is often considered a new modality for cancer therapy. Targeted therapy can be accomplished by using monoclonal antibodies (MAbs) alone or MAbs armed with radionuclides or toxins. The Food and Drugs Administration (FDA) recently approved the MAbs Rituximab and Herceptin, which are effective and well tolerated but 50% or more of patients do not respond and are in need of other therapy. This review will focus on the latter approach, where a monoclonal antibody is connected to a protein toxin to make an immunotoxin. Chimeric toxins containing a growth factor instead of a MAb are often considered a type of immunotoxin. To kill a cell the ligand of the immunotoxin must bind to the cell surface and internalize; within the cytoplasm the toxin must inhibit protein synthesis. This review will discuss the mechanism of action of immunotoxins, their production and their recent clinical results in patients with cancer.

Types of toxins

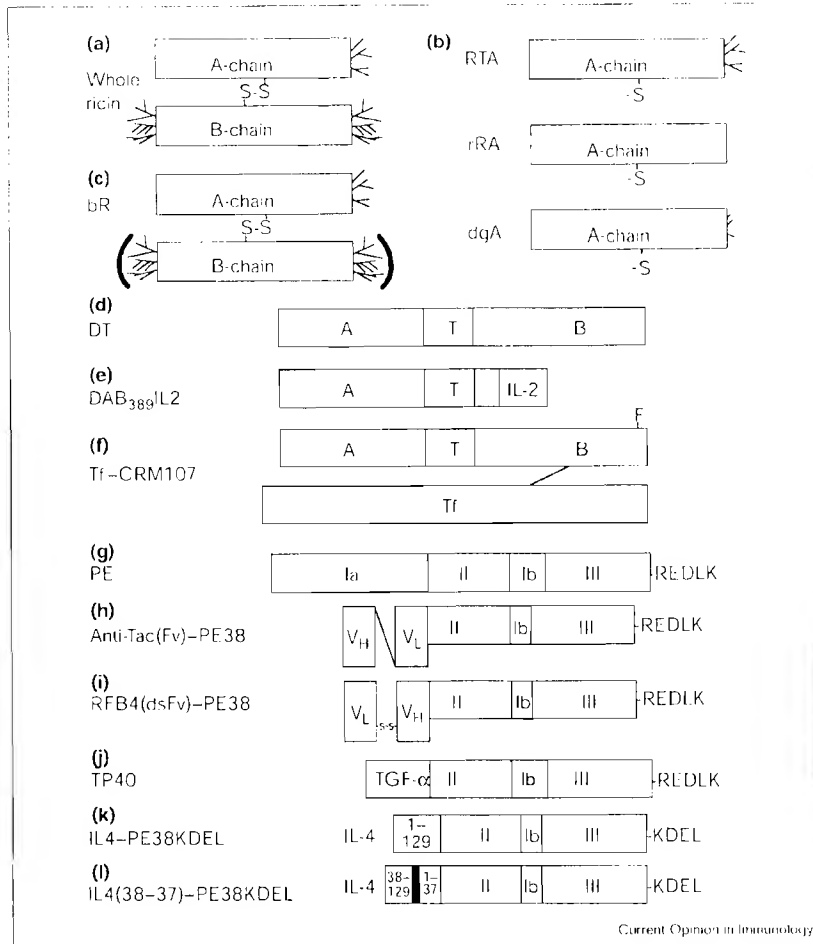
Schematic structures for the toxins discussed below are shown in Figure 1 and their modes of intoxication of cells are shown in Figure 2. Toxins originate from both plants and bacteria. Plant toxins are either holotoxins — composed of catalytic 'A-chains' disulfide bonded to 'B-chains', which bind the cell surface — or catalytic chains alone (hemotoxins). The bacterial toxins *Pseudomonas* exotoxin (PE) and diphtheria toxin (DT) are single chain proteins containing both binding and catalytic domains. The common features of plant and bacterial toxins — shown in Figure 2 — are binding to the cell surface, internalization into an endosome, translocation to the cytosol and then catalytic inhibition of protein synthesis, leading to cell death. As shown in Figure 1, immunotoxins contain toxins that have their binding domains either mutated or removed to prevent them from binding to normal cells and are either fused or chemically conjugated to a ligand specific for cancer cells.

Production of immunotoxins

Producing chemical conjugates requires purification of the ligand, either MAb or growth factor, and the toxin prior to the conjugation procedure [2]. The bond between the ligand and toxin is usually produced by disulfide bond chemistry. An exception is LMB-1 (see below), which contains a thioether linkage between the MAb and toxin [3]. The chemical conjugate must be purified to remove free ligand and toxin. If a 1:1 conjugate between toxin and ligand is desired, conjugates of higher molecular weight containing other ratios must be removed [4]. Recombinant

Figure 1

Schematic structure of immunotoxins. (a) Whole ricin is a plant holotoxin composed of a catalytic A chain disulfide bonded to a binding B-chain. Derivatives of the holotoxin have dramatically reduced uptake by the liver; they include (b) RTA (made by reducing whole ricin), rRA (made in *E. coli* without glycosylated amino acids), chemically deglycosylated RTA (dgA) and (c) chemically treated or 'blocked' whole ricin (bR). The bacterial toxins PE and DT are single-chain proteins suitable for forming recombinant fusion toxins. (d) DT is 535 amino acids in length and is composed of the enzymatic A domain (amino acids 1–193) [70,71] and the binding B domain (amino acids 382–535) [72,73]. The translocation or transmembrane (T) domain is located in-between [74]. (e) The fusion toxin DAB₃₈₉IL2 contains the initiator methionine, the first 388 amino acids of DT and human IL-2. (f) In the chemical conjugate Tf–CRM107, human Tf is chemically conjugated to a mutant of DT that contains phenylalanine (F) replacing serine at position 525 [55]. (g) PE is 613 amino acids long and contains three functional domains [75,76]. Domain Ia (amino acids 1–252) is the binding domain, domain II (amino acids 253–364) is the translocating domain and domain III (amino acids 400–613) contains the ADP-ribosylating enzyme which inactivates elongation factor 2 (EF-2) in the cytosol and results in cell death [77,78]. Domain Ib separates domains II and III and contains amino acids 365–399. PE38 is a truncated form of PE devoid of domain Ia and amino acids 365–380 of domain Ib. (h) The single-chain recombinant immunotoxin anti-Tac(Fv)–PE38 (or LMB-2) contains the variable heavy domain (V_H) of the anti-Tac MAb fused via the peptide linker (G₄S)₃ to the variable light domain (V_L), which in turn is fused to PE38. (i) The disulfide-stabilized recombinant immunotoxin RFB4(dsFv)–PE38 (or BL22) is composed of the V_L from the MAb RFB4 disulfide bonded to a fusion of V_H with PE38. The disulfide bond connecting V_H and V_L is formed between two cysteine residues replacing Arg44 of V_H and Gly100 of V_L. (j) TP40 is composed of human TGF- α fused to



a truncated form of PE containing amino acids 253–513 with cysteines at positions 265, 287, 372 and 379 converted to alanines. (k) In IL4–PE38KDEL, human IL-4 – composed of 129 amino acids – is fused to the amino terminus of a mutant of PE38, termed PE38KDEL, in which amino acids 609–613 of

PE, REDLK, are replaced with KDEL. (l) To fuse PE38KDEL to IL-4 residue 37 instead of IL-4 residue 129, the single-chain, circularly permuted IL-4 mutant IL-4 (38–37) was created; this contains amino acids 38–129 of IL-4, a GGNGG linker and amino acids 1–37 of IL-4 which are then fused to the toxin.

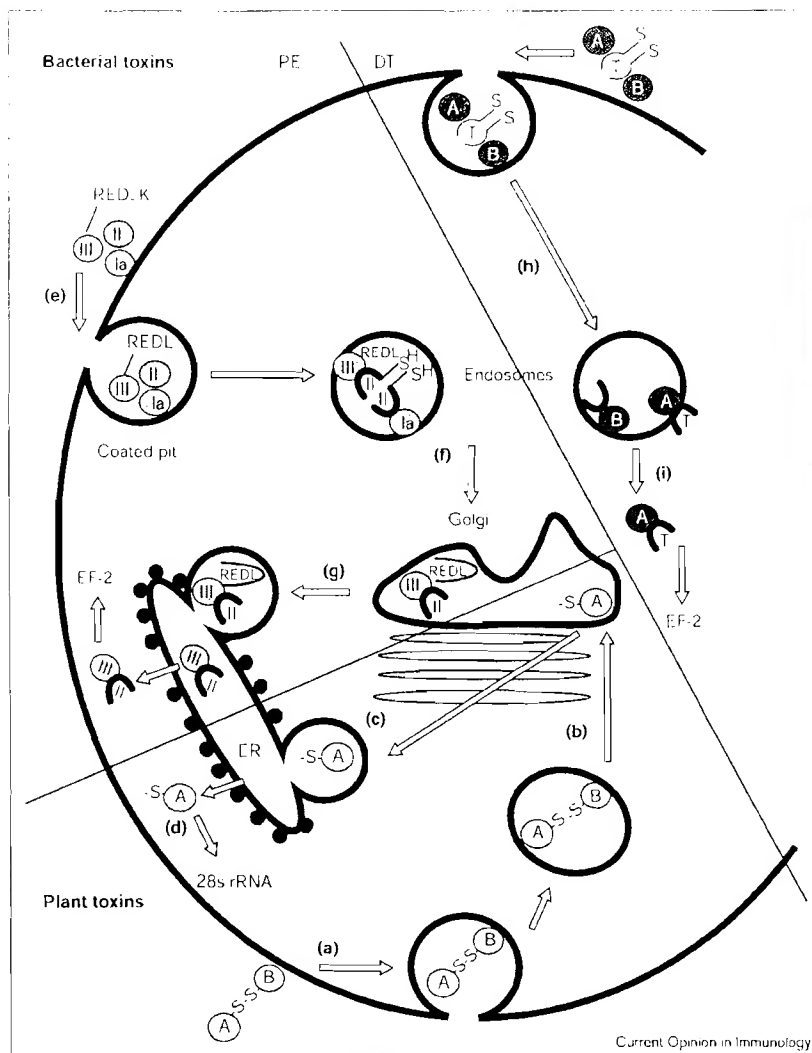
toxins can be produced by inserting the DNA encoding the fusion toxin into an expression plasmid [5]. *Escherichia coli* cells containing this plasmid can be grown in culture. Depending on the expression system, protein synthesis is induced either by addition of a lactose analog or by changing the temperature. After 1–2 hours, the recombinant protein can be harvested from one of several bacterial compartments such as the periplasm, cytoplasm or insoluble inclusion bodies. In our experience the latter compartment leads to recombinant protein with the highest yield, purity and activity but requires denaturation, reduction and refolding of the recombinant protein in redox buffer [6–8]. Purification of DT- or PE-containing fusion toxins can be accomplished by simple anion exchange and sizing chromatography [9] or by reverse-phase chromatography

followed by ultrafiltration [10**]. It is difficult to produce recombinant toxins using eukaryotic expression systems since such cells are sensitive to the toxin. Recently, however, high yields of recombinant toxin have been produced in baculovirus [11].

Preclinical development of recombinant toxins

Immunotoxins that are tested in clinical trials undergo several years of preclinical development to determine their efficacy and toxicity in several *in vitro* and *in vivo* models. A basic test involves measurement of cell-free enzymatic activity, namely ribosome-inactivating activity in the case of plant toxins and ADP-ribosylating activity in the case of bacterial toxins [12]. The binding affinity of immunotoxins to antigen can be tested on cells or purified antigen. Small

Figure 2



Intoxication of cells by toxins. The modes of intoxication of cells by toxins are shown for the plant toxins like ricin (bottom) and bacterial toxins PE and DT (top). See Figure 1 for schematic structures of the protein toxins. (a) After internalization, (b) plant toxins are believed to traffic through the Golgi and translocate to the cytosol, presumably (c) via the endoplasmic reticulum (ER). (d) Once in the cytosol, they inhibit protein synthesis by preventing the association of elongation factor-1 and -2 (EF-1 and EF-2) with the 60S ribosomal subunit by removing the base of A4324 in 28S rRNA [79,80]. The bacterial toxins PE and DT are single-chain proteins, which inhibit protein synthesis by ADP-ribosylating EF-2 [81]. Both PE and DT undergo proteolysis and disulfide-bond reduction to separate the catalytic domain (domain III for PE, A-chain for DT) from the binding domain (domain Ia for PE, B-chain for DT) [78,82–84]. PE undergoes both (e) removal of the carboxy-terminal lysine residue [85] and (f) processing between residues 279 and 280, resulting in a 37 kDa carboxy terminal toxin fragment ending in the residues REDL (which binds to the KDEL receptor). (g) This fragment is believed to be transported intracellularly via the KDEL receptor from the Golgi to the ER [86], where it translocates to the cytosol. (h) DT undergoes processing between residues 193 and 194 [84]. (i) The catalytic A-chain (amino acids 1–193) then translocates to the cytosol through the endosome with the help of translocation (T) domain residues 326–347 and 358–376 which form an ion channel [74,87–89]. Cell death caused by toxins has been shown to be facilitated by apoptosis [90,91].

recombinant toxins may lose binding affinity after radiolabeling, so their binding is often best tested by displacement or surface-plasmon-resonance assays [13]. Cytotoxicity assays are performed by incubating antigen-bearing cells with immunotoxins and then measuring either protein synthesis, proliferation, colony counts or cell viability. Malignant, single-cell suspensions directly obtained from patients are useful to test (if available) since such cells may contain a lower receptor density and may be less able to process the toxin than established cell lines [14–16]. *In vivo* efficacy of immunotoxins may be demonstrated in immunodeficient mice bearing xenografts of human tumor cells — either as subcutaneous solid tumors, orthotopic implants or disseminated leukemia [17–19]. Most targeted antigens are present at some level on some normal tissues and thus toxicology and pharmacokinetics should be tested in an animal that has normal cells capable

of binding the antigen. For most immunotoxins, this requires studies in monkeys to predict whether targeted damage to vital normal tissues will occur in humans [20,21]. The remainder of this review will focus briefly on those immunotoxins that have passed through preclinical development and have recently begun or finished clinical testing. These immunotoxins are summarized in Table 1.

Immunotoxins targeting hematologic tumors

Hematologic malignancies are easier to target than solid tumors for many reasons, including easy access of the immunotoxin to intravascular tumor cells and improved penetration of lymphomatous tumor cells without tight junctions. Moreover, fresh cells may be easily tested for immunotoxin binding and cytotoxic activity. Immunotoxins have also been developed for indirect treatment of malignancies by their killing of T cells that

Table 1

Results of recent clinical trials of chimeric toxins against cancer.

Chimeric toxin	Antigen	Diseases	Toxicities	Incidence of immunogenicity	Responses	Most recent trial Phase	References
HB5-rTA	CD5	Acute GVHD	Allergy, VLS	15 out of 93	51 out of 127 CR (4 weeks) 1 year survival unchanged	III	[92]
Anti-CD6-bR	CD6	CTCL	Ongoing	3 out of 5	N/A	I	[93]
Anti-CD7-dgA	CD7	T-NHL	VLS	1 out of 11	2 out of 11 PR	I	[94]
TX11-PAP	CD7	T-NHL	Ongoing				[20]
DAB ₃₈₉ IL-2	IL-2R	CTCL, HD, B-NHL	Asthenia, mild VLS	65 out of 71	13 out of 144 CR, 24 out of 144 PR	III	[10*,37]
Anti-Tac(Fv)-PE38 (LMB-2)	CD25	B, T cell lymphoma/leukemia, HD	AST, ALT, fever	11 out of 35	1 out of 34 CR, 7 out of 34 PR	I	[95], (a)
RFT5-SMPT-dgA	CD25	HD	VLS	7 out of 15	2 out of 20 PR	I	[43,44]
IgG-RFB4-dgA	CD22	NHL, CLL	VLS	21 out of 40	1 out of 42 CR, 9 out of 42 PR	I	[22,23]
D-dgA-RFB4	CD22	NHL, CLL	Ongoing	N/A	N/A		[4]
RFB4(dsFv)-PE38 (BL 22)	CD22	B-NHL, B-CLL	Ongoing	N/A	N/A	I	[32]
IgG-HD37-dgA	CD19	B-NHL, B-CLL	VLS	5 out of 24	1 out of 39 CR, 2 out of 39 PR	I	[26]
Anti-B4-bR	CD19	B-NHL	AST, ALT, PLTs	39 out of 75	3 out of 75 CR, 5 out of 75 PR	III	[28,29,30*]
Anti-B4-bR + chemotherapy		AIDS-NHL	AST, ALT	8 out of 26	3 out of 26 improved	I	[31]
Anti-My9-bR	CD33	AML	VLS, PLTs	N/A	0 out of 18	I	[93]
DT388-GM-CSF	GM-CSFR	AML	Ongoing	N/A	N/A		[96]
B3-Lys/PE38 (LMB-1)	LeY	Carcinoma	VLS	33 out of 38	1 out of 38 CR, 1 out of 38 PR	I	[3]
B3(Fv)-PE38 (LMB-7)	LeY	Carcinoma	N/A	33 out of 51	N/A	I	
B3(dsFv)-PE38 (LMB-9)	LeY	Carcinoma	N/A	Ongoing	N/A		
TP40	EGFR	Bladder cancer	None	0 out of 43	Improved CIS	I	[47]
DAB ₃₈₉ EGF	EGFR	Carcinoma	AST, ALT, renal, pain	52 out of 52	1 out of 52 PR	I/II	[48*]
454A12-rRA	TfR	CSF cancer	Inflammation	0 out of 8	4 out of 8 PR	I	[54]
Tf-CRM107	TfR	Glioma	Peritumoral injury	6 out of 14	2 out of 15 CR, 7 out of 15 PR	I	[59]
N901-bR	CD56	SCLC	VLS	19 out of 20	1 out of 21 PR	II	[60,93,97]

Toxins, which are shown schematically in Figure 1, include RTA, blocked ricin (bR), dgA, pokeweed antiviral protein (PAP), truncated DT (DT388 or DAB₃₈₉), truncated PE (PE38), recombinant RTA (rRA) and mutated DT (CRM107). Non-monoclonal antibody ligands include IL-2, granulocyte/macrophage colony-stimulating factor (GM-CSF), EGF and Tf. TP40 is a fusion of TGF- α with truncated PE. Diseases include acute GVHD, B or T cell non-Hodgkin's lymphoma (NHL), chronic

lymphocytic leukemia (CLL), AIDS-related NHL, acute myelogenous leukemia (AML), carcinoma *in situ* (CIS), metastatic tumor involving the CSF (CSF cancer) and small-cell lung carcinoma (SCLC). Toxicities include VLS, elevations of hepatic transaminases or aspartate aminotransferase (AST) and alanine aminotransferase (ALT), thrombocytopenia (PLTs) or are not available (N/A). (a) RJ Kreitman *et al.*, unpublished data

mediate graft-versus-host disease (GVHD) in the setting of allogeneic transplantation.

B cell lymphoma and leukemia

As shown in Table 1, B cell lymphoma and leukemia have been targeted using both anti-CD22 and anti-CD19 immunotoxins [22–29,30*,31]. The dose-limiting toxicity (DLT) is due to vascular leak syndrome (VLS) for both

deglycosylated ricin A chain (dgA)-containing immunotoxins IgG-RFB4-dgA (targeting CD22) and IgG-HD37-dgA (targeting CD19). Despite the higher antigen density of CD19 compared with CD22 on target cells, CD22 targeting led to higher response rates — including durable complete remissions (CRs) [24] — probably due to improved internalization or intracellular processing of the immunotoxin. One strategy for improving the therapeutic

index is to deliver two instead of one toxin molecule per MAb molecule and a clinical trial is currently underway using di-dgA-RFB4 [4]. Also in phase I testing is a 63 kDa recombinant immunotoxin, RFB4(dsFv)-PE38 (BL22), which — as shown in Figure 1 — contains only the variable domains (hence 'Fv') of MAb RFB4 fused to the truncated form of PE, PE38 [32]. Unlike LMB-2 (see later), BL22 contains a disulfide bond connecting the variable domains, which improves stability. Preclinical models suggest that this molecule might avoid dose-limiting VLS since PE38 is less toxic than dgA to endothelial cells [33,34] and because its smaller size might allow it to exit more quickly from the vasculature. However, as discussed below, the mechanisms causing VLS are not completely understood and results of clinical trials might not be predictable from animal models.

IL-2 receptor targeting

The recombinant fusions of IL-2 with truncated DT were shown to be cytotoxic toward IL-2 receptor (IL-2R)⁺ cells, providing all three subunits of the IL-2R — α (p55, Tac or CD25), β and γ — were present [35,36]. DAB₃₈₉IL2 (Figure 1) produced 5 CRs and 8 partial responses (PRs) in 35 patients with cutaneous T cell lymphoma (CTCL) and 1 CR and 2 PRs in 17 patients with non-Hodgkin's lymphoma [10**]. The maximum tolerated dose (MTD) was 27 μ g/Kg (daily for five doses), limited by asthenia. The most common toxicities were transient and well-tolerated transaminase elevations (62% of patients) and hypoalbuminemia (86%), hypotension (32%) and rashes (32%). The significant response rate in CTCL was recently confirmed in a Phase III trial in 71 CTCL patients in which 7 CRs and 14 PRs were observed and most of the patients had objective improvements in skin lesions [37]. DAB₃₈₉IL2 has just been approved by the FDA for salvage treatment of CTCL. This approval, which follows a decade of preclinical and clinical development [38], is proof of the principal that chimeric toxins can make useful pharmaceutical agents.

For improved IL-2R targeting, an alternative strategy is to target CD25 directly with an antibody rather than by IL-2, since IL-2 binds with low affinity to CD25 alone and since CD25 far outnumbers β and γ subunits of the IL-2R on most types of target cells [39,40]. In phase I testing, a recombinant immunotoxin containing anti-Tac(Fv) and PE38, termed LMB-2 [12,41], has been administered to 35 patients with chemotherapy-resistant leukemia, lymphoma and Hodgkin's disease (HD). Of 20 patients receiving $> 60 \mu$ g/kg/cycle, there was 1 CR and 7 PRs. A significant component of toxicity, including fever and transaminase elevations, appears to be mediated by cytokines and this is currently being defined. A Phase II trial is planned in patients with CD25⁺ hematologic malignancies and Phase I trials are planned for the prevention of GVHD in patients undergoing high-risk allotransplantation [42]. The goal in the latter approach is to selectively target CD25⁺, activated donor T cells which are reactive with patient cells while preserving CD25⁻ donor T cells which

are necessary for engraftment and protection against third-party antigens. The conventional immunotoxin RFT5-SMPT⁺ dgA has also been developed to target CD25 and has resulted in several responses in HD, one of which lasted over two years [43,44]. RFT5-SMPT⁺ dgA is already undergoing testing for the prevention of GVHD in patients undergoing allotransplantation and has recently been shown *ex vivo* to remove alloreactive donor T cells while preserving antileukemia and antiviral cytotoxic T cell responses [45].

Solid tumors

The treatment of solid tumors with immunotoxins is challenging due to tight junctions between tumor cells, high interstitial pressure within tumors and heterogeneous blood supply [46]. As described below, to deal with these obstacles some immunotoxins are being administered locally to solid tumors. Nevertheless, some systemically administered immunotoxins have recently shown efficacy in patients with solid tumors.

Targeting the epidermal growth factor receptor

In patients with superficial bladder carcinoma, the anti-EGFR (epidermal growth factor receptor) recombinant toxin TP40 — composed of transforming growth factor α (TGF- α ; this binds the EGFR) and truncated PE — resulted in pathologic improvement in carcinoma *in situ* when instilled into the bladder [47]. EGF itself was fused to DAB₃₈₉ for systemic therapy of EGFR⁺ carcinomas and has resulted in a response in lung cancer [48*]. Although EGFRs are present in liver, hepatic transaminase elevations were only observed in 52% of patients and decreased in severity during subsequent cycles. A Phase I/II study is currently being conducted in patients with non-small-cell lung cancer. It has been recently found that EGFRs expressed on cancers are often mutated and therefore preclinical development is underway for immunotoxins that bind specifically to tumors bearing mutant EGFRs and not to normal cells bearing EGFRs [49,50].

Targeting the Le^y antigen on solid tumors

One MAb that reacts with a carbohydrate antigen in the Le^y family is called B3 [51]. A chemical conjugate of B3 with PE38 — called LMB-1 — was tested in 38 patients with Le^y-expressing carcinomas of breast, ovarian and gastrointestinal origin [3]. The 1 CR and 1 PR were the first major responses to immunotoxins documented for metastatic breast and colon cancer, respectively. The dose-limiting toxicity was VLS but experiments with human umbilical vein endothelial cells (HUVECs) indicated that the MAb (B3) rather than PE38 was binding to the Le^y antigen on endothelial cells [33]. To target Le^y-expressing tumors with a smaller immunotoxin that would leave the vasculature sooner and not cause VLS, the variable domains of B3 were cloned and fused to PE38 [52]. B3(Fv)-PE38 (LMB-7) and B3(dsFv)-PE38 (LMB-9) are two recombinant immunotoxins that have recently undergone clinical testing, the former having a single-chain

structure like LMB-2 and the latter having a disulfide-stabilized structure like BL22 (Figure 1). A different recombinant single-chain immunotoxin, BR96(sFv)-PE40, was derived from the anti-Le^y MAb BR96 and is also currently undergoing clinical testing [53].

Targeting tumors in the central nervous system

Since the transferrin receptor (TfR) is expressed on tumor and normal hepatic cells but not in normal brain, several trials have targeted anti-TfR immunotoxins to brain tumors. The conjugate 454A12-rRA — composed of an anti-TfR MAb, 454A12, and recombinant ricin A chain — was used for intraventricular therapy of patients with leptomeningeal cancer and cleared > 50% of the malignant cells from the cerebrospinal fluid (CSF) in half of the patients [54]. These same investigators have also targeted the TfR to treat solid tumors in the brain, using a chemical conjugate of human Tf with a mutant form of DT [55]. Tf-CRM107 (Figure 1) was infused directly into the tumors of 18 patients using catheters placed stereotactically; 2 CRs and 7 PRs were documented in 15 evaluable patients. In 6 out of 9 responders and in some of the nonresponders, the tumor underwent early central necrosis with loss of central gadolinium enhancement up to 2–3 cm in diameter. There was evidence that the chimeric toxin escaped from the central nervous system, resulting in transient transaminase elevations, hypoalbuminemia and an increase in the anti-DT titer. At concentrations of at least 1 µg/ml of infused drug, peritumoral brain injury was observed — consisting of thrombosed cortical vessels, attributed to the presence of TfR on endothelial cells. A Phase II trial is underway to evaluate antitumor activity at the maximum tolerated concentration, 0.66 µg/ml. Several Phase I trials are also currently underway to test the recombinant IL-4 toxin IL4(38–37)-PE38KDEL (Figure 1) as an intratumoral therapy for high grade gliomas. These tumors, unlike normal brain tissues, overexpress IL-4R [21,56]. IL4(38–37)-PE38KDEL contains a circularly permuted variant of IL-4 that permits higher affinity binding to IL-4R [57,58]. IL4(38–37)-PE38KDEL was well tolerated at up to 7.3 µg/ml in the plasma of monkeys, up to 1.4 µg/ml in the CSF of monkeys and up to 100 µg/ml when directly instilled into the frontal cortex of rats [21]. Over 20 patients have so far been treated with concentrations up to 15 µg/ml and, although response determination will require further follow-up, essentially all patients experience at least central necrosis of injected tumors.

Specific challenges

Immunogenicity

Although durable partial and even complete responses have resulted from one cycle of immunotoxin therapy, immunogenicity is considered a major barrier to the clinical utility of chimeric toxins. Table 1 includes immunogenicity data from recent clinical trials, indicating that patients with solid tumors become immunized much more readily than those with hematologic tumors. Some

hematologic tumors may be associated with less immunogenicity than others. None of 14 patients with chronic lymphocytic leukemia treated with LMB2 (8 patients) or BL22 (6 patients) have shown any evidence of antibodies. Patients receiving DT containing chimeric toxins such as DAB₃₈₉IL2, DAB₃₈₉EGF and Tf-CRM107 often have pre-existing antibodies from prior vaccinations and experience increased titers after treatment but antibodies are probably not strongly neutralizing since they do not adversely affect response rates [10,48,59]. It has been suggested from clinical data that anti-B4-bR temporarily blocked immunogenicity through its anti-B cell activity [60]. In 11 patients receiving 22 cycles of the anti-CD22 recombinant immunotoxin BL22, evidence of immunogenicity has so far been observed in only one patient after four cycles. Several strategies are being developed to actively prevent immunogenicity. Recent strategies to prevent immunogenicity include cotreatment with CTLA4Ig — an inhibitor of the CD28/CTLA4–CD80/CD86 costimulation pathways [61] — or the anti-CD20 MAb Rituximab, which induces profound B cell depletion in the majority of patients and is itself nonimmunogenic [62]. LMB-1 is currently being tested in solid-tumor patients in combination with Rituximab to prevent immunogenicity.

VLS

As indicated in Table 1, the dose-limiting toxicity of many of the most successful immunotoxins — particularly those containing dgA — is VLS. Additionally, some evidence of mild VLS — such as hypoalbuminemia, hypotension and edema — is observed in nearly all immunotoxin clinical trials. This includes LMB-2, despite the observation that dgA but not LMB-2 was cytotoxic toward HUVECs [33]. Recent studies indicate that recombinant toxins, including those containing mutated forms of PE, produce VLS in rats [63–65] and that inflammation, which can be suppressed by steroidal or nonsteroidal anti-inflammatory drugs, mediates the VLS [63,64]. As reviewed recently — by Baluna and Vitetta [66] — endothelial cells and/or macrophages can be activated by cytokines such as TNF-α and IFN-γ to produce nitric oxide, which then can mediate oxidative damage to the endothelial cells and result in increased permeability. An *in vitro* model of VLS indicated that ricin A chain (RTA) causes intercellular gap formation following endothelial cell death that is caused by the enzymatic activity of the toxin [67]. However, experiments using an *in vivo* model composed of human neonatal foreskin xenografts in SCID (immunodeficient) mice [68] identified a 3-amino acid motif present in IL-2 and protein toxins that causes VLS without other toxin activity [69]. Thus, in the future, VLS induced by immunotoxins may be preventable by the use of anti-inflammatory agents to block cytokine action and by the use of mutations or peptide inhibitors to prevent binding to endothelial cells.

Conclusions

Chimeric toxins have become a new modality for the treatment of cancer. Despite difficulties with immunogenicity,

toxicity to normal tissues and limitations in tumor penetration, they are unique in their ability to rationally target tumor cells via cell surface receptors. The ability to kill a cell with only one or a few molecules of toxin in the cytoplasm permits successful targeting of cells displaying only a limited number of antigen molecules. Several immunotoxins can target cells mediating autoimmune disease, including GVHD. One chimeric toxin, DAB₃₈₉IL2, has finally become a drug that oncologists can prescribe and we anticipate that other agents of this class will be added to the list of useful anticancer agents.

References and recommended reading

Papers of particular interest, published within the annual period of review, have been highlighted as:

- of special interest
 - of outstanding interest
1. Landis SH, Murray T, Bolden S, Wingo PA. Cancer statistics, 1998. *CA Cancer J Clin* 1998; **48**:6-29.
 2. Ghetie V, Till MA, Ghetie MA, Uhr JW, Vitetta ES. Large scale preparation of an immunoconjugate constructed with human recombinant CD4 and deglycosylated ricin A chain. *J Immunol Methods* 1990; **126**:135-141.
 3. Par LH, Wittes R, Setser A, Willingham MC, Pastan I. Treatment of advanced solid tumors with immunotoxin LMB-1: an antibody linked to *Pseudomonas* exotoxin. *Nat Med* 1996; **2**:350-353.
 4. Ghetie V, Swindell E, Uhr JW, Vitetta ES. Purification and properties of immunotoxins containing one vs. two deglycosylated ricin A chains. *J Immunol Methods* 1993; **166**:117-122.
 5. Studier FW, Moffatt BA. Use of bacteriophage T7 polymerase to direct selective expression of cloned genes. *J Mol Biol* 1985; **189**:113-130.
 6. Buchner J, Pastan I, Brinkmann U. A method for increasing the yield of properly folded recombinant fusion proteins: single-chain immunotoxins from renaturation of bacterial inclusion bodies. *Anal Biochem* 1992; **205**:263-270.
 7. Kreitman RJ, Pastan I. Purification and characterization of IL6-PE^{4E}, a recombinant fusion of interleukin 6 with *Pseudomonas* exotoxin. *Bioconjug Chem* 1993; **4**:581-585.
 8. Kreitman RJ, Pastan I. Using cytokine receptors to target leukemia and lymphoma with fusion toxins. *Methods in Molecular Medicine: Drug Targeting* 1999, in press.
 9. Kreitman RJ, Pastan I. Recombinant toxins containing human granulocyte-macrophage colony-stimulating factor and either *Pseudomonas* exotoxin or diphtheria toxin kill gastrointestinal cancer and leukemia cells. *Blood* 1997; **90**:252-259.
 10. LeMaistre CF, Salen MN, Kuzel TM, Foss F, Platanius LC, Schwartz G, Rotain M, Rook A, Freytes CO, Craig F *et al.* Phase I trial of a ligand fusion-protein (DAB389IL-2) in lymphomas expressing the receptor for interleukin-2. *Blood* 1998; **91**:399-405.
 - LeMaistre *et al.* describe clinical results in patients tested with the recombinant single-chain IL-2-toxin DAB₃₈₉IL2 (Figure 1). Major responses were seen in 13 out of 35 patients with CTCL and 3 out of 17 patients with non-Hodgkin's lymphoma. The maximum tolerated dose was 27 µg/kg/day x5 due to asthenia. Most of the CTCL patients showed significant improvement in skin lesions.
 11. Williams MD, Rostovtsev A, Narla RK, Uckun FM. Production of recombinant DT(ct)GM-CSF fusion toxin in a baculovirus expression vector system for biotherapy of GM-CSF-receptor positive hematologic malignancies. *Protein Expr Purif* 1998; **13**:219-221.
 12. Kreitman RJ, Bailon P, Chaudhary VK, FitzGerald DIP, Pastan I. Recombinant immunotoxins containing anti-Tac(Fv) and derivatives of *Pseudomonas* exotoxin produce complete regression in mice of an interleukin-2 receptor-expressing human carcinoma. *Blood* 1991; **83**:426-434.
 13. Malmqvist M. BIACORE: an affinity biosensor system for characterization of biomolecular interactions. *Biochem Soc Trans* 1999; **27**:335-340.
 14. Kiyokawa T, Shirano K, Hattori T, Nishimura H, Zanoguie LK, Nishihara JC, Steens IB, Murphy JR, Iwakura K. Cytotoxicity of interleukin 2-toxin toward lymphocytes from patients with adult T-cell leukemia. *Cancer Res* 1989; **49**:4042-4046.
 15. Kreitman RJ, Chaudhary VK, Kozak RW, FitzGerald DIP, Waldmann TA, Pastan I. Recombinant toxins containing the variable domains of the anti-Tac monoclonal antibody to the interleukin-2 receptor kill malignant cells from patients with chronic lymphocytic leukemia. *Blood* 1992; **80**:2344-2352.
 16. Kreitman RJ, Chaudhary VK, Waldmann T, Willingham MC, FitzGerald DJ, Pastan I. The recombinant immunotoxin anti-Tac(Fv)-*Pseudomonas* exotoxin 40 is cytotoxic toward peripheral malignant cells from patients with adult T-cell leukemia. *Proc Natl Acad Sci USA* 1990; **87**:8291-8295.
 17. Engert A, Martin G, Amlot P, Wijdens J, Diehl V, Thorpe P. Immunotoxins constructed with anti-CD25 monoclonal antibodies and deglycosylated ricin A-chain have potent anti-tumour effects against human Hodgkin cells *in vitro* and solid Hodgkin tumours in mice. *Int J Cancer* 1991; **49**:450-456.
 18. Ghetie M-A, Richardson J, Tucker T, Jones D, Uhr JW, Vitetta ES. Antitumor activity of Fab' and IgG-anti-CD22 immunotoxins in disseminated human B lymphoma grown in mice with severe combined immunodeficiency disease: effect on tumor cells in extranodal sites. *Cancer Res* 1991; **51**:5876-5880.
 19. Skrepnik N, Zieske AW, Robert E, Bravo JC, Mera R, Hunt JD. Aggressive administration of recombinant oncotoxin AR209 (anti-ErbB-2) in athymic nude mice implanted with orthotopic human non-small cell lung tumours. *Eur J Cancer* 1998; **34**:1628-1633.
 20. Waurzyniak B, Schneider EA, Turner N, Yanishevsky Y, Gunther R, Chelstrom LM, Wendorf H, Myers DF, Irwin JD, Messenger Y *et al.* In vivo toxicity, pharmacokinetics, and antileukemic activity of TXU (anti-CD7)-pokeweed antiviral protein immunotoxin. *Clin Cancer Res* 1997; **3**:881-890.
 21. Puri RK, Hoon DS, Leland P, Snoy P, Rand RW, Pastan I, Kreitman RJ. Preclinical development of a recombinant toxin containing circularly permuted interleukin 4 and truncated *Pseudomonas* exotoxin for therapy of malignant astrocytoma. *Cancer Res* 1996; **56**:5631-5637.
 22. Amlot PL, Stone MJ, Cunningham D, Fay J, Newman J, Collins R, May R, McCarthy M, Richardson J, Ghetie V *et al.* A phase I study of an anti-CD22-deglycosylated ricin A chain immunotoxin in the treatment of B-cell lymphomas resistant to conventional therapy. *Blood* 1993; **82**:2624-2633.
 23. Sausville EA, Headlee D, Stetler-Stevenson M, Jaffe ES, Solomon D, Figg WD, Herdt J, Kopp WC, Rager H, Steinberg SM *et al.* Continuous infusion of the anti-CD22 immunotoxin IgG-RFB4-SMPT-dgA in patients with B-cell lymphoma: a phase I study. *Blood* 1995; **85**:3457-3465.
 24. Senderowicz AM, Vitetta E, Headlee D, Ghetie V, Uhr JW, Figg WD, Lush RM, Stetler-Stevenson M, Kershaw G, Kngma DW *et al.* Complete sustained response of a refractory, post-transplantation, large B-cell lymphoma to an anti-CD22 immunotoxin. *Ann Intern Med* 1991; **126**:882-885.
 25. Schreuermann RH, Racila F. CD19 antigen in leukemia and lymphoma diagnosis and immunotherapy. *Leuk Lymphoma* 1995; **18**:385-397.
 26. Stone MJ, Sausville EA, Fay JW, Headlee D, Collins RH, Figg WD, Stetler-Stevenson M, Jain V, Jaffe ES, Solomon D *et al.* A phase I study of bolus versus continuous infusion of the anti-CD19 immunotoxin, IgG-HD37-dgA, in patients with B-cell lymphoma. *Blood* 1996; **88**:1188-1197.
 27. Conry RM, Khazaeli MB, Salen MN, Ghetie V, Vitetta ES, Liu TP, LoBuglio AF. Phase I trial of an Anti-CD19 deglycosylated ricin A chain immunotoxin in non-Hodgkin's lymphoma: effect of an intensive schedule of administration. *J Immunother* 1995; **18**:231-241.
 28. Grossbard ML, Freedman AS, Ritz J, Coral F, Goldmacher VS, Fliseo L, Spector N, Dear K, Lambert JM, Blattler WA *et al.* Serotherapy of B-cell neoplasms with anti-B4-blocked ricin: a phase I trial of daily bolus infusion. *Blood* 1992; **79**:576-585.
 29. Grossbard ML, Lambert JM, Goldmacher VS, Spector NI, Kinsella J, Eliseo L, Coral F, Taylor JA, Blattler WA, Epstein CI, Nadler LM. Anti-B4-blocked ricin: a Phase I trial of 7-day continuous infusion in patients with B-cell neoplasms. *J Clin Oncol* 1993; **11**:126-137.

30. Mullan PS, O'Day S, Nadler LM, Grossbard M. Phase II clinical trial of bolus infusion anti-B4 blocked ricin immunoconjugate in patients with relapsed B-cell non-Hodgkin's lymphoma. *Clin Cancer Res* 1998, 4:2599-2604.
- Mullan *et al.* show that the chemical conjugate composed of the anti-CD19 MAb anti-B4 and 'blocked' whole ricin reaches tumor cells in the marrow more easily than tumor cells in lymph nodes, indicating that tumor penetration is a limiting factor in obtaining responses.
31. Scadder DT, Schenkein DP, Bernstein Z, Luskey B, Doweiko J, Tulpule A, Levine AM. Immunotoxin combined with chemotherapy for patients with AIDS-related non-Hodgkin's lymphoma. *Cancer* 1998, 83:2580-2587.
32. Kreitman RJ, Wang QC, FitzGerald DJP, Pastan I. Complete regression of human B-cell lymphoma xenografts in mice treated with recombinant anti-CD22 immunotoxin RFB4(dsFv)-PE38 at doses tolerated by Cynomolgus monkeys. *Int J Cancer* 1999, 81:148-155.
33. Kuan C, Pai LH, Pastan I. Immunotoxins containing *Pseudomonas* exotoxin targeting LeY damage human endothelial cells in an antibody-specific mode: relevance to vascular leak syndrome. *Clin Cancer Res* 1995, 1:1589-1594.
34. Soler-Rodríguez A-M, Ghetie M-A, Oppenheimer-Marks N, Uhr JW, Vitetta ES. Ricin A-chain and ricin A-chain immunotoxins rapidly damage human endothelial cells: implications for vascular leak syndrome. *Exp Cell Res* 1993, 206:227-234.
35. Re GG, Waters C, Posson L, Willingham MC, Sugamura K, Frankel AE. Interleukin 2 (IL-2) receptor expression and sensitivity to diphtheria toxin DAB(389)IL-2 in cultured hematopoietic cells. *Cancer Res* 1996, 56:2590-2595.
36. Waters CA, Schimke PA, Snider CE, Itoh K, Smith KA, Nichols JC, Strom TB, Murphy JR. Interleukin 2 receptor-targeted cytotoxicity. Receptor binding requirements for entry of a diphtheria toxin-related interleukin 2 fusion protein into cells. *Eur J Immunol* 1990, 20:785-791.
37. Duvic M, Kuzel T, Olsen E, Martin A, Foss F, Kim Y, Heald P, Bacha P, Nichols J, Cabanillas F. Quality of life is significantly improved in CTCL patients who responded to DAB389IL-2 (ONTAK) fusion protein. *Blood* 1998, 92(suppl 1):2572.
38. Williams DP, Snider CE, Strom TB, Murphy JR. Structure/function analysis of interleukin-2-toxin (DAB₄₈₆-IL-2). Fragment B sequences required for the delivery of fragment A to the cytosol of target cells. *J Biol Chem* 1990, 265:11885-11889.
39. Yagura H, Tamaki T, Furutsu T, Tomiyama Y, Nishiura T, Tominaga N, Katagiri S, Yonezawa T, Tarui S. Demonstration of high-affinity interleukin-2 receptors on B-chronic lymphocytic leukemia cells: functional and structural characterization. *Blood* 1990, 60:181-186.
40. Kodaka T, Uchiyama T, Ishikawa T, Kamio M, Onishi R, Itoh K, Hori T, Uchino H, Tsudo M, Araki K. Interleukin-2 receptor β -chain (p70-75) expressed on leukemic cells from adult T cell leukemia patients. *Jpn J Cancer Res* 1990, 81:902-908.
41. Kreitman RJ, Pastan I. Targeting *Pseudomonas* exotoxin to hematologic malignancies. *Semin Cancer Biol* 1995, 6:297-306.
42. Mavroudis DA, Jiang YZ, Hensel N, Lewalle P, Ccuriel D, Kreitman RJ, Pastan I, Barrett AJ. Specific depletion of alloreactivity against haplotype mismatched related individuals: a new approach to graft-versus-host disease prophylaxis in haploidentical bone marrow transplantation. *Bone Marrow Transplant* 1996, 17:793-799.
43. Engert A, Diehl V, Schnell R, Radszuhn A, Hatwig MT, Drillich S, Schon G, Bohlen H, Tesch H, Hansmann ML *et al.*: A phase-I study of an anti-CD25 ricin A-chain immunotoxin (RFT5-SMPT-dgA) in patients with refractory Hodgkin's lymphoma. *Blood* 1997, 89:403-410.
44. Schnell R, Vitetta E, Schindler J, Barth S, Winkler U, Borchmann P, Hansmann ML, Diehl V, Ghetie V, Engert A. Clinical trials with an anti-CD25 ricin A-chain experimental and immunotoxin (RFT5-SMPT-dgA) in Hodgkin's lymphoma. *Leuk Lymphoma* 1998, 30:525-537.
45. Montagna D, Yvon E, Calzavara V, Comoli P, Locatelli F, Maccario R, Fisher A, Cavazzana-Cavo M. Depletion of alloreactive T cells by a specific anti-interleukin-2 receptor p55 chain immunotoxin does not impair in vitro antileukemia and antiviral activity. *Blood* 1999, 93:3550-3557.
46. Jain RK. Delivery of molecular medicine to solid tumors. *Science* 1996, 271:1079-1080.
47. Goldberg MR, Heimbrook DC, Russo P, Sarady MI, Greenberg RL, Giantonio BJ, Linehan WM, Walther M, Fisher HAG, Messing F *et al.* Phase I clinical study of recombinant oncotxin TP40 in superficial bladder cancer. *Clin Cancer Res* 1995, 1:51-61.
48. Foss FM, Saleh MN, Krueger JC, Nichols JC, Murphy JR. Diphtheria toxin fusion proteins. In *Clinical Applications of Immunotoxins*. Edited by Frankel AF. Berlin: Springer-Verlag; 1998:63-81.
- This review by Foss *et al.* provides results of clinical trials of the IL-2-toxin DAB₃₈₉IL2, including Phase III results that led to the approval by the FDA of this agent for persistent or recurrent CD25⁺ CTCL. Data from clinical testing of DAB₃₈₉EGF are also given.
49. Lorimer IAJ, Wikstrand CJ, Batra SK, Bigner DD, Pastan I. Immunotoxins that target an oncogenic mutant epidermal growth factor receptor expressed in human tumors. *Clin Cancer Res* 1995, 1:859-864.
50. Lorimer IA, Keppler-Hafkemeyer A, Beers RA, Pegram CN, Bigner DD, Pastan I. Recombinant immunotoxins specific for a mutant epidermal growth factor receptor: targeting with a single chain antibody variable domain isolated by phage display. *Proc Natl Acad Sci USA* 1996, 93:14815-14820.
51. Pastan I, Lovelace ET, Gallo MG, Rutherford AV, Magnani JL, Willingham MC. Characterization of monoclonal antibodies B1 and B3 that react with mucinous adenocarcinomas. *Cancer Res* 1991, 51:3781-3787.
52. Brinkmann U, Pai LH, FitzGerald DJ, Willingham M, Pastan I. B3(Fv)-PE38KDEL, a single-chain immunotoxin that causes complete regression of a human carcinoma in mice. *Proc Natl Acad Sci USA* 1991, 88:8616-8620.
53. Siegall CB, Chace D, Mixan B, Garrigues U, Wan H, Paul L, Wolff F, Hellstrom L, Hellstrom KE. In vitro and in vivo characterization of BR96 sFv-PE40. A single-chain immunotoxin fusion protein that cures human breast carcinoma xenografts in athymic mice and rats. *J Immunol* 1994, 152:2377-2384.
54. Laske DW, Muraszko KM, Oldfield FH, DeVroom HL, Sung C, Dedrick RL, Simon TR, Colandrea J, Copeland C, Katz D *et al.* Intraventricular immunotoxin therapy for leptomeningeal neoplasia. *Neurosurgery* 1997, 41:1039-1049.
55. Greenfield L, Johnson VG, Youle RJ. Mutations in diphtheria toxin separate binding from entry and amplify immunotoxin selectivity. *Science* 1987, 238:536-539.
56. Puri RK, Leland P, Kreitman RJ, Pastan I. Human neurological cancer cells express interleukin-4 (IL-4) receptors which are targets for the toxic effects of IL4-*Pseudomonas* exotoxin chimeric protein. *Int J Cancer* 1994, 58:574-581.
57. Kreitman RJ, Puri RK, Pastan I. A circularly permuted recombinant interleukin 4 toxin with increased activity. *Proc Natl Acad Sci USA* 1994, 91:6889-6893.
58. Kreitman RJ, Puri RK, Pastan I. Increased antitumor activity of a circularly permuted interleukin 4-toxin in mice with interleukin 4 receptor-bearing human carcinoma. *Cancer Res* 1995, 55:3357-3363.
59. Laske DW, Youle RJ, Oldfield FH. Tumor regression with regional distribution of the targeted toxin TF-CRM107 in patients with malignant brain tumors. *Nat Med* 1997, 3:1362-1368.
60. Epstein C, Lynch T, Shefner J, Wen P, Maxted D, Braman V, Arniello P, Coral F, Ritz J. Use of the immunotoxin N901-blocked ricin in patients with small-cell lung cancer. *Int J Cancer* 1994, 57:51-59.
61. Siegall CB, Haggerty HG, Warner GL, Chace D, Mixan B, Unsley PS, Davidson T. Prevention of immunotoxin-induced immunogenicity by coadministration with CTLA4lg enhances antitumor efficacy. *J Immunol* 1997, 159:5168-5173.
62. McLaughlin P, Grillo-Lopez AJ, Link BK, Levy R, Czuczman MS, Williams ME, Heyman MR, Bence-Bruckler I, White CA, Cabanillas F *et al.* Rituximab chimeric Anti-CD20 monoclonal antibody therapy for relapsed indolent lymphoma: half of patients respond to a four-dose treatment program. *J Clin Oncol* 1998, 16:2825-2833.
63. Siegall CB, Liggitt D, Chace D, Mixan B, Sugai J, Davidson I, Steinitz M. Characterization of vascular leak syndrome induced by the toxin component of *Pseudomonas* exotoxin-based immunotoxins and its potential inhibition with nonsteroidal anti-inflammatory drugs. *Clin Cancer Res* 1997, 3:339-345.

64. Siegall CB, Eggitt D, Chace D, Tepper MA, Fell HP. Prevention of immunotoxin-mediated vascular leak syndrome in rats with retention of antitumor activity. *Proc Natl Acad Sci USA* 1994; 91:9514-9518.
 65. Rozenmuller H, Rombouts WJC, Jouw IP, FitzGerald DJP, Kreitman RJ, Pastan I, Hagenbeek A, Martens ACM. Treatment of acute myelocytic leukemia with interleukin-6 *Pseudomonas* exotoxin fusion protein in a rat leukemia model. *Leukemia* 1996; 10:1796-1803.
 66. Baluna R, Vitetta ES. Vascular leak syndrome: a side effect of immunotherapy. *Immunopharmacology* 1997; 37:117-132.
 67. Lindstrom AL, Erlandsen SL, Kersey JH, Pennell CA. An in vitro model for toxin-mediated vascular leak syndrome: ricin toxin A chain increases the permeability of human endothelial cell monolayers. *Blood* 1997; 90:2323-2334.
 68. Baluna R, Vitetta ES. An in vivo model to study immunotoxin-induced vascular leak in human tissue. *J Immunother* 1999; 22:41-47.
- Baluna and Vitetta performed skin grafting of foreskin or adult skin onto SCID mice and after systemic treatment of mice with immunotoxin measured changes in permeability via extravasation of Carbon Black or Evans Blue dye in the graft.
69. Baluna R, Rizo J, Gordon BE, Ghetie V, Vitetta ES. Evidence for a structural motif in toxins and interleukin-2 that may be responsible for binding to endothelial cells and initiating vascular leak syndrome. *Proc Natl Acad Sci USA* 1999; 96:3957-3962.
- Baluna *et al.* identify a tripeptide motif in RTA (LDV, using single-letter code for amino acids) which causes VLS as assessed by the *in vivo* model of skin transplants in SCID mice and also mediates binding to HUVECs. Similar sequences – such as GDL and GDV (in PE38), LDI (in IL-2) and VDS, IDS and LDV (in DT) – were also identified.
70. Uchida T, Pappenheimer AM Jr, Harper AA. Reconstitution of diphtheria toxin from two nontoxic cross-reacting mutant proteins. *Science* 1972; 175:901-903.
 71. Uchida T, Pappenheimer AM Jr, Greany R. Diphtheria toxin and related proteins I. Isolation and properties of mutant proteins serologically related to diphtheria toxin. *J Biol Chem* 1973; 248:3838-3844.
 72. Iwamoto R, Higashiyama S, Mitamura T, Taniguchi N, Klagsbrun M, Mekada E. Heparin-binding EGF-like growth factor, which acts as the diphtheria toxin receptor, forms a complex with membrane protein DRAP27/CD9, which up-regulates functional receptors and diphtheria toxin sensitivity. *EMBO J* 1994; 13:2322-2330.
 73. Rolf JM, Gaudin HM, Eidels L. Localization of the diphtheria toxin receptor-binding domain to the carboxyl-terminal M_r ~ 6000 region of the toxin. *J Biol Chem* 1990; 265:7331-7337.
 74. Kaul P, Silverman J, Shen WH, Blanke SR, Huynh PD, Finkelstein A, Collier RJ. Roles of Glu 349 and Asp 352 in membrane insertion and translocation by diphtheria toxin. *Protein Sci* 1996; 5:687-692.
 75. Hwang J, FitzGerald DJ, Achya S, Pastan I. Functional domains of *Pseudomonas* exotoxin identified by deletion analysis of the gene expressed in *E. coli*. *Cell* 1987; 48:129-136.
 76. Allred VS, Collier RJ, Carroll SF, McKay DB. Structure of exotoxin A of *Pseudomonas aeruginosa* at 3.0 Angstrom resolution. *Proc Natl Acad Sci USA* 1986; 83:1320-1324.
 77. Ogata M, Chaudhary VK, Pastan I, FitzGerald DJ. Processing of *Pseudomonas* exotoxin by a cellular protease results in the generation of a 37,000-Da toxin fragment that is translocated to the cytosol. *J Biol Chem* 1990; 265:20678-20685.
 78. Ogata M, Fryling CM, Pastan I, FitzGerald DJ. Cell-mediated cleavage of *Pseudomonas* exotoxin between Arg²⁷⁹ and Gly²⁸⁰ generates the enzymatically active fragment which translocates to the cytosol. *J Biol Chem* 1992; 267:25396-25401.
 79. Endo Y, Mitsui K, Motizuki M, Tsurugi K. The mechanism of action of ricin and related toxic lectins on eukaryotic ribosomes. *J Biol Chem* 1987; 262:5908-5912.
 80. Zamboni M, Brigotti M, Rambelli F, Montanaro L, Sperti S. High pressure liquid chromatographic and fluorimetric methods for the determination of adenine released from ribosomes by ricin and gelonin. *Biochem J* 1989; 259:639-643.
 81. Carroll SF, Collier RJ. Active site of *Pseudomonas aeruginosa* exotoxin A. Glutamic acid 553 is photolabeled by NAD and shows functional homology with glutamic acid 148 of diphtheria toxin. *J Biol Chem* 1981; 256:8701-8711.
 82. Chiron MF, Fryling CM, FitzGerald DJ. Cleavage of *Pseudomonas* exotoxin and diphtheria toxin by a furin-like enzyme prepared from beef liver. *J Biol Chem* 1994; 269:18167-18176.
 83. Fryling C, Ogata M, FitzGerald DJ. Characterization of a cellular protease that cleaves *Pseudomonas* exotoxin. *Infect Immun* 1992; 60:497-502.
 84. Williams DP, Wen Z, Watson RS, Boyd J, Ström TB, Murphy JR. Cellular processing of the interleukin-2 fusion toxin DAB₄₈₅-IL-2 and efficient delivery of diphtheria fragment A to the cytosol of target cells requires Arg¹⁹⁴. *J Biol Chem* 1990; 265:20673-20677.
 85. Hessler JL, Kreitman RJ. An early step in *Pseudomonas* exotoxin action is removal of the terminal lysine residue, which allows binding to the KDEL receptor. *Biochemistry* 1991; 36:14511-14582.
 86. Kreitman RJ, Pastan I. Importance of the glutamate residue of KDEL in increasing the cytotoxicity of *Pseudomonas* exotoxin derivatives and for increased binding to the KDEL receptor. *Biochem J* 1995; 307:29-37.
 87. vanderSpek J, Cassidy D, Genbauffe F, Huynh PD, Murphy JR. An intact transmembrane helix 9 is essential for the efficient delivery of the diphtheria toxin catalytic domain to the cytosol of target cells. *J Biol Chem* 1994; 269:21455-21459.
 88. Zhan H, Choe S, Huynh PD, Finkelstein A, Eisenberg D, Collier RJ. Dynamic transitions of the transmembrane domain of diphtheria toxin: disulfide trapping and fluorescence proximity studies. *Biochemistry* 1994; 33:11254-11263.
 89. Cabiiaux V, Mindell J, Collier RJ. Membrane translocation and channel-forming activities of diphtheria toxin are blocked by replacing isoleucine 364 with lysine. *Infect Immun* 1993; 61:2200-2202.
 90. Brinkmann U, Brinkmann E, Gallo M, Pastan I. Cloning and characterization of a cellular apoptosis susceptibility gene, the human homologue to the yeast chromosome segregation gene CSE1. *Proc Natl Acad Sci USA* 1995; 92:10427-10431.
 91. Williams JM, Lea N, Lord JM, Roberts LM, Milford DV, Taylor CM. Comparison of ribosome-inactivating proteins in the induction of apoptosis. *Toxicol Lett* 1997; 91:121-127.
 92. Martin PJ, Nelson BJ, Appelbaum FR, Anasetti C, Deeg HJ, Hansen JA, McDonald GB, Nash RA, Sullivan KM, Witherspoon RP *et al.* Evaluation of a CD5-specific immunotoxin for treatment of acute graft-versus-host disease after allogeneic marrow transplantation. *Blood* 1996; 88:824-830.
 93. O'Toole JE, Esseltine D, Lynch TJ, Lambert JM, Grossbard M. Clinical trials with blocked ricin immunotoxins. *Curr Top Microbiol Immunol* 1998; 234:35-56.
 94. Frankel AE, Laver JH, Willingham MC, Burns LJ, Kersey JH, Valleria DA. Therapy of patients with T-cell lymphomas and leukemias using an anti-CD7 monoclonal antibody-ricin A chain immunotoxin. *Leuk Lymphoma* 1997; 26:287-298.
 95. Kreitman RJ, Wilson WH, Robbins D, Margules I, Stetler-Stevenson M, Waldmann TA, Pastan I. Responses in refractory hairy cell leukemia to a recombinant immunotoxin. *Blood* 1999; in press.
 96. Hall PD, Willingham MC, Kreitman RJ, Frankel AE. DT388-GM-CSF, a novel fusion toxin consisting of a truncated diphtheria toxin fused to human granulocyte-macrophage colony stimulating factor, prolongs survival in a SCID model of acute myelogenous leukemia. *Leukemia* 1999; 13:629-633.
 97. Lynch TJ, Lambert JM, Coral F, Shefiar J, Wen P, Blattler WA, Collinson AR, Arniello PD, Braman G, Cook S *et al.* Immunotoxin therapy of small-cell lung cancer: a phase I study of N901-blocked ricin. *J Clin Oncol* 1997; 15:723-734.

Clinical trials of targeted toxins

Arthur E. Frankel, Edward P. Tagge* and Mark C. Willingham†

Immunotoxins (monoclonal antibodies chemically coupled to peptide toxins) and fusion toxins (peptide ligands fused genetically to peptide toxins) have been used to treat a variety of malignancies over the last 20 years. Problems with normal tissue toxicities (vascular leak syndrome, hepatotoxicity, and neurotoxicities), poor penetration to tumor interstitium, and humoral immune responses have limited clinical efficacy. Higher response rates were observed with systemic therapy of leukemias and lymphomas and regional therapy of primary brain tumors. Ongoing studies are examining the role of targeted toxins in combination with chemoradiotherapy and in minimal residual disease settings.

Key words: immunotoxins / fusion toxins / ricin / diphtheria toxin / *Pseudomonas* exotoxin / pokeweed antiviral protein / saporin

©1995 Academic Press Ltd

CHEMORADIO THERAPY IS TOXIC to mitotically active cells and, consequently, produces clinical responses in a number of rapidly proliferating human neoplasms including germ cell and hematopoietic malignancies, childhood cancers, breast and ovarian epithelial cancers, and small cell lung carcinoma. However, even in patients with responsive neoplasms, a fraction of patients are refractory to treatment or relapse after a brief remission. Explanations for failure of cytotoxic regimens include a low growth fraction for portions of the cancer¹ and altered tumor cell metabolism leading to removal of the drug or repair of drug-induced damage.² In addition, many common malignancies including melanomas, gliomas, gastrointestinal (GI) malignancies, sarcomas, non-small cell lung carcinomas and prostate cancer are minimally responsive to available chemoradiotherapy. Again, this primary refractory state has been attributed to low growth fraction and multiple drug resistance phenotypes.

As discussed by FitzGerald, peptide toxins are a new class of cancer therapeutics with a unique mechanism

of cell killing.³ Initially, two small clinical studies were done in the mid 1970's to 1980's using unmodified native whole toxin to treat refractory metastatic cancer patients.^{4,5} Topically and intratumorally applied ricin induced transient cytoreduction (5/18 partial responses) in patients with locally advanced cervical carcinomas, without any reported toxicities.¹ Intravenously administered ricin (4.5–23 µg/m² every two weeks) led to significant side effects (myalgias, fatigue, nausea and vomiting) and one partial response and four stable disease in 38 evaluable patients with advanced refractory metastatic carcinomas.⁵ However, most clinical studies have used either immunotoxins or fusion toxins, molecules that contain targeting functions with some degree of specificity for tumor cells. Immunotoxins consist of monoclonal antibodies covalently attached to peptide toxins via heterobifunctional linkers or intermolecular disulfide bonds.⁶ Fusion toxins consist of peptide ligands such as growth factors, hormones or single chain Fv's fused to peptide toxins via amide bonds.⁷ In each case, the toxin moiety has been modified to reduce normal cell binding. The growth factor or antibody delivers the molecule to the target cell surface, and the toxin then enters the cytosol and catalytically inactivates protein synthesis.

Synthesis of immunotoxins and fusion toxins requires the elimination of binding to normal tissues. The three dimensional atomic structures of several toxins^{8–11} along with the cDNA clones for these toxins^{12–15} has facilitated chemical derivatization and genetic engineering to alter toxin binding sites. After toxin modification, targeting ligands must be added to direct the toxin to tumor cell surface receptors. These receptors must be absent or at lower density on accessible normal human tissue cells. The targeting ligand must also trigger endocytosis and intracellular metabolism similar to the native toxins in order to yield potent immunotoxins or fusion toxins.

The structure and physiology of the toxins employed in the clinic were reviewed by FitzGerald.³ In this review we will focus on the clinical pharmacology of immunotoxins and fusion toxins. We will document the toxicities, pharmacodynamics, immune responses, and anti-tumor efficacy observed in clinical

From the Departments of Medicine, *Surgery and †Pathology, Medical University of South Carolina, 171 Ashley Avenue, Charleston, SC 29425, USA

©1995 Academic Press Ltd

1044-579X/95/050307+11 \$12.00/0

Table 1. Systemic immunotoxin trials*

Conjugate	Disease	Specific toxicity	Response rate	Ref
Anti-proteog-RTA	Melanoma	VLS	5/102	16,18
Anti-gp12-RTA	Colorectal Ca	VLS	2/16	19
Anti-CD5 RTA	CLL	VLS	2/18	20,21
Anti-CD5 RTA	CTCL	VLS	4/14	22
Anti-CD25 PE	ATL	Hepatic	0/4	23
Anti-gp55-rRTA	Breast Ca	Schwann. VLS	1/9	24,25
Anti-ov. ant. PE	Ovarian Ca	CNS	0/23	26
Anti-TfR-rRTA	AdenoCa	CNS	0/19	27
Anti-TfR-rRTA	Leptom. Ca	Arachnoid	0/8	28
Anti-CD22 dgRTA	NHL	VLS	9/40	31,51
Anti-CD22-dgRTA	HIV+ NHL	VLS	3/6	51
α CD22Fab-dgRTA	NHL	VLS	4/16	32
Anti-CD25-dgRTA	Hodgkin's	VLS	1/14	47
Anti-CD19-dgRTA	NHL	VLS	2/19	51
Anti-CD19 bR	NHL	Hepatic	8/59	33,34
Anti-CD30 SAP	Hodgkin's	VLS	5/12	36
DAB ₄₈₆ IL2	CD25+ malign.	None	11/109	37
DAB ₃₈₉ IL2	CTCL	None	12/35	38,39
DAB ₃₈₉ IL2	HNL	None	3/17	39
DAB ₃₈₉ IL2	Hodgkin's	None	0/19	39
Anti-CD19 PAP	B-ALL	VLS	9/26	35
LMB1	Carcinomas	VLS	1/35	40
Anti-CD56-bR	SCLC	VLS	1/21	41
Tf-CRM107	Brain	None	9/18	43
TP40	Bladder	None	8/43	42

*Response rate is (CR+PR)/total. VLS, vascular leak syndrome; RTA, ricin, toxin A chain; PE, *Pseudomonas* exotoxin; rRTA, recombinant ricin toxin A chain; dgRTA, deglycosylated ricin toxin A chain; bR, blocked ricin; Leptom. Ca, leptomeningeal neoplasms; SAP, saporin; PAP, pokeweed antiviral protein; Tf, human transferrin; CRM107, mutant DT with binding site inactive; TP40, TGF α fused to a 40 kilodalton fragment of PE; LMB1, Anti-Lewis y conjugated to a 38 kilodalton fragment of PE with a single Lys at the N-terminus for derivatization; SCLC, small cell lung cancer; CD25+ malign., hematopoietic malignancies with IL2 receptor including chronic lymphocytic leukemia, cutaneous T cell lymphoma, non-Hodgkin's lymphoma and Hodgkin's disease; B-ALL, B-cell acute lymphoblastic leukemia; CTCL, cutaneous T cell lymphoma; NHL, non-Hodgkin's lymphoma; TfR, transferrin receptor.

trials. In addition, we will postulate molecular mechanisms for these results, as well as propose favorable clinical settings for future clinical studies.

First generation clinical studies

Based on the extreme *in-vitro* potency of these hybrid proteins (approximately one-million fold more active on a molar basis than current cytotoxic drugs), 10 clinical studies were conducted with these molecules between 1985 and 1990.¹⁶⁻²⁸ In seven studies, patients with advanced refractory neoplasms were treated with short daily systemic infusions of immunotoxins (Table 1). 102 patients with melanoma received anti-proteoglycan-ricin toxin A chain (RTA) conjugate,¹⁶⁻¹⁸ 16 patients with metastatic colon carcinoma received anti-gp72-RTA conjugate,¹⁹ 18 patients with chronic lymphocytic leukemia (CLL)^{20,21} and 14 patients with cutaneous T-cell lymphoma (CTCL)²² received anti-CD5-RTA (CD refers to 'cluster of differentiation' to

denote an antigen recognized by different antibodies), four patients with adult T cell leukemia (ATL) were given one to two doses of anti-CD25-*Pseudomonas* exotoxin (PE),²³ and nine patients with refractory metastatic breast carcinoma were given anti-gp55-recombinant RTA.^{24,25} Three clinical trials were conducted using intracavitary treatment to expose local tumor deposits to high concentrations of immunotoxins (Table 1). Twenty-three patients with refractory stage III ovarian cancer received several intraperitoneal infusions of anti-adenocarcinoma antigen-PE conjugate.²⁶ 20 patients with peritoneal metastases of adenocarcinoma were given intraperitoneal infusions of anti-transferrin receptor antibody-recombinant RTA.²⁷ The same anti-transferrin receptor-recombinant RTA conjugate was given intrathecally to eight patients with leptomeningeal neoplasms.²⁸

In most studies where RTA was used, the dose-limiting toxicity was vascular leak syndrome (VLS) monitored by dyspnea, hypoalbuminemia, edema, weight gain, malaise, anorexia and fatigue. This

toxicity was seen with a number of RTA conjugates, suggesting the toxicity was not due to antibody targeting. VLS was seen with infusions of anti-proteoglycan-RTA, anti-gp72-RTA, anti-CD5-RTA, anti-gp55-recombinant RTA, and anti-transferrin receptor-recombinant RTA. VLS has been postulated as secondary to direct endothelial cell injury from exposure to high toxin concentrations and was reproduced in an *in-vitro* model by exposure of human umbilical cord endothelial cells to RTA alone.²⁹ Anti-gp72-RTA produced additional toxicities including proteinuria and a transient toxic encephalopathy (mental status changes, diffuse slowing on electroencephalograms, and normal computerized tomographic scans). This syndrome may have constituted a central nervous system form of VLS based on its time of occurrence and transient course. Anti-CD5-RTA produced additional side effects including arthralgias, rash, renal insufficiency and rhabdomyolysis, though these patients showed no evidence of serum sickness or anti-toxin antibodies. The dose-limiting toxicity of anti-CD25-PE was hepatotoxicity, apparently due to residual hepatocyte binding by domain Ia of the PE moiety. Central nervous system (CNS) toxicity due to antibody-specific targeting produced dose-limiting toxicity in four studies.^{24,26-28} A profound peripheral motor-sensory neuropathy occurred in three patients one month after treatment with anti-gp55-recombinant RTA. The gp55 antigen was found on normal human Schwann cells.²⁴ The anti-adenocarcinoma antigen-PE produced severe encephalopathy in three patients with brainstem inflammation on magnetic resonance imaging (MRI) in two patients and death in one patient. The antibody reacts with an antigen in the CNS.²⁶ Anti-transferrin receptor-recombinant RTA administered intraperitoneally produced abdominal pain, mucositis, and a fatal encephalopathy. In the latter patient, CT scan showed cerebral edema at 12 hours and postmortem exam showed hemorrhagic capillary necrosis of the basal ganglia. Transferrin receptor was subsequently identified on brain capillaries.²⁷ After intrathecal administration of anti-transferrin receptor-recombinant RTA for leptomeningeal malignancy, patients developed headaches, vomiting, decreased mental status, and elevated intracranial pressure which responded to steroids and cerebrospinal fluid (CSF) drainage. The meningitis may have been secondary to an inflammatory response to necrotic tumor cells or a direct effect of the immunotoxin on meningeal capillaries.²⁸

The pharmacology of immunotoxins in these stud-

ies was affected both by physical properties of the drug and biological aspects of the disease. The large size of most of the conjugates (around 200,000 daltons) led to high circulating levels of immunotoxin in the systemic trials and elevated intracavitary immunotoxin levels in the intraperitoneal and intrathecal therapy trials. The slow clearance from the infused compartment was likely secondary to low permeability. Penetration of immunotoxin into tumor interstitium was poor. While some anti-proteoglycan-RTA escaped the circulation and bound melanoma cells in skin nodules,¹⁶ neither anti-CD5-RTA nor anti-gp55-recombinant RTA conjugates were detected in extravascular sites (nodes, marrow, skin nodules) in patients with chronic lymphocytic leukemia and metastatic breast carcinoma, respectively.^{21,24} The plasma half-life was less than one hour for antibody conjugated to plant RTA which contained mannose-terminated oligosaccharides.¹⁶⁻²² Clearance was mediated by mannose receptors on reticuloendothelial cells.³⁰ As anticipated, deglycosylated RTA conjugate showed a longer blood half-life of 6-8 hours.^{24,25}

Immune responses were seen to all conjugates with the exception of 16/18 patients with CLL treated with anti-CD5-RTA. Presumably, the CLL patients were severely immunosuppressed. On the other hand, tolerance could not be produced in melanoma patients using either cyclophosphamide or azathioprine.^{17,18}

Clinical responses in these first generation phase I studies were rare (Table 1). There was one complete response and four partial responses lasting 6 weeks to one year in 102 metastatic melanoma patients treated with anti-proteoglycan-RTA. There were two partial responses in 16 metastatic colon cancer patients and one ovarian cancer patient treated with anti-gp72-RTA. Two partial responses were seen in 18 CLL patients given anti-CD5-RTA. Four out of 14 CTCL patients given 1-6 cycles of anti-CD5-RTA had partial responses. No responses were observed with anti-CD25-PE in 4 ATL patients. Similarly, there were no responses in 23 patients with ovarian cancer treated with intraperitoneal anti-adenocarcinoma antigen-PE. One partial response occurred in nine metastatic breast cancer patients infused with anti gp55-recombinant RTA. Finally, there were no responses observed after treatment of 19 metastatic intraperitoneal carcinomatosis patients given intraperitoneal anti-transferrin receptor-recombinant RTA or in eight leptomeningeal cancer patients given intrathecal anti-transferrin receptor-recombinant RTA.

Second generation clinical trials

Between 1990 and 1995, a series of clinical trials were conducted with immunotoxins and fusion toxins showing improved *in-vitro* efficacy (Table 1). Eleven different studies were performed with systemically administered toxin conjugates and two trials employed regional or cavity administered toxins.

Bolus infusions of anti-CD22 antibody (intact or Fab) conjugated to deglycosylated (dg) RTA were used to treat 25 and 16 patients, respectively, with refractory B-cell non-Hodgkin's lymphoma (NHL).^{31,32} In a third study, 18 B-cell NHL patients received continuous infusions of anti-CD22 Ig-dgRTA given at 9.6–28.8 mg/m² total dose over 8 days.⁵¹ Anti-CD25-dgRTA was given intravenously over 4 hours on days 1, 3, 5 and 7 at 5–20 mg/m² total dose to 15 patients with refractory CD25 positive Hodgkin's disease.⁴⁷ Anti-CD19-dgRTA was given to 19 B-cell NHL patients by bolus infusion and 10 B-cell NHL patients by continuous infusion.⁵¹ Anti-CD19 antibody conjugated to blocked ricin was given either by bolus or continuous infusion to 25 and 34 patients, respectively, with NHL.^{33,34} Anti-CD19-pokeweed antiviral protein (PAP) was given to 26 patients with B-cell acute lymphoblastic leukemia (B-ALL).³⁵ Anti-CD30-saporin (SAP) was administered as one or two infusions lasting three hours to 12 patients with refractory Hodgkin's disease.³⁶ IL2 was fused to fragments of diphtheria toxin (DAB₄₈₆IL2 and DAB₃₈₉IL2) and used to treat 109 and 73 patients, respectively, with IL2 receptor positive hematopoietic malignancies.^{37–39} Antibody to Lewis^y antigen coupled to a 38 kilodalton fragment of PE (LMB-1) was used to treat 35 patients with Lewis^y antigen positive metastatic carcinomas.⁴⁰ Anti-CD56-blocked ricin was administered by a seven day continuous infusion to 23 patients with small cell lung carcinoma.⁴¹

Two regional/cavity protocols were used to treat patients with bladder carcinoma and brain tumors. Transforming growth factor α (TGF α) peptide was fused to a 40 kilodalton fragment of PE (TP40) and repeatedly instilled into the bladder of 43 patients with refractory superficial bladder carcinoma.⁴² Human transferrin coupled to a binding defective S525F mutant of diphtheria toxin, CRM107, was inoculated into the lesions of 25 patients with refractory brain tumors.⁴³

VLS continued to be the dose-limiting toxicity for many of the trials, but qualitative and quantitative information has been gained about the syndrome which may help elucidate its mechanism and define

preventive measures. Both the anti-CD22 Fab-dgRTA and anti-CD22 Ig-dgRTA produced VLS, suggesting antibody Fc does not play a major role in pathogenesis. PAP, SAP, PE38, and blocked ricin conjugates also produced VLS, showing the toxicity is not restricted to RTA conjugates. This general toxicity may be secondary to greater sensitivity of endothelial cells to peptide toxins compared to other tissues. Alternatively, endothelial cells may have receptors and endocytosis for these diverse protein compounds, and evidence for each hypothesis exists. Primary pig endothelial cells lack bcl 2 expression and are poised for apoptosis.⁴⁴ Since toxin conjugates can induce apoptotic cell death,⁴⁴ these cells will be more sensitive. Various toxins may bind fibronectin receptors, α 2-macroglobulin receptors, or Lys-Asp-Glu-Leu (KDEL endoplasmic reticulum retention signal) receptors on endothelial cell surfaces and undergo receptor-mediated endocytosis. Binding of toxins to each of these receptors has been demonstrated and each may be present on endothelial cells.^{44–46} Patients with low tumor burden lacking an antigen sink and patients with high peak serum concentrations and total drug exposure (AUC) were more likely to show VLS in clinical studies with anti-CD22 Ig-RTA and LMB-1.^{31,40} Patients treated with DAB₄₈₆IL2, DAB₃₈₉IL2, transferrin-CRM107 and TP40 had low serum concentrations of drug, and the drug was rapidly cleared from the circulation.^{37–39,42,43} VLS was not observed in these studies, even though toxicity to cultured endothelial cells could be demonstrated *in vitro* with each toxin at concentrations identical to that producing endothelial cell toxicity for RTA, PAP, SAP, blocked ricin and PE40. These findings further support a local effect of high concentrations of conjugate on endothelial cell integrity. Other toxicities were seen in this group of trials. Blocked ricin conjugates produced transaminasemia and thrombocytopenia which were dose-limiting.^{33,34,41} The diphtheria toxin fusion proteins also produced dose-limiting transaminasemia which, interestingly, reduced in severity on subsequent cycles of drug. Protection appeared to correlate with development of anti-diphtheria toxin antibodies.^{37–39} TP40 fusion toxin produced no significant side effects and the maximal tolerated dose was not reached in the study.⁴² The limiting toxicity of interstitial transferrin-CRM107 for brain tumors was neurotoxicities secondary to extravasation of drug into surrounding normal brain tissues with transient neurological deficits.⁴³

Small conjugates showed dramatically shorter

plasma half-lives, attributable to kidney clearance and more rapid distribution outside the vasculature. The anti-CD22 Fab-dgRTA had a circulating $t_{1/2}$ of 1.3 hours versus 10.8 hours for the anti-CD22 Ig-dgRTA conjugate.^{31,32} The former molecule was 80,000 daltons and the latter molecule 180,000 daltons. As in the first generation trials, deglycosylation of RTA showed clearance. Bolus administration of 50 µg/kg anti-CD19-blocked ricin yielded peak levels of 0.2 µg/ml and a half-life of about one hour.³³ Continuous infusions of 40 µg/kg/day produced steady-state levels of also 0.2 µg/ml.³⁴ Continuous infusion of 30 µg/kg/day anti-CD56-blocked ricin produced steady-state levels of 0.1 µg/ml.⁴¹ Thus, blocked ricin conjugates behaved similarly to RTA conjugates. Since one-fifth the dose was administered, peak levels were one-fifth as high, and half-lives were about the same. Plant hemitoxins and PE40 conjugates had half-lives in the same range as deglycosylated RTA conjugates. This was expected since PAP, SAP and PE40 lack attached oligosaccharides. The plasma half-life of anti-CD30-SAP was 19 hours, the half-life of anti-CD19-PAP was 6 hours and the half-life of LMB-1 was 8.5 hours.^{35,36,40} The fusion toxins, DAB₃₈₉IL2 and DAB₄₈₆IL2, demonstrated much shorter plasma half-lives, on the order of 15 minutes, consistent with more rapid equilibrium with extravascular tissues and renal clearance.³⁷⁻³⁹ No measurements were made of circulating toxin in the two regional/cavitary studies.^{42,43} Only two studies addressed tumor penetration. Two refractory Hodgkin's disease patients underwent lymph node biopsies 18–24 hours after infusion of anti-CD30-SAP. Immunostaining revealed the presence of some toxin conjugate on Reed-Sternberg cells in the nodes.⁴⁹ Comparable *in-vivo* binding was documented in lung tumor and bone marrow of one patient after systemic administration of anti-CD56-blocked ricin.⁴¹ The role of drug size and dose in tumor penetration was not documented in any of the second generation trials.

Immune responses to both ligands and toxin moieties were again commonly observed in these second generation trials. Patients with B-cell malignancies appeared to have blunted responses to toxins. Out of 14 evaluable B-cell NHL patients treated with anti-CD22 Fab-dgRTA, only one patient produced high level antibody to RTA (500 µg/ml); two other patients developed low level antibody to RTA at 42 days (40–80 µg/ml) and one patient produced low level antibody to RTA (26 g/ml) and mouse Ig (5 µg/ml) at 28 days.³¹ Thus, 11/14 patients showed no immune response to toxin conjugate. Similarly, among 24 evaluable B-cell NHL patients treated with

bolus anti-CD22 Ig-dgRTA, most did not make antibodies (15/24); one patient made antibody to mouse Ig alone; two patients made antibody to RTA alone and six patients made antibodies to both RTA and mouse Ig.³² Antibody levels were low (0.1–68 µg/ml). Only 1/6 B-cell NHL patients on steroids produced antibody to anti-CD22 Ig-dgRTA. Only 9/25 B-cell NHL patients receiving bolus anti-CD19-blocked ricin developed antibodies to ricin and mouse Ig.³³ After multiple cycles of continuous infusion anti-CD19-blocked ricin in 34 B-cell NHL patients, six patients developed anti-ricin antibodies, five patients had anti-mouse Ig antibodies, and 13 patients showed both antibodies — although levels were not reported.³⁴ 17 B-ALL patients given intravenous anti-CD19-PAP did not develop immune responses to either the PAP or mouse Ig components.⁴⁸ In contrast, patients with small cell lung cancer given anti-CD56-blocked ricin almost uniformly developed anti-ricin antibodies (over 90% of patients).⁴¹ All refractory Hodgkin's disease patients given anti-CD19-SAP developed antibodies to both SAP and mouse Ig.⁴⁹ Most patients with IL2-receptor positive malignancies receiving DAB₄₈₆IL2 or DAB₃₈₉IL2 had significant anti-diphtheria toxin titers.^{37,39} This immune response was expected, since the U.S. population is immunized in childhood with diphtheria toxoid. Immune responses after intravesicle TP40 were not observed, presumably due to low systemic absorption of drug.⁴² Systemic immune responses to interstitial transferrin-CRM107 were not reported.⁴³

Response rates approaching 40% were observed in the second generation trials of leukemias and lymphomas. Leukemia and lymphoma cells may be more easily reached by targeted toxins than solid tumor cells. Most solid tumors have poor blood supply, absent lymphatic drainage and large interstitial pressures.⁵⁰ In contrast, clonal malignant stem cells for hematopoietic malignancies may circulate between blood, marrow and other organs. Bolus anti-CD22 Ig dgRTA yielded 5/24 partial responses (PR) and bolus infusions of anti-CD22 Fab-dgRTA produced 4/16 PR in evaluable patients with refractory B-cell NHL.^{31,32} Using anti-CD22 Ig-dgRTA in human immunodeficiency virus (HIV) positive patients with B-cell NHL, there were three complete responses (CR) among six evaluable patients.⁵¹ An eight-day continuous infusion of anti-CD22 Ig dgRTA in non-HIV B-cell NHL patients at 9.6–28.8 mg/m² total dose yielded 4/16 PR.⁵¹ Bolus infusions of anti-CD19-dgRTA produced one CR and one PR among 19 B-NHL patients, and continuous infusions of anti-CD19-dgRTA produced

one PR among 10 B-NHL patients.⁵¹ Anti-CD25-dlgRTA produced one PR lasting 2 months in 14 evaluable patients with refractory Hodgkin's disease.¹⁷ Anti-CD19-blocked ricin given as bolus daily infusion for five days to 25 patients with B-cell NHL produced one CR lasting 21 months and two PR.³³ The same drug continuously infused over seven days in 34 B-cell NHL patients produced two CR lasting 16 and 33 months and three PR lasting 1–3 months.³⁴ Anti-CD30-SAP produced PR lasting 2–4 months in five out of 12 patients with advanced refractory Hodgkin's disease.³⁶ Among 26 children with B-ALL treated with five daily boluses of anti-CD19-PAP, there were 6CR and 3PR.³⁵ DAB₄₈₆IL2 was given by bolus infusion in several schedules to 109 patients with CD25 positive lymphoid malignancies, and there were three unmaintained CR of over 18 months' duration including one patient each with intermediate-grade NHL, cutaneous T-cell lymphoma and bone marrow transplant refractory Hodgkin's disease. In addition, eight PR lasting 2–12 months were noted.³⁸ DAB₃₈₉IL2 has been given in 21 day cycles of five daily bolus infusions to patients with CD25 positive CTCL, NHL and Hodgkin's disease.³⁹ There were five CR and seven PR among 35 evaluable patients with CTCL. There was one CR and two PR among 17 patients with NHL. One of 10 evaluable patients with Hodgkin's disease, there have been no responses. Thus, even in the case of a smaller diffusible fusion toxin (60,000 daltons), *in vivo* efficacy is reduced for solid tumors. Consistent with these observations, only one PR was observed in 21 evaluable refractory small cell lung cancer patients treated with anti-CD56-blocked ricin.⁴¹ Only one CR lasting 2 months was observed in 35 patients with metastatic carcinomas treated with LMB-1.⁴⁰ Intracavitary therapy was relatively ineffective both in the second generation intravesicle TP40 trial⁴² and the previously reported intrathecal anti-transferrin receptor-recombinant RTA study.²⁸ Among 43 patients with refractory superficial bladder cancer, no evidence of antitumor activity was seen in patients with Pa or T1 lesions (Ta: papillary tumors with no invasion of bladder wall; T1: papillary tumors with lamina propria invasion).⁴² Eight of nine patients with carcinoma *in situ* showed clinical improvement following TP40 therapy, however urine and bladder washings continued to show malignant cells. In contrast, interstitial therapy using transferrin-CRM107 of 18 evaluable patients with unifocal brain neoplasms (12 glioblastoma multiforme, six anaplastic astrocytoma) yielded two CR and 7PR. The mean duration of response has not been reached and is greater than 40

weeks.¹³ Thus, while conclusions about efficacy are premature from Phase I dose escalation studies, these observations suggest the best disease targets are (a) leukemias and lymphomas for systemic therapy and (b) local disease treated by regional therapy rather than cavitary treatment.

Closer analysis showed responders had lower initial tumor burdens than nonresponders. If patient tumor burden must fall below a critical value for long term remissions or cure, and targeted toxin therapy like chemoradiotherapy causes fractional or log cell kill, response rates would be expected to be higher when initial tumor burdens are lower.⁵² Below a certain number, residual clonogenic tumor cells may not be able to expand perhaps due to host defenses.⁵³

Ongoing trials

Between 1993 and 1995, three types of targeted toxin trials were initiated (Table 2). Novel potent fusion toxins and more efficacious immunotoxins are being used systemically in four phase I studies in hopes that smaller or more potent toxic polypeptides will penetrate tumors more effectively and yielded better clinical activity. Previously developed toxin conjugates are being used in cocktails or combined with chemotherapy or bone marrow transplantation in 10 phase II trials to achieve greater log tumor cell kill. Finally, toxin conjugates are being used in three late phase II and phase III trials in selected disease states in which 1–2 log cytoreduction of circulating target cells can improve patient well-being.

A phase I dose-escalation study of DAB₃₈₉EGF for treatment of patients with EGF receptor bearing advanced malignancies was recently commenced.⁵⁴ To date 47 patients have been treated with 30-minute infusions of 0.3–15 µg/kg/day for five days every 28 days for six cycles or with 30 minute infusions on days 1, 8, 9, 15 and 16 every 28 days for six cycles. Twenty patients have received the 5 consecutive-day treatment and 27 have received the episodic treatment schedule. Dose-limiting toxicity has not been reached, but side effects including transient elevated creatinine, transient elevated transaminases, fatigue, pain, chills, fever, hypotension, hypertension, nausea and vomiting have been experienced. There have been no responses to date, although 4 patients have stable disease. A fusion protein consisting of a single chain Fv (immunoglobulin variable fragment) reactive with Lewis' antigen coupled to a 38 kilodalton fragment of PE (LMB-7) is being given intravenously over 30

Table 2. Ongoing immunotoxin trials*

Conjugate	Disease	Setting	Ref
Anti-CD19-bR	NHL	Post-AutoBMT	55,56
Anti-CD19-bR	NHL	Refrac. with chemo	56
Anti-CD19-bR	HIV+NHL	With chemo	57
Anti-CD56-bR	SCLC	Refrac. with chemo	41
DAB ₃₈₉ -IL2	CTCL	Stages I-III	39
DAB ₃₈₉ -IL2	Psoriasis	Refractory	60
Anti-CD19-PAP	B-ALL	With chemo	35
Tf CRM107	Brain tumors	Unifocal	43
Anti-CD7-dgRTA	T-ALL	Refractory	J.Kersey, unpublished
Anti-CD25-dgRTA	Hodgkin's	Refractory, CD25+	47
Anti-CD30-SAP	Hodgkin's	Post-AutoBMT	36
Anti-CD19-SAP	B-ALL	Refractory	D.Flavell, unpublished
α CD19&22-dgRTA	NHL	Refractory	51
DAB ₃₈₉ -EGF	Carcinomas	Refractory	54
LMB-7	Carcinomas	Refractory	40

*Abbreviations as in Table 1. HIV-NHL, HIV positive patients with NHL; T-ALL, T cell acute lymphoblastic leukemia; DAB₃₈₉-EGF, EGF fused to 389 amino acid fragment of DT; LMB-7, Anti Lewis^x Fv-PE38KDEL; AutoBMT, autologous bone marrow transplantation; chemo, combination chemotherapy; α CD19&22 dgRTA, cocktail of both immunotoxins.

minutes on days 1, 3 and 5 every four weeks for patients with metastatic Lewis^x positive carcinomas.⁴⁰ To date eight colorectal cancer patients and one breast cancer patient have received 2–7 μ g/kg doses without side effects. The $t_{1/2}$ was 60 minutes and the peak drug level was 90 ng/ml. 70% of patients developed anti-PE antibodies. A third new targeted toxin phase I study tests anti-CD7-dgRTA in patients with refractory T-cell acute lymphoblastic leukemia (J.Kersey, unpublished data). Six patients have received 0.05–0.1 mg/kg/day by one hour intravenous infusions for five days. There have been no side effects or responses. Finally, anti-CD19-SAP is given in a dose-escalation fashion to children with refractory B-ALL (D. Flavell, personal communication).

A phase II study on anti-CD19-blocked ricin has been conducted in minimal residual disease B-cell NHL.⁵⁵ Patients must have relapsed after one or more chemotherapy regimens, had chemosensitive disease, undergo myeloablative therapy with cyclophosphamide (60 mg/kg/day for two days) and total body irradiation (200 cGy bid \times 3 days) followed by rescue with antibody and complement purged autologous marrow grafts, and remain in complete remission 60 days post-transplant. Seven-day continuous infusions of 30–40 μ g/kg/day drug are administered on a 14–28 day cycle. To date 12 patients have been treated at 40 μ g/kg/day for seven-day infusions monthly and 49 patients have received 30 μ g/kg/day for seven days every two weeks. 29/59 evaluable patients have developed antibodies to mouse Ig and ricin between day 11 and 200, and infusions were stopped once

immune responses were documented. Toxicities included asthenia, anorexia, arthralgias, dyspnea, thrombopenia, hypotension, chills and thrombophlebitis. 60% of patients remain in continuous complete remission an average of 3 years post-transplant. These results compare favorably with other transplant regimens for B-cell NHL.⁵⁶ Based on these results, Cancer and Acute Leukemia Group B (CALGB) began a 48-center phase III trial (CALGB9254) in which relapsed or refractory B-cell NHL patients receive any myeloablative regimen followed by marrow or peripheral stem cell rescue (with or without purging) and, once achieving a complete remission, half the patients receive anti-CD19-blocked ricin infusions for seven days at 30 μ g/kg/day for two courses between day 60 and 120 post-transplant. The study has accrued half the 232 patients needed for randomization.⁵¹ In a phase II study, anti-CD19-blocked ricin is being given in combination with etoposide, vincristine, doxorubicin, cyclophosphamide, and prednisone (EPOCH) combination chemotherapy for relapsed B-cell NHL.⁵¹ To date, eight patients have been enrolled. The cytoreduction from combination targeted toxin and chemotherapy should lead to a greater log tumor cell kill. Similarly, a phase II study of anti-CD19-blocked ricin in combination with low dose cyclophosphamide, adriamycin, vincristine and prednisone (CHOP) combination chemotherapy is being given to HIV positive B-cell NHL patients in an effort to improve the short remission duration in this disease.⁵⁷ Continuous infusion of 20 μ g/kg/day for seven days is given, and to date, 46 patients have been enrolled. Another phase II study employs anti-CD56-blocked

ricin for treatment of minimal residual disease small cell lung cancer.⁴¹ After six cycles of chemotherapy and radiotherapy for limited small cell lung cancer, responding patients are receiving drug by continuous infusion at 30 µg/kg/day for seven days. Nine patients have been treated so far, and transaminasemia, VLS, elevated serum creatinine phosphokinase (CPK) and one episode of ventricular tachycardia have been observed. B-ALL patients with detectable minimal residual disease after induction chemotherapy will be entered on a Children's Cancer Study Group (CCG) protocol employing five daily bolus infusions of anti-CD19-PAP followed by consolidative chemotherapy.³⁵ Refractory Hodgkin's disease patients will receive 0.4 mg/kg twice of anti-CD30-SAP one month after autologous bone marrow transplant.³⁶ Two other phase II studies of targeted toxins attempted to improve response rates by adapting treatment to the biology of the particular tumor. Anti-CD25-dgRTA will be tested at 15 mg/m² total dose in patients with greater than 30% CD25 positive Reed-Sternberg cells.⁴⁷ This subset of patients showed a higher response rate in the phase I dose-escalation study. Higher antigen density should facilitate toxin binding and internalization.⁵⁸ A final phase II study employs a cocktail of two immunotoxins, anti-CD19-dgRTA and anti-CD22-dgRTA, to treat refractory B-cell NHL patients.⁵¹ Anti-CD19 antibody induces cell activation and primes cells for apoptosis.⁵⁹ Further, more of the tumor cells express the combination of CD19 and CD22 antigens than either alone. Among the three patients treated so far, there is one PR and one minimal response. Interestingly, the $t_{1/2}$'s of the two conjugates are different.

Three phase II-III trials will use targeted toxins in conditions where 1-2 log target cell depletion will result in significant disease palliation. Patients with stage Ia-III (stage Ia-limited plaques without nodal or visceral involvement, stage III-erythroderma without nodal or visceral involvement) CTCL having received fewer than three previous therapies will be given five daily bolus infusions of 9 or 18 µg/kg/day DAB₃₈₉IL2 on 21-day cycles for eight cycles.³⁹ The disease produces disfiguring skin lesions, with malignant cells circulating between the skin and bloodstream. Alternative palliative treatments require elaborate equipment (extracorporeal photophoresis) or have significant side effects (chemotherapy or radiotherapy). Another late phase II study is testing DAB₃₈₉IL2 at 5, 10 or 15 µg/kg/day for three days every 4 weeks for patients with psoriasis. A pilot phase I study of DAB₃₈₉IL2 at 2-9 µg/kg/day for 5 days monthly for

six cycles yielded 10/24 partial remissions.⁶⁰ Abnormal psoriatic T cells infiltrate the skin and release interferon γ which induces keratinocyte proliferation.⁶¹ Alternative treatments (steroids, methotrexate, cyclosporin) have not been proven efficacious and have significant side effects. Finally, patients with glioblastoma multiforme and anaplastic astrocytoma who have received maximal surgery and radiotherapy have a very short survival with great morbidity due to locally growing tumor. These patients will be treated in a late phase II trial with two infusions of interstitial transferrin-CRM107.⁴³ Slowing the spread of these locally destructive neoplasms should improve both disease-free survival and overall survival.

Future clinical strategies

Toxicities to normal tissues have limited the therapeutic usefulness of a number of targeted toxins. More careful screening of normal tissues prior to clinical testing, particular nervous system tissues, have reduced ligand-induced toxicities. However, in two trials preclinical cross-reactivities require careful clinical monitoring. Anti-CD56-blocked ricin targets the neural cell adhesion molecule (NCAM) antigen found on neural tissues⁶² and hence observations for late neurological sequelae are necessary. Similarly, LMB-7 targets the Lewis^x antigen present on GI tissues and severe gastritis has been encountered with BR96-DOX (antibody-doxorubicin conjugate) which targets the same antigen.⁶³ DAB₃₈₉EGF may bind the EGF receptor on hepatocytes⁶⁴ and continued monitoring of liver function tests will be necessary. Transferrin-CRM107 may be toxic to normal brain capillaries⁶⁵ and hence careful monitoring for acute and chronic CNS toxicities will be required in the interstitial therapy study. Most of the other targeted toxins in trials are directed towards differentiation antigens on hematopoietic tissues and have minimal cross-reactivity with other normal tissues. The major toxicity of targeted toxins independent of ligand continues to be VLS. While the smaller size of fusion toxins may reduce vascular endothelial exposure, adequate doses to produce clinical benefit are likely to expose the endothelial cells to toxic levels of drug. *In-vitro* models of VLS suggest endothelial cells are sensitive to toxins, but fail to provide methods of prevention. While no animal model exactly reproduces human VLS, a syndrome of hydrothorax, hypoalbuminemia, hemoconcentration and neutrophilia has been described in rats after intravenous injection of anti-Lewis^x Fv

PE40.⁶⁶ The syndrome was prevented by prophylaxis with steroids or non-steroidal anti-inflammatory drugs (NSAIDs).⁶⁷ No molecular mechanism was demonstrated. Anti-CD30-SAP is being administered to patients with refractory Hodgkin's disease one month post-autologous bone marrow transplant with 8 mg/kg methylprednisolone daily starting 24 hours before immunotoxin therapy. In the first two patients treated no VLS has been observed.³⁶

Poor tumor penetration continues to plague targeted toxin therapy. *In-vitro* studies with multicellular tumor spheroids and mathematical models using data from other proteins suggest smaller-sized fusion toxins and permeability enhancers — such as cisplatinum or hyaluronidase — may improve tumor uptake.^{68,69}

Immunotoxins and fusion toxins generate humoral immune responses in most patients except immunosuppressed patients with B-cell neoplasms. Although anti-toxin may not block killing of circulating tumor cells, the immune complexes likely inhibit extravascular tumor uptake and limit effective treatment periods for non-hematologic malignancies. Immuno-dominant neutralizing epitopes have been identified for both PE⁷⁰ and ricin⁷¹ and may serve as targets for genetic engineering. 15-deoxyspergualin and CTLA4Ig (a chimeric immunoglobulin fusion protein incorporating the extracellular domain of CTLA-4 retaining the high binding avidity for B7/BB1; induces blockade of a costimulatory pathway on T cells) given systemically reduce humoral immune responses to foreign proteins in animals and patients and may permit repeated treatment schedules with immunotoxins and fusion toxins.^{72,73} Finally, the use of human ribonucleases as the toxophore may be an additional method for reducing conjugate immunogenicity.⁷⁴

Efficacy of targeted toxins in patients may be greatest where cyto-reductions of several logs of target cells can produce a change in clinical condition. As noted above, trials in early stage CTCL, refractory unifocal gliomas, or minimal residual disease leukemia, lymphoma, Hodgkin's disease or small cell lung cancer may provide such a setting. A number of autoimmune disorders appear to respond to intravascular depletion of activated T lymphocytes including graft-versus-host disease,⁷⁵ rheumatoid arthritis,⁷⁶ early type I diabetes mellitus,⁷⁷ and, most recently, psoriasis.⁶⁰ Another presumed autoimmune disease with horrendous morbidity is multiple sclerosis and this may be a candidate for targeted toxin clinical trials, especially with MRI monitoring of disease activity.⁷⁸

Conclusions

Protein engineering to optimize drug design and selection of disease states based on tumor cell biology is leading to a niche for targeted toxin therapy in the treatment of minimal residual disease leukemias and lymphomas and small volume residual brain tumors. A number of autoimmune diseases may be better controlled with intermittent use of targeted toxins than chronic use of immunosuppressants. Applications of cocktails of targeted toxins and combination therapy with chemoradiation may eventually lead to use of these agents in the front-line treatment of a number of malignant diseases.

References

1. Skipper H (1979) Historic milestones in cancer biology: a few that are important to cancer treatment (revisited). *Semin Oncol* 6:506-514
2. Morrow C, Cowan K (1993) Drug resistance and cancer. *Adv Exp Med Biol* 330:287-305
3. FitzGerald D (1995) Why toxins? *Semin Cancer Biol*, in press
4. Hus C, Lin Y, Tung T (1974) Further report on therapeutic effect of abrin and ricin on human cancers. *J Form Med Assoc* 73:526-542
5. Fodstad O, Kvalheim G, Godal A, Lotsberg J, Aamdal S, Host H, Pihl A (1984) Phase I study of the plant protein ricin. *Cancer Res* 44:862-865
6. Vitetta E, Fulton R, May R, Till M, Uhr J (1987) Redesigning major positions to create antitumor reagents. *Science* 238:1098-1104
7. Pastan I, FitzGerald D (1992) Recombinant toxins for cancer treatment. *Science* 254:1173-1177
8. Choe S, Bennett M, Fujii G, Curmi P, Kantardjiev K, Collier R, Eisenberg D (1992) The crystal structure of diphtheria toxin. *Nature* 357:216-222
9. Brandhuber B, Allured V, Falbel T, McKay D (1988) Mapping the enzymatic active site of *Pseudomonas aeruginosa* exotoxin A. *Proteins* 3:146-154
10. Montfort W, Villafraanca J, Monzingo A, Ernst S, Katzin B, Rutenber E, Xuong N, Hamlin R, Robertus J (1987) The three-dimensional structure of ricin at 2.8 Angstroms. *J Biol Chem* 262:5398-5403
11. Monzingo A, Collins E, Ernst S, Irvin J, Robertus J (1993) The 2.5 Angstrom structure of pokeweed antiviral protein. *J Mol Biol* 233:705-715
12. Greenfield L, Bjorn M, Horn G, Fong D, Buck G, Collier R, Kaplan D (1983) Nucleotide sequence of the structural gene for diphtheria toxin carried by corynebacteriophage β . *Proc Natl Acad Sci USA* 80:6853-6857
13. Gray G, Smith D, Baldrige J, Harkins R, Vasil M, Chen E, Heneyker H (1984) Cloning, nucleotide sequence, and expression in *Escherichia coli* of the exotoxin A structural gene of *Pseudomonas aeruginosa*. *Proc Natl Acad Sci USA* 81:2645-2649
14. Lamb F, Roberts L, Lord J (1985) Nucleotide sequence of cloned cDNA coding for preproricin. *Eur J Biochem* 148:265-270
15. Benatti L, Saccardo M, Dani M, Nitti G, Sassano M, Lorenzetti R, Lippi D, Soria M (1989) Nucleotide sequence of cDNA coding for saporin-6, a type-I ribosome-inactivating protein from *Saponaria officinalis*. *Eur J Biochem* 183:465-470

16. Spittler L, del Rio M, Kientigan A, Wedel N, Brophy N, Miller L, Harkonen W, Rosendorf L, Lee H, Mischak R, Kawahata R, Stoudemire J, Fradkin L, Bautista E, Scannon P (1987) Therapy of patients with malignant melanoma using a monoclonal anti-melanoma antibody-ricin A chain immunotoxin. *Cancer Res* 47:1717-1723
17. Oratz R, Speyer J, Wernz J, Hochster H, Meyers M, Mischak R, Spittler L (1990) Antimelanoma monoclonal antibody-ricin A chain immunoconjugate (XMMME-001-RTA) plus cyclophosphamide in the treatment of metastatic malignant melanoma: results of a phase II trial. *J Biol Res Med* 9:345-354
18. Spittler L, Mishak R, Scannon P (1989) Therapy of metastatic melanoma with Xomazyme Mel, a murine monoclonal antibody-ricin A chain immunotoxin. *Int J Rad Appl Instrum [B]* 16:625-627
19. Byers V, Rodvien R, Grant K, Durrant L, Hudson K, Baldwin R, Scannon P (1989) Phase I study of monoclonal antibody ricin A chain immunotoxin XOMAZYME-791 in patients with metastatic colon cancer. *Cancer Res* 47:6153-6160
20. Hertler A, Schlossman D, Borowitz M, Blythman H, Casellas P, Frankel A (1989) An anti-CD5 immunotoxin for chronic lymphocytic leukemia: enhancement of cytotoxicity with human serum albumin-monsensin. *Int J Cancer* 43:215-219
21. LeMaistre F, Deisseroth A, Fogel B, Meneghetti C, Ma J, Anderson J, Saria E, Lomen P, Byers V (1990) Phase I trial of H65-RTA in patients with chronic lymphocytic leukemia. *Blood* 76 suppl 1:295a
22. LeMaistre C, Rosen S, Frankel A, Kornfeld S, Saria E, Meneghetti C, Drakes J, Fishwild D, Scannon P, Byers V (1991) Phase I trial of H65-RTA immunoconjugate in patients with cutaneous T-cell lymphoma. *Blood* 76:1173-1182
23. Waldman T, Pastan I, Gansow O, Junghans R (1992) The multichain interleukin-2 receptor: a target for immunotherapy. *Ann Intern Med* 116:148-160
24. Gould B, Borowitz M, Groves E, Carter P, Anthony D, Weiner J, Frankel A (1989) A phase I study of a continuous infusion anti-breast cancer immunotoxin: report of a targeted toxicity not predicted by animal studies. *JNCI* 81:775-781
25. Weiner L, O'Dwyer J, Kitson J, Comis R, Frankel A, Bauer R, Konrad M, Groves E (1989) Phase I evaluation of an anti-breast ca monoclonal antibody 260F9-recombinant ricin A chain immunoconjugate. *Cancer Res* 49:4062-4067
26. Pai L, Bookman M, Ozols R, Young R, Smith J, Longo D, Gould B, Frankel A, McClay E, Howell S, Reed E, Willingham M, FitzGerald D, Pastan I (1991) Clinical evaluation of intraperitoneal Pseudomonas exotoxin immunoconjugate OVB3-PE in patients with ovarian cancer. *J Clin Oncol* 9:2095-2103
27. Bookman M, Godfrey S, Padavic K, Griffin T, Corda J, Hamilton T, Ozols R, Groves E (1990) Anti-transferrin receptor immunotoxin (iT) therapy: phase I intraperitoneal (i.p.) trial. *Proc Am Soc Clin Oncol* 9:187
28. Laske D, Muraszko K, Oldfield E, DeVroom H, Sung C, Dedrick R, Simon T, Solomon D, Copeland C, Katz D, Groves E, Greenfield L, Houston L, Youle R (1992) Intraventricular immunotoxin therapy for leptomeningeal neoplasia. *Proc Third Intl Symp Immunotoxin*. Orlando, p 124
29. Soler-Rodriguez A, Ghetie M, Oppenheimer-Marks N, Uhr J, Vitetta E (1993) Ricin A-chain and ricin A-chain immunotoxins rapidly damage human endothelial cells: implications for vascular leak syndrome. *Exp Cell Res* 206:227-234
30. Blakey D, Watson G, Knowles P, Thorpe P (1987) Effect of chemical deglycosylation of ricin A-chain on the in vivo fate and cytotoxic activity of an immunotoxin composed of ricin A-chain and anti-Thy 1.1 antibody. *Cancer Res* 47:947-952
31. Amlot P, Stone M, Cunningham D, Fay J, Newman J, Collins R, May R, McCarthy M, Richardson J, Ghetie V, Ramilo O, Thorpe P, Uhr J, Vitetta E (1993) A phase I study of an anti-CD22-deglycosylated ricin A chain immunotoxin in the treatment of B cell lymphomas resistant to conventional therapy. *Blood* 82:2624-2633
32. Vitetta E, Stone M, Amlot P, Fay J, May R, Tidl M, Newman J, Clark P, Collins R, Cunningham D, Ghetie V, Uhr J, Thorpe P (1991) Phase I immunotoxin trial in patients with B cell lymphoma. *Cancer Res* 51:4052-4058
33. Grossbard M, Freedman A, Ritz J, Coral F, Goldmacher V, Eliseo L, Spector N, Dear K, Lambert J, Blatter W, Taylor J, Nadler L (1992) Serotherapy of B cell neoplasms with anti-B4-blocked ricin: a phase I trial of daily bolus infusion. *Blood* 79:576-585
34. Grossbard M, Lambert J, Goldmacher V, Spector N, Kinsella J, Eliseo L, Coral F, Taylor J, Blatter W, Epstein C, Nadler L (1993) Anti-B4 blocked ricin: a phase I trial of 7 day continuous infusion in patients with B cell neoplasms. *J Clin Oncol* 11:726-737
35. Uckun F (1995) B43-pokeweed antiviral protein (B43-PAP) immunotoxin. *Proc Fourth Intl Symp on Immunotoxins*. Myrtle Beach, p 162
36. Falini B, Pasqualucci L, Flenghi L, Bolognesi A, Kadin M, Stein H, Martelli M, Stürpe F (1995) Anti-CD30 immunotoxins: experimental and clinical studies. *Proc Fourth Intl Symp on Immunotoxins*. Myrtle Beach, p 160
37. Strom T, Kelley V, Murphy J, Nichols J, Woodworth T (1994) Interleukin-2 receptor directed therapies: antibody or cytokine-based targeting molecules. *Adv Nephrol* 23:347-356
38. Foss F, Borkowski T, Gilliom M, Stettin-Stevenson M, Jaffe E, Figg W, Tompkins A, Bastian A, Nylen P, Woodworth T, Udey M, Sausville E (1994) Chimeric fusion protein toxin DAB486IL2 in advanced mycosis fungoides and the Sezary syndrome: correlation of activity and interleukin-2 receptor expression in a phase II study. *Blood* 84:1765-1774
39. Foss F, Nichols J, Parker K (1995) Phase I/II trial of DAB389IL-2 in patients with NHL, HD and CTCL. *Proc Fourth Intl Symp on Immunotoxins*. Myrtle Beach, p 159
40. Pai L, Wittes R, Setser A, Goldspiel B, FitzGerald D, Willingham M, Pastan I (1995) Phase I and pharmacokinetic study of the immunotoxin LMB-1 (B3-LysPE38). *Proc Fourth Intl Symp Immunotoxins*. Myrtle Beach, p 163
41. Lynch T, Grossbard M, Fidas P, Bartholomay M, Coral F, Saigra R, Elias A, Skarin A, Sheffner J, Wen P, Arinello P, Bramen G, Esseltine D, Ritz J (1995) Immunotoxin therapy of small cell lung cancer (SCLC): clinical trials of N901 blocked ricin (N901-bR). *Proc Fourth Intl Symp on Immunotoxins*. Myrtle Beach, p 164
42. Goldberg M, Heimbrook D, Russo P, Sarosdy M, Greenberg R, Giantonio B, Linehan W, Walther M, Fisher H, Messing E, Crawford E, Oliff A, Pastan I (1995) *Clin Cancer Res* 1:57-61
43. Laske D, Oldfield E, Youle R (1995) Immunotoxins for brain tumor therapy. *Proc Fourth Intl Symp Immunotoxins*. Myrtle Beach, p 166
44. Willingham M, Brothier T, Tagge D, Frankel A (1995) Endothelial apoptosis in immunotoxin-induced vascular leak syndrome: an *in vitro* model. *Modern Path* 8:36A
45. Cavallaro U, Nykjaer A, Nielsen M, Soria M (1995) agr2: macroglobulin receptor mediates binding and cytotoxicity of plant ribosome-inactivating proteins. *Proteins*, in press
46. Baluna R, Ghetie V, Oppenheimer-Marks N, Vitetta E (1995) The binding of ricin A-chain to fibronectin: possible implications for vascular leak syndrome in immunotoxin-treated patients. *Proc Fourth Intl Symp Immunotoxins*. Myrtle Beach, p 144
47. Schnell R, Hatwig M, Radzuhn A, Cebe E, Drillich S, Schön G, Böhlen H, Tesch H, Hausmann M, Schindler J, Ghetie V, Uhr J, Diehl V, Vitetta E, Engel A (1995) A clinical phase I study of an anti-CD25-deglycosylated ricin A-chain immunotoxin (RFT5-SMPT-dgA) in patients with refractory Hodgkin's disease. *Proc Fourth Intl Symp Immunotoxins*. Myrtle Beach, p 161
48. Uckun F (1993) Annotation: immunotoxins for the treatment of leukaemia. *Br J Haematol* 85:435-438

49. Falini B, Bolognesi A, Flenghi L, Tazzari P, Broc M, Stein H, Durkop H, Aversa F, Corneli P, Pizzolo G, Barbabietola G, Sabatini E, Pileri S, Martelli M, Stirpe F (1992) Response of refractory Hodgkin's disease to monoclonal anti-CD30 immunotoxin. *Lancet* 339:1195-1196
50. Jain R (1994) Barriers to drug delivery in solid tumors. *Sci Am* 271:58-65
51. Esseltine D, Grossbard M, McLaughlin P, Murray J, Freedman A, Braman G, Nadler L (1995) Anti-B4-blocked ricin (anti-B4 bR) immunotoxin (IT) in the treatment of B-cell lymphoma and leukemia. *Proc Fourth Intl Symp on Immunotoxins*. Myrtle Beach, p 157
52. Skipper H, Perry S (1970) Kinetics of normal and leukemic leucocyte populations and relevance to chemotherapy. *Cancer Res* 30:1883-1897
53. Skipper H, Goh C, Wang T (1995) Shifting the cancer paradigm: must we kill to cure? *J Clin Oncol* 13:801-807
54. Theodoulou M, Baselga J, Scher H, Dantis L, Trainor K, Mendelsohn J, Howes L, Elledge R, Ravdin P, Bacha P, Braudt-Sarif T, Osborne K (1995) Phase I dose-escalation study of the safety, tolerability, pharmacokinetics and biologic effects of DAB389EGF in patients with solid malignancies that express EGF receptors (EGFR). *Proc Am Soc Clin Oncol* 14:480
55. Grossbard M, Gribben J, Freedman A, Lambert J, Kinsella J, Rabinow S, Eliseo L, Taylor J, Blatter W, Epstein C, Nadler L (1993) Adjuvant immunotoxin therapy with anti-B4-blocked ricin after autologous bone marrow transplantation for patients with B-cell non-Hodgkin's lymphoma. *Blood* 81:2263-2271
56. Verdonck L, van Putten W, Hagenbeek A, Schouten H, Sonneveld P, van Imhoff G, Kluin-Nelemans H, Raemaekers J, van Oers R, Haak H, Schots R, Dekker A, de Gast G, Lowenberg B (1995) Comparison of CHOP chemotherapy with autologous bone marrow transplantation for slowing responding patients with aggressive non-Hodgkin's lymphoma. *New England J Med* 332:1045-1051
57. Scadden D, Doweiko J, Bernstein Z, Schenkein D, Luskey B, Bresnahan J, Stram D, Esseltine D, Levine A (1995) Combined immunotoxin and chemotherapy for initial treatment of AIDS lymphoma. *Proc Fourth Intl Symp Immunotoxins*. Myrtle Beach, p 169
58. Bjorn M, Ring D, Frankel A (1985) Evaluation of monoclonal antibodies for the development of breast cancer immunotoxins. *Cancer Res* 45:1214-1221
59. Vitetta E, Uhr J (1994) Monoclonal antibodies as agonists: an expanded role for their use in cancer therapy. *Cancer Res* 54:5301-5309
60. Estis L, Krueger J, Nichols J, Parker K (1995) Psoriasis: a potential target for DAB₃₈₉IL-2. *Proc Fourth Intl Symp Immunotoxins*. Myrtle Beach, p 167
61. Greaves M, Weinstein G (1995) Treatment of psoriasis. *New Engl J Med* 332:581-588
62. Seki T, Aral Y (1993) Distribution and possible roles of the highly polysialylated neural cell adhesion molecule (NCAM-H) in the developing and adult central nervous system. *Neurosci Res* 17:265-290
63. Saleh M, LoBuglio A, Sugarman S, Murray J, Onetto N, Warner G, Mezza L, Davidson T, Grizzle W, Daniel C, LeBherz D, Healey D, Baron T, van Leeuwen D, Canetta R, Hellstrom K (1995) Gastrointestinal effects of chimeric BR96-Doxorubicin (DOX) conjugate. *Proc Am Assoc Cancer Res* 36:483
64. Carpenter G (1987) Receptors for epidermal growth factor and other polypeptide mitogens. *Annu Rev Biochem* 56:881-914
65. Frankel A, Ring D, Tringale F (1985) Tissue distribution of breast cancer associated antigens defined by monoclonal antibodies. *J Biol Res Mod* 4:273-286
66. Siegall C, Liggitt D, Chace D, Tepper M, Fell H (1994) Prevention of immunotoxin-mediated vascular leak syndrome in rats with retention of antitumor activity. *Proc Natl Acad Sci USA* 91:9514-9518
67. Chace D, Siegall C (1995) Characterization of immunotoxin induced vascular leak syndrome in rats. *Proc Fourth Intl Symp Immunotoxins*. Myrtle Beach, p 139
68. Ohnuma T, Kikuchi T, Kohno N, Spittler L, Holland J (1995) Penetration of immunotoxin and cytotoxic agents into multicellular spheroids and their cell kill effects. *Proc Fourth Intl Symp on Immunotoxins*. Myrtle Beach, p 119
69. Sung C, van Osdol W (1995) Effects of molecular weight and intracellular processing on tumor penetration of immunotoxins. *Proc Fourth Intl Symp Immunotoxins*. Myrtle Beach, p 118
70. Roscoe D, Jung S, Benhar I, Pai L, Lee B, Pastan I (1994) Primate antibody response to immunotoxin: serological and computer-aided analysis of epitopes on a truncated form of *Pseudomonas* exotoxin. *Infect Immun* 62:5055-5060
71. Lemley P, Amanatides P, Wright D (1994) Identification and characterization of a monoclonal antibody that neutralizes ricin toxicity in vitro and in vivo. *Hybridoma* 13:417-421
72. Pai L, FitzGerald D, Tepper M, Schachter B, Spitalny G, Pastan I (1990) Inhibition of antibody response to *Pseudomonas* exotoxin and an immunotoxin containing *Pseudomonas* exotoxin by 15-deoxyspergualin in mice. *Cancer Res* 50:7750-7760
73. Noon E, Shanahan S, Linsley P, Noelle R, Vitetta E (1995) Reduction in the murine anti-immunotoxin antibody response using novel immunosuppressive agents. *Proc Fourth Intl Symp Immunotoxins*. Myrtle Beach, p 150
74. Rybak S, Hoogenboom H, Meade H, Youle R (1992) Humanization of immunotoxins. *Proc Natl Acad Sci USA* 89:3165-3169
75. Byers V, Henslee P, Kernan N (1990) Use of an anti-pan T-lymphocyte ricin A chain immunotoxin in steroid-resistant acute graft-versus-host disease. *Blood* 75:1426-1432
76. Strand V, Lipsky P, Cannon G (1991) Treatment of rheumatoid arthritis with an anti-CD5 immunoconjugate: final results of phase II studies. *Arthritis Rheum* 34:S91
77. Woodworth T, Parker K, Sewell K (1992) Pilot studies demonstrating DAB486IL2 (DAB) associated safety and improvement in parameters of disease activity in patients with severe, refractory rheumatoid arthritis (RA) and early autoimmune type I diabetes mellitus (DM). *Proc Third Intl Symp on Immunotoxins*. Orlando, p 130
78. The IFNB Multiple Sclerosis Study Group. (1993) Interferon beta-1b is effective in relapsing remitting multiple sclerosis. I. Clinical results of a multicenter randomized, double-blind, placebo-controlled trial. *Neurology* 43:655-661

Athens Authentication Point

Welcome!

To use the personalized features of this site, please log in or register.

If you have forgotten your username or password, we can help.

My SpringerLink

Marked Items

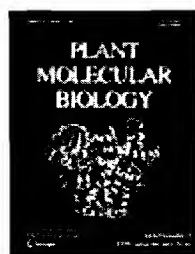
Alerts

Order History

Saved Items

All

Favorites



Characterization of a cDNA encoding ricin E, a hybrid ricin-*Ricinus communis* agglutinin gene from the castor plant *Ricinus communis*

Journal Plant Molecular Biology
 Publisher Springer Netherlands
 ISSN 0167-4412 (Print)
 1573-5028 (Online)
 Subject Biomedical and Life Sciences
 Issue Volume 9, Number 3 / May, 1987
 DOI 10.1007/BF00166464
 Pages 287-295
 SpringerLink Date Tuesday, November 09, 2004

Add to marked items

Add to shopping cart

Add to saved items

Request Permissions

Recommend this article

Beth F. Ladin^{1, 2}, Elizabeth E. Murray^{1, 3},
 Amy C. Halling¹, Kevin C. Halling¹,
 Nanda Tilakaratne¹, George L. Long⁴,
 L. L. Houston^{1, 5} and Robert F. Weaver¹

- (1) Department of Biochemistry, University of Kansas, 66045 Lawrence, KS, USA
- (2) *Present address:* Henkel Corporation, Santa Rosa, CA
- (3) *Present address:* Agrigenetics Advanced Research Laboratory, Madison, WI
- (4) Eli Lilly and Company, Indianapolis, IN
- (5) *Present address:* Cetus Corporation, Emeryville, CA

Find more options

Go

☒ Within this issue

☐ Within this journal

☐ Within all content

Export this article

Export this article as RIS | Text

Text

PDF

The size of this document is 683 kilobytes. Although it may be a lengthier download, this is the most authoritative online format.

Open: Entire document


Referenced by

1 newer article

1. WOOD, Katherine A. (1991) Preproabrin: genomic cloning, characterisation and the expression of the A-chain in *Escherichia coli*. *European Journal of Biochemistry* 198 (3) [CrossRef]

Received: 5 June 1986 Accepted: 4 June 1987

Abstract Two classes of ricin cDNA clones have been identified and sequenced. The cDNA clone pBL-1 closely matches in nucleotide sequence the ricin genomic clone pAKG previously described by Halling *et al.*, 1985 (Nucl. Acids Res. 13:8019). A second group of cDNA clones, represented by pBL-3, encode a hybrid protein (ricin E), having a ricin-like A chain and N-terminal half of the B chain and an RCA (*Ricinus communis* agglutinin)-like C-terminal half of the B chain.


 Beth F. Ladin

Phone: (913) 864-3399

 Elizabeth E. Murray

Phone: (913) 864-3399

20. Davis, G. L., Dibner, D. M. & Battey, F. J. (1986) *Basic methods in molecular biology*, Elsevier Science Publishing Co., Amsterdam.
21. Messing, J. & Vieira, J. (1982) *Gene* 19, 269–276.
22. Ullrich, A., Berman, C. H., Dull, T. J., Gray, A. & Lee, J. M. (1984) *EMBO J.* 3, 361–364.
23. Von Heijne, G. (1986) *Nucleic Acids Res.* 14, 4683–4690.
24. Bianchi, M. W. & Viotti, A. (1988) *Plant Mol. Biol.* 11, 203–214.
25. Dani, M., Benatti, L., Lorenzetti, R., Martini, D., Minganti, C., Sassano, M., Sidoli, S. & Soria, M. (1988) *Nucleic Acids Res.* 16, 3103.
26. Boer, P. H. & Gray, M. W. (1988) *Cell* 55, 399–411.
27. Pan, Y. E., Stern, A. S., Familletti, P. C., Khan, R. F. & Chizzonite, R. (1987) *Eur. J. Biochem.* 166, 145–149.
28. Shinshi, H., Wenzler, H., Neuhaus, J. M., Felix, G., Hofsteenge, J. & Mein, F. Jr. (1988) *Proc. Natl Acad. Sci. USA* 85, 5541–5545.
29. Zhang, X. & Wang, J. (1986) *Nature* 321, 477–478.
30. Asano, K., Svensson, B., Svendsen, I., Poulsen, F. M. & Roepstorff, P. (1986) *Carlsberg Res. Commun.* 51, 129–141.
31. Calderwood, S. B., Auclair, F., Donohue-Rolfe, A., Keusch, G. T. & Mekalanos, J. J. (1987) *Proc. Natl Acad. Sci. USA* 84, 4364–4368.
32. Hovde, C. J., Calderwood, S. B., Mekalanos, J. J. & Collier, R. J. (1988) *Proc. Natl Acad. Sci. USA* 85, 2568–2572.
33. Monfort, W., Villafranca, J. E., Monzingo, A. F., Ernst, S. R., Katzin, B., Rutenber, E., Xuong, N. H., Hamlin, R. & Robertus, J. D. (1987) *J. Biol. Chem.* 262, 5398–5403.
34. Ready, M. P., Katzin, B. J. & Robertus, J. D. (1988) *Proteins* 3, 53–59.
35. Gelfi, C., Bossi, M. L., Bjellqvist, B. & Righetti, P. G. (1987) *J. Biochem. Biophys. Methods* 15, 41–48.
36. Thorpe, P. E., Brown, A. N., Bremner, J. A. G. Jr., Foxwell, B. M. J. & Stirpe, F. (1985) *J. Natl Cancer Inst.* 75, 151–159.
37. Siena, S., Lippi, D. A., Bregni, M., Formosa, A., Villa, S., Soria, M., Bonadonna, G. & Gianni, M. A. (1988) *Blood* 72, 756–765.
38. Bregni, M., Lippi, D. A., Siena, S., Villa, S., Formosa, A., Bonadonna, G., Soria, M. & Gianni, A. M. (1988) *J. Natl Cancer Inst.* 80, 511–517.
39. Siena, S., Bregni, M. D., Formosa, A., Martineau, D., Lippi, D. A., Bonadonna, G. & Gianni, A. M. (1989) *Transplantation* 46, 747–753.
40. Marcucci, F., Lippi, D. A., Ghislieri, M., Martineau, D., Formosa, A., Siena, S., Bregni, M., Soria, M. & Gianni, A. M. (1989) *J. Immunol.* 142, 2955–2960.
41. Kelley, V. E., Bacha, P., Pankewycz, O., Nichols, J. C., Murphy, J. R. & Strom, T. B. (1988) *Proc. Natl Acad. Sci. USA* 85, 3980–3984.
42. Chaudhary, V. K., FitzGerald, D. J., Adhya, S. & Pastan, I. (1987) *Proc. Natl Acad. Sci. USA* 85, 4538–4542.
43. Chaudhary, V. K., Mizukami, Y., Fuerst, T. R., FitzHerald, D. J., Moss, B., Pastan, I. & Berger, E. A. (1988) *Nature* 335, 369–372.
44. Lorberboum-Galski, H., FitzGerald, D., Chaudhary, V. K., Adhya, S. & Pastan, I. (1988) *Proc. Natl Acad. Sci. USA* 85, 1922–1926.

 **Amy C. Halling**


Phone: (913) 864-3399

 **Kevin C. Halling**

Phone: (913) 864-3399

 **Nanda Tilakaratne**

Phone: (913) 864-3399

 **L. L. Houston**

Phone: (913) 864-3399

 **Robert F. Weaver**

Phone: (913) 864-3399

References secured to subscribers.

Ads by Goooooogle

Protein Characterization
Use a DynaPro for Fast &
Accurate Protein
Characterization
www.wyatt.com

Antibodies
Your Online Source For
Antibody! Comprehensive
Info. And Pricing.
Antibodysonet.net

AbD Serotec Antibodies
10,000+ antibodies &
reagents Free e-catalog,
posters & brochures
www.ab-direct.com

TNF alpha ELISA Kit
\$410.00 US for 96 tests
Assay Range: 4-2000
pg/mL
www.anogen.ca

**Recombinant
Heparanase**
rh HPA-1 Bioactive, Highly
pure
www.insight.co.il

Advertise on this site

[Frequently asked questions](#) | [General information on journals and books](#) | [Send us your feedback](#) | [Impressum](#)

© **Springer**. Part of Springer Science+Business Media

[Privacy](#), [Disclaimer](#), [Terms and Conditions](#), [Copyright Information](#)

Remote Address: 206.166.115.173 • Server: mpower04

HTTP User Agent: Mozilla/4.0 (compatible; MSIE 6.0; Windows NT 5.0; .NET CLR 1.1.4322)



European Journal of Biochemistry

Volume 235 Issue 1-2 Page 159 - January 1996

To cite this article: John A. Chaddock, Arthur F. Monzingo, Jon D. Robertus, J. Michael Lord, Lynne M. Roberts (1996) Major Structural Differences between Pokeweed Antiviral Protein and Ricin A-Chain do not Account for their Differing Ribosome Specificity *European Journal of Biochemistry* 235 (1-2), 159–166.
doi:10.1111/j.1432-1033.1996.00159.x



[Prev Article](#) [Next Article](#)

Original Article

Major Structural Differences between Pokeweed Antiviral Protein and Ricin A-Chain do not Account for their Differing Ribosome Specificity

John A. Chaddock¹, Arthur F. Monzingo², Jon D. Robertus¹, J. Michael Lord¹, Lynne M. Roberts¹

¹Department of Biological Sciences, University of Warwick, Coventry, UK ²Department of Chemistry and Biochemistry, University of Texas, Austin, TX USA

L. M. Roberts, Department of Biological Sciences, University of Warwick, Coventry, West Midlands, United Kingdom, CV4 7AL
Fax: +44 1203 523701

Abstract

Pokeweed antiviral protein (PAP) and the A-chain of ricin (RTA) are two members of a family of ribosome-inactivating proteins (RIPs) that are characterised by their ability to catalytically depurinate eukaryotic ribosomes, a modification that makes the ribosomes incapable of protein synthesis. In contrast to RTA, PAP can also inactivate prokaryotic ribosomes. In order to investigate the reason for this differing ribosome specificity, a series of PAP/RTA hybrid proteins was prepared to test for their ability to depurinate prokaryotic and eukaryotic ribosomes. Information from the X-ray structures of RTA and PAP was used to design gross polypeptide switches and specific peptide insertions. Initial gross polypeptide swaps created hybrids that had altered ribosome inactivation properties. Preliminary results suggest that the carboxy-terminus of the RIPs (PAP 219–262) does not contribute to ribosome recognition, whereas polypeptide swaps in the amino-terminal half of the proteins did affect ribosome inactivation. Structural examination identified three loop regions that were different in both structure and composition within the amino-terminal region. Directed substitution of RTA sequences into PAP at these sites, however, had little effect on the ribosome inactivation characteristics of the mutant PAPs, suggesting that the loops were not crucial for prokaryotic ribosome recognition. On the basis of these results we have identified regions of RIP primary sequence that may be important in ribosome recognition. The implications of this work are discussed.

This article is cited by:

This article is cited by the following articles in Blackwell Synergy and CrossRef

- K. Szalai, I. Schöll, E. Förster-Waldl, L. Polito, A. Bolognesi, E. Untersmayr, A. B. Riemer, G. Boltz-Nitulescu, F. Stirpe and E. Jensen-Jarolim. (2005) Occupational sensitization to ribosome-inactivating proteins in researchers. *Clinical & Experimental Allergy* **35**:10, 1354–1360
[Abstract](#) [Abstract and References](#) [Full Text](#) [Article Full](#) [Article PDF](#)

This Article

Abstract

References

Full Text PDF (1,411 KB)

Rights & Permissions

Search

In

- ☒ Synergy
- ☐ PubMed (MEDLINE)
- ☐ CrossRef

By keywords

- ☐ ribosome-inactivating proteins
- ☐ pokeweed antiviral protein
- ☐ ricin
- ☐ ribosome recognition
- ☐ *N*-glycosidase

By author

- ☐ John A. Chaddock
- ☐ Arthur F. Monzingo
- ☐ Jon D. Robertus
- ☐ J. Michael Lord
- ☐ Lynne M. Roberts
- ☐ _____

GO 

[Privacy Statement](#) | [Terms & Conditions](#) | [Contact](#) | [Help](#)



**Blackwell
Publishing**

Blackwell Publishing is a registered trademark
of Blackwell Publishing Ltd, Oxford, UK, USA, Malaysia and Singapore

Technology platform: Atypion Systems, Inc.

**Catalogue de documents pour le chercheur****Titre du document / Document title**

Cloning and expression of a gene encoding gelonin, a ribosome-inactivating protein from *Gelonium multiflorum*

Auteur(s) / Author(s)

NOLAN P. A. ; GARRISON D. A. ; BETTER M. ;

Affiliation(s) du ou des auteurs / Author(s) Affiliation(s)

XOMA Corp., Santa Monica CA 90404, ETATS-UNIS

Résumé / Abstract

A cDNA copy of the gel gene, encoding gelonin (Gel), has been cloned from the seeds of the Asian plant, *Gelonium multiflorum*. Gel is a type-I ribosome-inactivating protein which has been produced in *Escherichia coli* as a secreted protein under the transcriptional control of the *Salmonella typhimurium* araB promoter and linked to the pectate lyase (pelB) leader sequence from *Erwinia carotovora*. Recombinant, soluble Gel (re-Gel) can be recovered from the *E. coli* culture supernatant at a yield of greater than 1 mg/ml, and it inhibits protein synthesis in vitro to the same extent as the native protein isolated from plant seeds

Revue / Journal Title

Gene (Gene) ISSN 0378-1119 CODEN GENED6

Source / Source

1993, vol. 134, n°2, pp. 223-227 (25 ref.)

Langue / Language

Anglais

Editeur / Publisher

Elsevier, Amsterdam, PAYS-BAS (1977) (Revue)

Mots-clés anglais / English Keywords

Complementary DNA ; Nucleotide sequence ; Homology ; Gene expression ; Recombinant protein ; Ribosome inactivating protein ; Euphorbiaceae ; Dicotyledones ; Angiospermae ; Spermatophyta ;

Mots-clés français / French Keywords

DNA complémentaire ; Séquence nucléotide ; Homologie ; Expression génique ; Protéine recombinante ; Gélonine ; Gène gel ; *Gelonium multiflorum* ; Protéine inactivant ribosome ; Euphorbiaceae ; Dicotyledones ; Angiospermae ; Spermatophyta ;

002a04c02 ;

Mots-clés espagnols / Spanish Keywords

DNA complementario ; Secuencia nucleótido ; Homología ; Expresión genética ; Proteína recombinante ; Euphorbiaceae ; Dicotyledones ; Angiospermae ; Spermatophyta ;

Localisation / Location

INIST-CNRS, Cote INIST : 17570, 35400002402312.0100

Copyright 2006 INIST-CNRS. All rights reserved

Toute reproduction ou diffusion même partielle, par quelque procédé ou sur tout support que ce soit, ne pourra être faite sans l'accord préalable écrit de l'INIST-CNRS.

No part of these records may be reproduced or distributed, in any form or by any means, without the prior written permission of INIST-CNRS.



Services

- ▶ [Similar articles in this journal](#)
- ▶ [Similar articles in PubMed](#)
- ▶ [Alert me to new issues of the journal](#)
- ▶ [Download to citation manager](#)
- ▶ [Cited by other online articles](#)

Google Scholar

- ▶ [Articles by Benatti, L.](#)
- ▶ [Articles by Soria, M.](#)
- ▶ [Articles citing this Article](#)

PubMed

- ▶ [PubMed Citation](#)
- ▶ [Articles by Benatti, L.](#)
- ▶ [Articles by Soria, M.](#)

European Journal of Biochemistry, Vol 183, 465-470. Copyright © 1989 by Federation of European Biochemical Societies

ARTICLES

Nucleotide sequence of cDNA coding for saporin-6, a type-1 ribosome- inactivating protein from *Saponaria officinalis*

L Benatti, MB Saccardo, M Dani, G Nitti, M Sassano, R Lorenzetti, DA Lappi and M Soria

Biotechnological Research, Farmitalia Carlo Erba, Milano, Italy.

We have isolated and sequenced partial cDNA clones that encode SO-6, a ribosome-inactivating protein from *Saponaria officinalis*. A cDNA library was constructed from the leaves of this plant and screened with synthetic oligonucleotide probes representing various portions of the protein. The deduced amino acid sequence shows the signal peptide and a coding region virtually accounting for the entire amino acid sequence of SO-6. The sequence reveals regions of similarity to other ribosome- inactivating proteins, especially in a region of the molecule where critical amino acid residues might participate in the active site.

This article has been cited by other articles: (Search Google Scholar for Other Citing Articles)



the **FEBS** Journal

▶ [HOME](#)

M. T den Hartog, C. Lubelli, L. Boon, S. Heerkens, A. P Ortiz Buijsse, M. de Boer, and F. Stirpe

Cloning and expression of cDNA coding for bouganin: A type-I ribosome-inactivating protein from *Bougainvillea spectabilis* Willd

FEBS J., March 15, 2002; 269(6): 1772 - 1779.

[\[Abstract\]](#) [\[Full Text\]](#) [\[PDF\]](#)



THE FASEB JOURNAL

▶ [HOME](#)

M. S. FABBRINI, D. CARPANI, M. R. SORIA, and A. CERIOTTI

Cytosolic immunization allows the expression of preATF-saporin chimeric toxin in eukaryotic cells

FASEB J, February 1, 2000; 14(2): 391 - 398.

[\[Abstract\]](#) [\[Full Text\]](#)



PubMed
Central

Search

Journal List

Biochemical Journal

Home | Current issue | Editorial board | Subscriptions

Note: Performing your original search, **+saporin +cdna**, in PubMed Central will retrieve 17 citations.

Journal List > Biochem J > v.322(Pt 3); Mar 15, 1997

■ Summary

Selected References
PDF (498K)
Contents
Archive

Related material:

PubMed related arts



PubMed articles by:

Fabbrini, M.
Rappocciolo, E.
Carpani, D.
Soria, M.

Biochem J. 1997 March 15; 322(Pt 3): 719–727.

Copyright notice

Characterization of a saporin isoform with lower ribosome-inhibiting acti

M S Fabbrini, E Rappocciolo, D Carpani, M Solinas, B Valsasina, U Breme, U Cavallaro, A Nykj
Rovida, G Legname, and M R Soria

Department of Biological and Technological Research-Dibit, San Raffaele Scientific Institute, via Olgettina 58, 2013

ABSTRACT

We have expressed in *Escherichia coli* five isoforms of saporin, a single-chain ribosome-inactivating protein. Translation inhibition activities of the purified recombinant polypeptides in vitro were compared with those of recombinant dianthin 30, a less potent and closely related RIP, and of ricin A chain. Dianthin 30, and a saporin encoded by a cDNA from leaf tissue (SAP-C), both had about one order of magnitude lower activity in translation inhibition assays than all other isoforms of saporin tested. We recently demonstrated that saporin extracted from *Saponaria officinalis* binds to alpha2-macroglobulin receptor (alpha2MR; also termed low density lipoprotein receptor-related-protein), indicating a general mechanism of interaction of plant RIPs with the alpha2MR system [Cavallaro U, Nielsen and Soria (1995) *Eur. J. Biochem.* 232, 165–171]. Here we report that SAP-C bound to alpha2MR equally well as native saporin. However, the same isoform had about ten times lower cytotoxicity than the other isoforms towards different cell lines. This indicates that the lower cell-killing ability of the SAP-C isoform is due to its altered interaction with the protein synthesis machinery of target cells. Since saporin binding to alpha2MR is competed by heparin, we also tested in cell-killing experiments Chinese hamster ovary cell lines defective in the expression of either heparan sulphates or proteoglycans. No differences were observed in cytotoxicity using saporin or the recombinant isoforms. Therefore saporin binding to the cell surface should not be mediated by proteoglycans, as is the case for other alpha2MR ligands.

FULL TEXT

The Full Text of this article is available as a PDF (498K).

SELECTED REFERENCES

This list contains those references that cite another article in PMC or have a citation in PubMed. It may not include all the original references.

- Stirpe F, Barbieri L, Battelli MG, Soria M, Lappi DA. Ribosome-inactivating proteins from plants: present status and future perspectives. *Biotechnology (N Y)*. 1992 Apr;10(4):405–412. [PubMed]
- Lappi DA, Ying W, Barthelemy I, Martineau D, Prieto I, Benatti L, Soria M, Baird A. Expression and activities of a recombinant fibroblast growth factor-saporin fusion protein. *J Biol Chem*. 1994 Apr 29;269(17):12552–12558. [PubMed]
- Falini B, Bolognesi A, Flenghi L, Tazzari PL, Broe MK, Stein H, Dürkop H, Aversa F, Corneli P, Pizzolo G, et al. Response to Hodgkin's disease to monoclonal anti-CD30 immunotoxin. *Lancet*. 1992 May 16;339(8803):1195–1196. [PubMed]
- Casscells W, Lappi DA, Olwin BB, Wai C, Siegman M, Speir EH, Sasse J, Baird A. Elimination of smooth muscle cells in experimental restenosis: targeting of fibroblast growth factor receptors. *Proc Natl Acad Sci U S A*. 1992 Aug 1;89(15):7159–7163. [PubMed]
- Cavallaro U, del Vecchio A, Lappi DA, Soria MR. A conjugate between human urokinase and saporin, a type-I ribosome-inactivating protein, is selectively cytotoxic to urokinase receptor-expressing cells. *J Biol Chem*. 1993 Nov 5;268(31):23186–23190. [PubMed]
- McGrath MS, Hwang KM, Caldwell SE, Gaston I, Luk KC, Wu P, Ng VL, Crowe S, Daniels J, Marsh J, et al. GLQ223: an HIV-1 immunodeficiency virus replication in acutely and chronically infected cells of lymphocyte and mononuclear phagocyte lineage. *Proc Natl Acad Sci U S A*. 1989 Apr;86(8):2844–2848. [PubMed]
- Lodge JK, Kaniewski WK, Tumer NE. Broad-spectrum virus resistance in transgenic plants expressing pokeweed antiviral protein. *Proc Natl Acad Sci U S A*. 1992 Apr 15;89(8):4000–4004. [PubMed]

Proc Natl Acad Sci U S A. 1993 Aug 1;90(15):7089–7093. [PubMed]

- Taylor S, Massiah A, Lomonosoff G, Roberts LM, Lord JM, Hartley M. Correlation between the activities of five ribosome-proteins in depurination of tobacco ribosomes and inhibition of tobacco mosaic virus infection. *Plant J*. 1994 Jun;5(6):827–8. [PubMed]
- Barra D, Maras B, Schininà ME, Angelaccio S, Bossa F. Assessment of sequence features in internal regions of proteins. *Biotechnol Appl Biochem*. 1991 Feb;13(1):48–53. [PubMed]
- Barthelemy I, Martineau D, Ong M, Matsunami R, Ling N, Benatti L, Cavallaro U, Soria M, Lappi DA. The expression of a ribosome-inactivating protein from the plant *Saponaria officinalis*, in *Escherichia coli*. *J Biol Chem*. 1993 Mar 25;268(9):654 [PubMed]
- Benatti L, Saccardo MB, Dani M, Nitti G, Sassano M, Lorenzetti R, Lappi DA, Soria M. Nucleotide sequence of cDNA coding for a type-1 ribosome-inactivating protein from *Saponaria officinalis*. *Eur J Biochem*. 1989 Aug 1;183(2):465–470. [PubMed]
- Benatti L, Nitti G, Solinas M, Valsasina B, Vitale A, Ceriotti A, Soria MR. A Saporin-6 cDNA containing a precursor sequence with a carboxyl-terminal extension. *FEBS Lett*. 1991 Oct 21;291(2):285–288. [PubMed]
- Hartley MR, Legname G, Osborn R, Chen Z, Lord JM. Single-chain ribosome inactivating proteins from plants depurinate *Escherichia coli* 23S ribosomal RNA. *FEBS Lett*. 1991 Sep 23;290(1-2):65–68. [PubMed]
- Legname G, Gromo G, Lord JM, Monzini N, Modena D. Expression and activity of pre-dianthin 30 and dianthin 30. *Biochem Biophys Res Commun*. 1993 May 14;192(3):1230–1237. [PubMed]
- Habuka N, Murakami Y, Noma M, Kudo T, Horikoshi K. Amino acid sequence of Mirabilis antiviral protein, total synthesis and expression in *Escherichia coli*. *J Biol Chem*. 1989 Apr 25;264(12):6629–6637. [PubMed]
- Chaddock JA, Lord JM, Hartley MR, Roberts LM. Pokeweed antiviral protein (PAP) mutations which permit *E. coli* growth and catalytic activity towards prokaryotic ribosomes. *Nucleic Acids Res*. 1994 May 11;22(9):1536–1540. [PubMed]
- Legname G, Fossati G, Monzini N, Gromo G, Marcucci F, Mascagni P, Modena D. Heterologous expression, purification, and conformational studies of different forms of dianthin 30. *Biomed Pept Proteins Nucleic Acids*. 1995;1(2):61–68. [PubMed]
- Edgell CJ, McDonald CC, Graham JB. Permanent cell line expressing human factor VIII-related antigen established by hybridoma technology. *Proc Natl Acad Sci U S A*. 1983 Jun;80(12):3734–3737. [PubMed]
- Esko JD, Stewart TE, Taylor WH. Animal cell mutants defective in glycosaminoglycan biosynthesis. *Proc Natl Acad Sci U S A*. 1985 May;82(10):3197–3201. [PubMed]
- Esko JD, Rostand KS, Weinke JL. Tumor formation dependent on proteoglycan biosynthesis. *Science*. 1988 Aug 26;241(4866):101–103. [PubMed]
- Feng DF, Doolittle RF. Progressive sequence alignment as a prerequisite to correct phylogenetic trees. *J Mol Evol*. 1987;25(4):41–50. [PubMed]
- Bernstein FC, Koetzle TF, Williams GJ, Meyer EF Jr, Brice MD, Rodgers JR, Kennard O, Shimanouchi T, Tasumi M. The Protein Data Bank: a computer-based archival file for macromolecular structures. *J Mol Biol*. 1977 May 25;112(3):535–542. [PubMed]
- Sutcliffe MJ, Haneef I, Carney D, Blundell TL. Knowledge based modelling of homologous proteins. Part I: Three-dimensional structure derived from the simultaneous superposition of multiple structures. *Protein Eng*. 1987 1(5):377–384. Oct–Nov. [PubMed]
- Ready MP, Katzin BJ, Robertus JD. Ribosome-inhibiting proteins, retroviral reverse transcriptases, and RNase H share common elements. *Proteins*. 1988;3(1):53–59. [PubMed]
- Lappi DA, Esch FS, Barbieri L, Stirpe F, Soria M. Characterization of a *Saponaria officinalis* seed ribosome-inactivating protein: immunoreactivity and sequence homologies. *Biochem Biophys Res Commun*. 1985 Jun 28;129(3):934–942. [PubMed]
- Lord JM, Roberts LM, Robertus JD. Ricin: structure, mode of action, and some current applications. *FASEB J*. 1994 Feb;8(2):1–10. [PubMed]
- Cavallaro U, Nykjaer A, Nielsen M, Soria MR. Alpha 2-macroglobulin receptor mediates binding and cytotoxicity of plant ribosome-inactivating proteins. *Eur J Biochem*. 1995 Aug 15;232(1):165–171. [PubMed]
- Moestrup SK. The alpha 2-macroglobulin receptor and epithelial glycoprotein-330: two giant receptors mediating endocytosis of ligands. *Biochim Biophys Acta*. 1994 Jun 29;1197(2):197–213. [PubMed]
- Reisbig RR, Bruland O. Dianthin 30 and 32 from *Dianthus caryophyllus*: two inhibitors of plant protein synthesis and their toxicity. *Arch Biochem Biophys*. 1983 Jul 15;224(2):700–706. [PubMed]
- Ferreras JM, Barbieri L, Girbés T, Battelli MG, Rojo MA, Arias FJ, Rocher MA, Soriano F, Mendez E, Stirpe F. Distribution of major ribosome-inactivating proteins (28 S rRNA N-glycosidases) of the plant *Saponaria officinalis* L. (Caryophyllaceae). *Biochim Biophys Acta*. 1993 Oct 19;1216(1):31–42. [PubMed]
- Houston LL, Ramakrishnan S, Hermodson MA. Seasonal variations in different forms of pokeweed antiviral protein, a potent ribosome inactivator. *J Biol Chem*. 1983 Aug 25;258(16):9601–9604. [PubMed]
- Taylor BE, Irvin JD. Depurination of plant ribosomes by pokeweed antiviral protein. *FEBS Lett*. 1990 Oct 29;273(1-2):144–148. [PubMed]
- Prestle J, Schönfelder M, Adam G, Mundry KW. Type I ribosome-inactivating proteins depurinate plant 25S rRNA without loss of specificity. *Nucleic Acids Res*. 1992 Jun 25;20(12):3179–3182. [PubMed]
- Fabbrini MS, Valsasina B, Nitti G, Benatti L, Vitale A. The signal peptide of human preproendothelin-1. *FEBS Lett*. 1991 Jul 29;286(1-2):91–94. [PubMed]
- Machamer CE, Rose JK. Influence of new glycosylation sites on expression of the vesicular stomatitis virus G protein at the plasma membrane. *J Biol Chem*. 1988 Apr 25;263(12):5948–5954. [PubMed]
- Fordham-Skelton AP, Taylor PN, Hartley MR, Croy RR. Characterisation of saporin genes: in vitro expression and ribosome inactivation. *Mol Gen Genet*. 1991 Oct;229(3):460–466. [PubMed]
- Montfort W, Villafranca JE, Monzingo AF, Ernst SR, Katzin B, Rutenber E, Xuong NH, Hamlin R, Robertus JD. The three-dimensional structure of ricin at 2.8 Å. *J Biol Chem*. 1987 Apr 15;262(11):5398–5403. [PubMed]
- Munishkin A, Wool IG. Systematic deletion analysis of ricin A-chain function. Single amino acid deletions. *J Biol Chem*. 1995 Dec 22;270(51):30581–30587. [PubMed]

- Monzingo AF, Collins EJ, Ernst SR, Irvin JD, Robertus JD. The 2.5 Å structure of pokeweed antiviral protein. *J Mol Biol.* 1993 Oct 20;233(4):705-715. [PubMed]
- Hung CH, Lee MC, Chen JK, Lin JY. Cloning and expression of three abrin A-chains and their mutants derived by site-specific mutagenesis in *Escherichia coli*. *Eur J Biochem.* 1994 Jan 15;219(1-2):83-87. [PubMed]
- Chaddock JA, Monzingo AF, Robertus JD, Lord JM, Roberts LM. Major structural differences between pokeweed antiviral protein A-chain do not account for their differing ribosome specificity. *Eur J Biochem.* 1996 Jan 15;235(1-2):159-166. [PubMed]
- Bravi G, Legname G, Chan AW. Substrate recognition by ribosome-inactivating protein studied by molecular modeling and electrostatic potentials. *J Mol Graph.* 1995 Apr;13(2):83-8-109. [PubMed]
- Bandziulis RJ, Swanson MS, Dreyfuss G. RNA-binding proteins as developmental regulators. *Genes Dev.* 1989 Apr;3(4):431-441.
- Oubridge C, Ito N, Evans PR, Teo CH, Nagai K. Crystal structure at 1.92 Å resolution of the RNA-binding domain of the U1 protein complexed with an RNA hairpin. *Nature.* 1994 Dec 1;372(6505):432-438. [PubMed]
- Query CC, Bentley RC, Keene JD. A common RNA recognition motif identified within a defined U1 RNA binding domain of a small nuclear ribonucleoprotein. *Cell.* 1989 Apr 7;57(1):89-101. [PubMed]
- Mikhailenko I, Kounnas MZ, Strickland DK. Low density lipoprotein receptor-related protein/alpha 2-macroglobulin receptor-mediated cellular internalization and degradation of thrombospondin: A process facilitated by cell-surface proteoglycans. *J Biol Chem.* 1995 Apr 21;270(16):9543-9549. [PubMed]
- Nykjaer A, Nielsen M, Lookene A, Meyer N, Roigaard H, Ertter M, Beisiegel U, Olivecrona G, Gliemann J. A carboxyl-terminal domain of lipoprotein lipase binds to the low density lipoprotein receptor-related protein and inhibits lipase-mediated uptake of lipoproteins. *J Biol Chem.* 1994 Dec 16;269(50):31747-31755. [PubMed]

Cloning and Expression of Recombinant, Functional Ricin B Chain

Ming-Shi Chang, David W. Russell, Jonathan W. Uhr, and Ellen S. Vitetta

PNAS 1987;84:5640-5644
doi:10.1073/pnas.84.16.5640

This information is current as of February 2007.

	This article has been cited by other articles: www.pnas.org#otherarticles
E-mail Alerts	Receive free email alerts when new articles cite this article - sign up in the box at the top right corner of the article or click here.
Rights & Permissions	To reproduce this article in part (figures, tables) or in entirety, see: www.pnas.org/misc/rightperm.shtml
Reprints	To order reprints, see: www.pnas.org/misc/reprints.shtml

Notes:

Cloning and expression of recombinant, functional ricin B chain

(toxin/immunotoxin/DNA/lectin)

MING-SHI CHANG^{*†}, DAVID W. RUSSELL[‡], JONATHAN W. UHR^{*†}, AND ELLEN S. VITETTA^{*†§}

^{*}Department of Microbiology, [†]Microbiology Graduate Program, and [‡]Department of Molecular Genetics, University of Texas Health Science Center, Southwestern Medical School, Dallas, TX 75235

Contributed by Jonathan W. Uhr, May 1, 1987

ABSTRACT The cDNA encoding the B chain of the plant toxin ricin has been cloned and expressed in monkey kidney COS-M6 cells. The recombinant B chain was detected by labeling the transfected cells with [³⁵S]methionine and [³⁵S]-cysteine and demonstrating the secretion of a protein with a *M_r* of 30,000–32,000 that was not present in the medium of mock-transfected COS-M6 cells. This protein was specifically immunoprecipitated by an anti-ricin or anti-B-chain antibody and the amount of recombinant B chain secreted by the COS-M6 cells was determined by a radioimmunoassay. Virtually all of the recombinant B chain formed active ricin when mixed with native A chain; it could also bind to the galactose-containing glycoprotein asialofetuin as effectively as native B chain. These results indicate that the vast majority of recombinant B chains secreted into the medium of the COS-M6 cells retain biological function.

Ricin is a potent toxin produced by beans of the plant *Ricinus communis*. The toxin consists of two disulfide-bonded subunits (A and B), each with a *M_r* of ≈32,000 (1–3). The B chain is a galactose-specific lectin that mediates binding of the toxin to a wide variety of cells (2–4). After binding and internalization of ricin, the A chain translocates across the membrane of an endocytic vesicle into the cytoplasm where it catalytically inactivates 60S ribosomal subunits (2–4) and thereby inhibits protein synthesis and causes cell death.

The A chain of ricin has been purified biochemically and conjugated to monoclonal antibodies reactive with normal and neoplastic cells using disulfide-containing crosslinkers (reviewed in refs. 5–7). Such conjugates or immunotoxins (ITs) have been used to kill cells, both *in vitro* and *in vivo* (8). Many A-chain-containing ITs (IT-As) are less potent than ricin-containing ITs (IT-Rs) (6, 7). There is evidence to suggest that this reduced toxicity is due to the absence of B chain, which has a second function—i.e., it can enhance the translocation of A chain into the cytosol where it exerts its cytotoxic effect (9, 10). The use of IT-Rs *in vivo* has been limited by their marked nonspecific toxicity. To provide the A-chain-enhancing function of B chain, IT-As have been used in the presence of free B chain (9, 10) or B-chain-containing ITs (IT-Bs) (11, 12). Both approaches enhance the specific toxicity of IT-As *in vitro* and free B chains can also enhance specific killing by IT-As *in vivo* (13). With regard to IT-Bs, some lectin activity remains that could lead to nonspecific interactions *in vivo*. Recent data (14, 15) indicate that lectin activity may not be essential for the A-chain-enhancing function of B chain but other data argue against this conclusion (6, 9). A definitive answer to whether or not the galactose-binding sites on the B chain play a role in A-chain-enhancing function requires deleting the galactose-binding site on the B chain prior to preparing and testing a IT-B. To this end, we have cloned and expressed a functional ricin

B-chain cDNA to carry out site-specific mutagenesis of the galactose-binding site. Our results indicate that recombinant B chain can be expressed in small amounts in monkey COS-M6 cells and that the B chain has A-chain-enhancing function and lectin activity.

MATERIALS AND METHODS

cDNA Cloning. Castor bean seeds were obtained from a local source. Total RNA was isolated from the endosperm of maturing seeds by homogenizing in 4 M guanidinium thiocyanate; this was followed by sedimentation through 5.7 M CsCl. Poly(A)⁺ mRNA was purified by chromatography on oligo(dT)-cellulose (16). Two micrograms of this mRNA was employed as a template in cDNA cloning procedures described by Okayama and Berg (17). Double-stranded cDNAs were used to transform *Escherichia coli* K-12 (strain HB101), and ≈3 × 10⁵ independent transformants were obtained from the starting mRNA. To identify ricin cDNA clones, 3 × 10⁴ colonies were plated on nitrocellulose filters and screened with a mixture of oligonucleotides 20 bases in length representing all possible mRNA sequences encoding amino acids 495–501 (Trp-Met-Phe-Lys-Asn-Asp-Gly). This protein sequence corresponds to the COOH terminus of the B chain (2). Colonies hybridizing to this probe were then rescreened with a unique probe (AGGATCCATACAAAC-ATCAGC) corresponding to amino acids 280–287 at the NH₂ terminus of the B chain, as derived from the DNA sequence of a ricin cDNA (18). Colonies hybridizing to both probes were characterized by restriction enzyme mapping and DNA sequencing. Both ricin and agglutinin were identified by these methods. A ricin cDNA clone encoding the complete B chain and part of the A chain was used in the subsequent genetic engineering of the plasmid.

Construction of Ricin B-Chain Expression Vector. A plasmid containing an insert capable of expressing the ricin B chain in mammalian cells was constructed using standard techniques (16). Briefly, a synthetic DNA fragment of 82 base pairs (bp) containing an *Xba* I site at the 5' end and a *Bam*HI site at the 3' end and encoding a 21 amino acid signal sequence for the low density lipoprotein receptor (LDLR) (19) and 5 amino acids of the NH₂ terminus of the B chain was synthesized as two complementary oligonucleotides. One microgram each of the oligonucleotides was hybridized in 30 μl of 10 mM Tris-HCl, pH 8.0/1 mM EDTA/300 mM NaOAc for 16 hr at 42°C. The resulting double-stranded DNA was phosphorylated at the 5' end using an excess of ATP and T4 polynucleotide kinase. A cDNA fragment encoding amino

The publication costs of this article were defrayed in part by page charge payment. This article must therefore be hereby marked "advertisement" in accordance with 18 U.S.C. §1734 solely to indicate this fact.

Abbreviations: IT, immunotoxin; IT-A, ricin A-chain-containing IT; ASF, asialofetuin; IT-B, ricin B-chain-containing IT; GAMlg, goat anti-mouse Ig; GARlg, goat anti-rabbit Ig; LDLR, low density lipoprotein receptor; OVA, ovalbumin; RAB, rabbit anti-ricin B-chain antibody; RAR, rabbit anti-ricin antibody; RAOVA, rabbit anti-ovalbumin antibody; IT-Rs, ricin-containing ITs; mAb-anti-A, monoclonal antibody anti-ricin A chain; SV40, simian virus 40.

[§]To whom reprint requests should be addressed.

acids 285–541 of the ricin B chain and 250 bp of 3' untranslated sequence was excised from a ricin cDNA clone by a complete *Pvu* II digestion and partial *Bam*HI digestion. Equimolar amounts of the 82-bp and the 1021-bp cDNA fragments were then ligated with an equimolar amount of a derivative of the pCD-X expression vector (20). This vector contains a simian virus 40 (SV40) early region promoter and the SV40 late region transcription termination and poly(A) sites. The desired expression vector (pES-B, Fig. 1) containing both the synthetic DNA encoding the signal sequence and the ricin B-chain cDNA fragment in the proper orientation was selected by colony hybridization after transformation of *E. coli* HB101. The plasmid was further characterized by restriction mapping and DNA sequencing of the cloning junctions.

Cell Growth and Transfection. COS-M6 cells (21, 22) were provided by Tim Osborne of this institution. Cells were grown in high-glucose (4 g/liter) Dulbecco's modified Eagle's medium (DMEM) containing 10% fetal calf serum, penicillin, streptomycin, and L-glutamine. Transfection of COS-M6 cells was carried out using a DEAE-dextran-chloroquine procedure (23). Briefly, COS-M6 cells at 3×10^5 cells per ml were transfected with 5 μ g of plasmid DNA per ml. Following transfection, cells were washed with Tris-buffered saline (TBS; pH 7.4) and incubated in DMEM for 40 hr, after which the medium was replaced with fresh, cysteine-free and methionine-free DMEM containing 0.1 M galactose and 1 g of glucose per liter. [35 S]Cysteine and [35 S]methionine were then added to the medium at a specific activity of 400 μ Ci/ml (1 Ci = 37 GBq). After 8 hr, the medium was collected and assayed for the presence of B chain as described below. Medium used for the analysis of lectin activity and toxicity of reconstituted ricin contained unlabeled cysteine (48 mg/liter) and methionine (30 mg/liter).

Immunoprecipitation. Immunoprecipitation was carried out with rabbit anti-ricin (RAR), rabbit anti-ricin B chain (RAB), or rabbit anti-ovalbumin (RAOVA) antibodies complexed to goat anti-rabbit Ig (GARIG) (immunocomplexes) (24). The RAR was raised against boiled ricin and recognizes both native and denatured A and B chains (14). In radioimmunoassays (RIA) it is about 2-fold more active against denatured than native B chain. One hundred microliters of the immune complex suspension was added to 500 μ l of COS-M6 medium and incubated by continuous rotation for 1 hr at 4°C. Immunocomplexes were sedimented through sucrose gradients (24). The resulting pellet was washed in 0.5 ml of phosphate-buffered saline (PBS), dissolved in 40 μ l of sample buffer (125 mM Tris-HCl, pH 6.8/2.5% NaDodSO₄/5% 2-mercaptoethanol), and analyzed by NaDodSO₄/PAGE (25).

Detection of B Chain by RIA. Media from mock-transfected or transfected COS-M6 cells were concentrated 10- to 20-fold by centrifugation through an Amicon Centricon 10 micro-concentrator. The molar concentration of B chain was then determined by RIA as described (26). A standard curve was constructed using the values obtained with the native B chain and the concentration of recombinant B chain was determined from this curve. The assay could detect 0.01 nM B chain.

Lectin Activity Analysis. The lectin activity of secreted recombinant B chain in the medium of the COS-M6 cells was determined by a RIA (14). Briefly, wells of microtiter plates were coated with asialofetuin (ASF), a galactose-rich glycoprotein. Native B chain (in PBS or in medium from mock-transfected COS-M6 cells), medium from pES-B-transfected cells, or medium from mock-transfected cells was added to the plates and binding was subsequently detected with [125 I]-labeled RAR. Negative controls included ovalbumin (OVA; a protein with no lectin activity) or PBS. The assay could detect 0.01 nM B chain.

Ricin Formation. The ability of recombinant or native ricin B chain and native A chain to reform toxic ricin was evaluated in two ways. (i) One milliliter of 35 S-labeled media was dialyzed against PBS/2-mercaptoethanol. This was mixed with 1 μ g (0.03 μ M) of unlabeled, reduced native A chain. Controls included medium alone, native 125 I-labeled B chain alone, and native 125 I-labeled B chain mixed with native A chain. The mixture was dialyzed at 37°C for 16 hr. Following incubation, the mixture was immunoprecipitated with monoclonal antibody anti-ricin A-chain (mAb-anti-A)-goat anti-mouse Ig (GARIG) immunocomplexes as described above. The washed immune complexes were dissolved in sample buffer without reducing agent and analyzed by NaDodSO₄/PAGE (25). (ii) Concentrated media from unlabeled COS-M6 cells were dialyzed for 16 hr against PBS at 4°C to remove galactose. Fifty microliters of this medium containing no B chain (mock-transfected COS-M6 cells) or 0.3 nM recombinant B chain (transfected COS-M6 cells) was mixed with 1 μ g of A chain per ml (0.03 μ M) for 1 hr at 37°C. Native B chain at concentrations of 0.01–1 nM was used as a positive control. Additional negative controls included A chain alone, native B chain alone, medium from transfected cells alone (recombinant B chain), or medium from mock-transfected cells plus native A chain. Daudi cells (10^5) in 100 μ l were then added and cultured for 40 hr. After this time, cells were labeled with [3 H]leucine for 4 hr. Incorporation of [3 H]leucine into protein was determined by harvesting the cells on a multiple automated harvester and counting the radioactivity in a liquid scintillation spectrometer. The assay could detect 1 pM B chain.

RESULTS

Rationale for the Construction of a Ricin B-Chain Expression Vector. In the endosperm of castor bean seeds, the ricin B-chain gene is normally expressed as part of a prepro-ricin precursor containing a signal sequence (24 amino acids) and a 12 amino acid linker between the A and B chains (18). The prepro-ricin molecule is processed posttranslationally to yield an A chain that is disulfide bonded to B chain. The ricin B chain itself has four intrachain disulfide bonds and two glycosylation sites (2). In the absence of galactose, it undergoes conformational changes resulting in gradual loss of lectin activity, which is accelerated at 37°C (E. Wawrzyn-czak, P. E. Thorpe, and E.S.V., unpublished results). Our aim was to construct an expression vector that would yield a B chain with optimal tertiary structure and intrachain disulfide bonds. To this end, a signal sequence was ligated 5' to the coding sequence of the B chain to facilitate processing, glycosylation, and secretion of soluble B chain (Fig. 1). Although the ricin cDNA contains a signal sequence (18), it was not clear whether this sequence would be recognized by the appropriate enzymes in the COS-M6 cells. Since LDLRs have been successfully expressed in COS-M6 cells (19) and the NH₂-terminal amino acid of the LDLR is the same as that of the ricin B chain (alanine), it was postulated that the COS-M6 cells would effectively cleave the signal sequence. We also included galactose in the COS-M6 cell medium during expression to preserve the lectin function of the B chain at 37°C and prevent it from binding back to the COS-M6 cells.

Detection of Ricin B Chain in the Medium of COS-M6 Cells. To analyze proteins secreted into the medium by pES-B-transfected and mock-transfected COS-M6 cells, we labeled cells with [35 S]methionine and [35 S]cysteine and then precipitated media with 10% trichloroacetic acid. The trichloroacetic acid precipitates were dissolved, reduced, and electrophoresed on NaDodSO₄/polyacrylamide gels. As shown in Fig. 2, lane B, mock-transfected COS-M6 cells secreted a variety of proteins ranging in M_r from 12,000 to 200,000. As

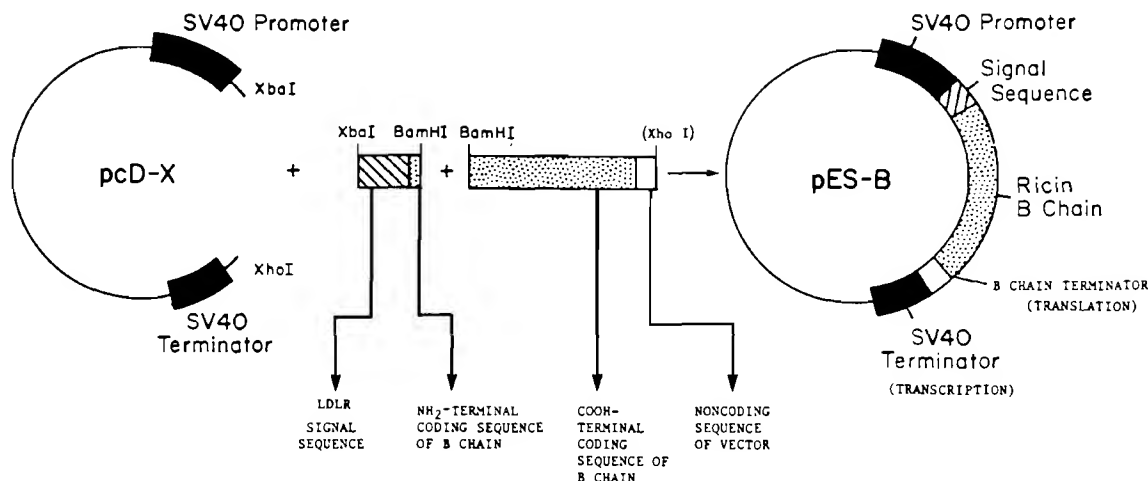


FIG. 1. Construction of the ricin B-chain expression vector. An expression vector containing B chain DNA was assembled by means of a three-fragment ligation. The vector backbone was a derivative of PCD-X (21) containing an *Xba*I site at the 3' end of the SV40 early region promoter. An 82-bp fragment encoding the 21 amino acids of LDLR signal sequence (20) and the first five residues of the ricin B chain was synthesized as two oligonucleotides on an Applied Biosystems model 380A DNA synthesizer. The nucleotides were hybridized and then phosphorylated at their 5' ends with ATP and T4 polynucleotide kinase. A third DNA fragment encoding the remaining 267 amino acids of the ricin B chain was isolated from a ricin cDNA plasmid. These three DNA fragments were mixed in an equimolar ratio and ligated with T4 DNA ligase. After transformation into *E. coli* HB101, the desired expression vector was identified by colony hybridization and characterized extensively by restriction endonuclease mapping and DNA sequencing.

seen in lane C, a similar array of proteins was secreted by the transfected cells, but, in addition, there was a protein of $\approx 30,000\text{--}32,000 M_r$ that was not present in lane B.

Immunoprecipitation of COS-M6 Cell Medium. To determine whether the M_r 30,000–32,000 molecule secreted by the pES-B-transfected COS-M6 cells was ricin B chain, media from transfected and mock-transfected COS-M6 cells were treated with immunocomplexes containing antibodies directed against ricin, ricin B chain, and OVA (control). Approximately 3–5% of the acid-precipitable radioactivity in the medium of the pES-B transfected COS-M6 cells was specifically immunoprecipitated by RAR or RAB (data not shown)

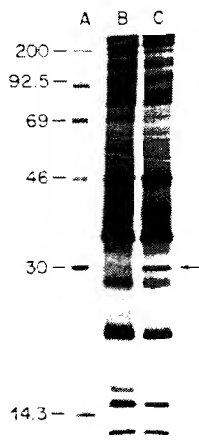


FIG. 2. Trichloroacetic acid-precipitable ^{35}S -labeled proteins released into the medium of COS-M6 cells. Media from the mock-transfected or pES-B-transfected cells were precipitated with 10% trichloroacetic acid. Precipitates were dissolved, reduced, and electrophoresed on 12% NaDodSO₄ slab gels. The gels were fluorographed in Enhancer solution (DuPont, New England Nuclear) and dried. Lanes: A, size markers (shown as $M_r \times 10^{-3}$); B, medium from mock-transfected cells; C, medium from pES-B-transfected cells. The position of the B chain is noted by the arrow.

antibodies. Immunoprecipitates were washed, dissolved, and electrophoresed in 12% NaDodSO₄/polyacrylamide gels. As shown in Fig. 3, only the native B chain (lane F) and the 30,000–32,000 M_r protein from the transfected cells (lane E) were specifically precipitated. No proteins were immunoprecipitated with the anti-OVA immunocomplexes (lanes B and C) nor were any proteins recognized by the anti-ricin antibodies in the media of mock-transfected cells (lane D). These



FIG. 3. Immunoprecipitation of the medium of pES-B-transfected COS-M6 cells. Immunocomplexes consisting of RAOVA and GAR1g or RAR and GAR1g were added to 500 μl of medium or 20 ng (0.6 nM) of ^{125}I -labeled B chain. All samples were immunoprecipitated in 0.1 M galactose. The immunoprecipitates were washed, dissolved, and electrophoresed on 12% NaDodSO₄ slab gels. The bands were visualized by fluorography. Lanes: A, size markers (shown as $M_r \times 10^{-3}$); B and C, RAOVA immunoprecipitates of medium from mock-transfected (lane B) and pES-B-transfected (lane C) cells; D and E, RAR immunoprecipitates of medium from mock-transfected (lane D) and pES-B-transfected (lane E) cells; F, ^{125}I -labeled native B chain. Similar results were obtained using RAB instead of RAR (data not shown).

results indicate that the 30,000–32,000 M_r protein secreted by the pES-B-transfected cells has the antigenicity of ricin B chain. The slower mobility of this protein under reducing conditions versus nonreducing conditions (data not shown) indicates that the secreted protein has intrachain disulfide bonds. As determined by RIA, the amount of B chain in the medium before concentration was 0.03–0.5 nM and, hence, is lower by a factor of about 10 than most proteins secreted by transfected COS-M6 cells (27). In the immunoprecipitates, the molecular weight of recombinant B chain was slightly larger than that of native B chain, which may be due to glycosylation differences when synthesized in plant versus mammalian COS-M6 cells or by the failure of the COS-M6 cells to cleave the entire signal sequence at the 5' end of the B-chain coding sequence.

Reconstitution of Recombinant B Chain with Native A Chain. To test the ability of recombinant B chain to form active ricin when mixed with native A chain (28–31), reduced A chain (or controls; see *Materials and Methods*) was mixed with reduced medium from ^{35}S -labeled, pES-B-transfected COS-M6 cells and dialyzed for 16 hr at 37°C against PBS in the presence of 0.1 M galactose. The medium was precipitated with immunocomplexes containing mAb-anti-A (32) (which does not react with native or denatured B chain). Washed immunoprecipitates were analyzed under nonreducing conditions by NaDodSO₄/PAGE. As shown in Fig. 4, a molecule containing A and B chains with a molecular weight similar to that of ricin was observed only in those samples containing mixtures of medium from ^{35}S -labeled, pES-B-transfected cells and native A chain (lane C) or ^{125}I -labeled native B chain and native A chain (lane E). These data indicate that the recombinant B chain forms a covalent heterodimer with the native A chain.

To determine whether the recombinant B-chain-native A heterodimer was toxic to cells, medium from unlabeled, pES-B-transfected COS-M6 cells (containing a known concentration of B chain as determined by RIA) was mixed with native A chain and tested for its toxicity to Daudi cells. The positive and negative controls are described in *Materials and Methods*. In a representative experiment shown in Table 1, medium containing 0.3 nM recombinant B chain effectively reconstituted the toxic activity of ricin when mixed with native A chain. In comparing this toxicity with that of native B chain mixed with the same concentration of native A chain, the concentration of recombinant B chain forming ricin was estimated to be ≈ 0.4 nM, which was similar to the concentration of B chain in the medium as determined by RIA. This



FIG. 4. Reconstitution of ricin heterodimers from native A chain and ^{35}S -labeled medium of pES-B-transfected COS-M6 cells. One microgram (0.03 μM) of native, reduced, unlabeled ricin A chain was mixed with the reduced medium and dialyzed against PBS for 16 hr at 37°C. Immunocomplexes (100 μl) consisting of mAb-anti-A and GAMlg (lanes B–F) were added to the mixture. The immunoprecipitates were washed, dissolved, and electrophoresed on 12% NaDodSO₄ slab gels. Bands were visualized by fluorography. Lanes: A, size markers (shown as $M_r \times 10^{-3}$); B, 1 ml of medium from ^{35}S -labeled mock-transfected cells incubated with 1 μg of unlabeled native A chain; C, 1 ml of medium from pES-B-transfected cells incubated with unlabeled native A chain; D, 1 ml of medium from pES-B-transfected cells incubated alone; E, native ^{125}I -labeled ricin B chain incubated with unlabeled native A chain; F, native ^{125}I -labeled ricin B chain incubated alone.

Table 1. Toxicity of ricin formed by recombinant B chain and native A chain

Addition to Daudi cells	B chain, nM	% of control protein synthesis*
None	0	—
Native B chain	5	99
A chain	0	100
+ mock-transfected medium	0	100
+ transfected medium	0.3†	13
+ native B chain	0.5	16
+ native B chain	1	0.7

Aliquots of concentrated media were mixed with native A chain (1 $\mu\text{g}/\text{ml}$ or 0.03 μM) in 96-well microtiter cell culture plates at 37°C for 1 hr; this was followed by addition of Daudi cells. Cells were incubated for 40 hr at 37°C in a CO₂ incubator. The ability of recombinant B chain in medium from pES-B-transfected cells to reform ricin with native A chain and kill Daudi cells was measured by [³H]leucine incorporation. A representative experiment (one of six) is shown. The native B chain used in this experiment has an IC₅₀ of >0.1 μM when cultured for 40 hr with Daudi cells.

*No addition = 320,722 \pm 3720 cpm per 10⁵ cells.

†As determined by RIA.

observation suggests that virtually all of the recombinant B chain could form heterodimers with native ricin A chain and these heterodimers were as toxic to cells as those formed with the two native polypeptides. This finding suggests that the recombinant B chain has both lectin and potentiating activity for the A chain.

Analysis of the Lectin Activity of Recombinant B Chain. Native B chain binds to galactose-containing glycoproteins and glycolipids. To test the ability of recombinant B chain to bind to the galactose-containing protein ASF, a RIA was utilized as described in *Materials and Methods*. As shown in Table 2, medium containing 5 nM recombinant B chain bound to the galactose-containing ASF and this binding was inhibitable by 0.1 M galactose. The addition of medium from mock-transfected cells to native B chain reduced its binding to ASF by 36%, presumably due to the complexing of native B chain with secreted proteins in the medium of the COS-M6 cells. Thus, in comparing the concentration of the B chain in the medium of the transfected cells to native B chain that

Table 2. Lectin activity of ricin B chain in the medium of pES-B-transfected COS-M6 cells

Sample	B chain, nM	cpm	
		No galactose	0.1 M galactose
OVA (5 nM)	0	0	ND
Mock-transfected medium	0	0	ND
Transfected medium	5*	1606	0
Native B chain	5	2445	0
+ mock-transfected medium	5	1554	0

Microtiter plates (96-well) were coated with 10 μg of ASF and washed five times in distilled H₂O. The concentrated media were added to ASF-coated plates and incubated for 2 hr at room temperature. The amount of ricin B chain bound to ASF was detected by adding ^{125}I -labeled RAR to the wells. The effect of galactose on binding to ASF was measured by adding 0.1 M galactose to the medium or native B chain during the 2-hr incubation period with ASF. This is one experiment of two performed. The cpm in the PBS control (270 cpm) have been subtracted from all values. ND, not determined.

*As determined by RIA. The concentrations of B chain were determined from the linear portion of the standard curve (limit of detection, 0.01 nM).

bound to the ASF substrate in the presence of medium from mock-transfected cells (Table 2), all of the recombinant B-chain molecules appear to have lectin activity.

DISCUSSION

In the present study, we have described the cloning and expression of ricin B chain in a transient expression system—i.e., monkey COS-M6 cells. The recombinant B chain reacts with antibody to ricin B chain, retains lectin activity, and can dimerize with A chain to form toxic ricin. By quantifying the amount of recombinant B chain in the medium of the transfected cells by a sensitive RIA and by constructing dose-response curves for the functional studies in question, it was possible to determine quantitatively the retention of biological activity of the recombinant B chain. The results suggest that the B chain has full biological activity, although it was expressed at low levels (0.1 nM) compared to other proteins expressed in this cell line. These low levels could be due to binding of the B chain to intracellular or cell-surface glycoproteins or glycolipids during transport and secretion, toxicity to the cells, degradation by secreted proteases, or improper posttranslational processing.

Recent studies (14, 15) indicate that the ability of the B chain to potentiate the toxicity of a IT-A is retained when it is targeted to cells as a IT-B, even when the lectin activity is destroyed by chemical modification. Hence, it would be desirable to produce a IT-B (to be used in conjunction with a IT-A) in which the galactose-binding sites of the B chain have been selectively eliminated. The development of a system for expressing recombinant B chain with both A-chain-enhancing function and lectin activity makes this approach possible. Moreover, the amino acids in the galactose-binding sites of the B chain have been identified by x-ray crystallography (33). If a lectin-deficient ricin B chain with A-chain-potentiating activity could be generated, a IT-B prepared with this B chain could then be utilized in conjunction with a IT-A as a highly specific therapeutic agent.

We thank Dr. C. Geoff Davis for the COS-M6 cell transfection protocol, Ms. L. Trahan, Ms. N. Yen, Ms. R. Nisi, Ms. B. Smith, and Mr. Y. Chinn for technical assistance, and Ms. G. A. Cheek for secretarial assistance. We are grateful to Drs. P. E. Thorpe and R. J. Fulton for helpful comments concerning the manuscript. This work was supported by NIH Grants CA-28149, CA-41081, HL-20948 and a grant from the Robert A. Welch Foundation (I-0947).

- Olsnes, S. & Pihl, A. (1981) *Pharmacol. Ther.* **15**, 355–381.
- Olsnes, S. & Pihl, A. (1982) in *Molecular Action of Toxins and Viruses*, eds. Cohen, P. & van Heyningen, S. (Elsevier, New York), pp. 51–105.
- Olsnes, S., Saltvedt, E. & Pihl, A. (1974) *J. Biol. Chem.* **249**, 803–810.
- Olsnes, S. & Sandvig, K. (1983) in *Receptor-Mediated Endocytosis*, eds. Pastain, I. & Willingham, M. (Plenum, New York), pp. 189–236.
- Vitetta, E. S. & Uhr, J. W. (1985) *Annu. Rev. Immunol.* **3**, 197–212.
- Neville, D. M., Jr., & Youle, R. J. (1982) *Immunol. Rev.* **62**, 75–91.
- Thorpe, P. E. & Ross, W. C. J. (1982) *Immunol. Rev.* **62**, 119–158.
- Blakey, D. C., Wawrzynczak, E. J., Wallace, P. M. & Thorpe, P. E. (1987) *Progress in Allergy: Monoclonal Antibodies*, in press.
- Youle, R. J. & Neville, D. M., Jr. (1982) *J. Biol. Chem.* **257**, 1598–1601.
- McIntosh, D. P., Edwards, D. C., Cumber, A. J., Parnell, G. D., Dean, C. J., Ross, W. C. J. & Forrester, J. A. (1983) *FEBS Lett.* **164**, 17–20.
- Vitetta, E. S., Cushley, W. & Uhr, J. W. (1983) *Proc. Natl. Acad. Sci. USA* **80**, 6332–6335.
- Vitetta, E. S., Fulton, R. J. & Uhr, J. W. (1984) *J. Exp. Med.* **160**, 341–346.
- Eccles, S. A., McIntosh, D. P., Purvies, H. P., Cumber, A. J., Parnell, G. D., Forrester, J. A., Styles, J. M. & Dean, C. J. (1987) *Cancer Immunol. Immunother.* **24**, 37–41.
- Vitetta, E. S. (1986) *J. Immunol.* **136**, 1880–1887.
- Thorpe, P. E., Ross, W. C. J., Brown, A. N. F., Myers, C. D., Cumber, A. J., Foxwell, B. M. J. & Forrester, J. T. (1984) *Eur. J. Biochem.* **140**, 63–71.
- Maniatis, T., Fritsch, E. F. & Sambrook, J. (1982) *Molecular Cloning: A Laboratory Manual* (Cold Spring Harbor Laboratory, Cold Spring Harbor, NY), pp. 187–198.
- Okayama, H. & Berg, P. (1982) *Mol. Cell. Biol.* **2**, 161–170.
- Lamb, F. I., Roberts, L. M. & Lord, J. M. (1985) *Eur. J. Biochem.* **148**, 265–270.
- Yamamoto, T., Davis, C. G., Brown, M. S., Schneider, W. J., Casey, M. L., Goldstein, J. L. & Russell, D. W. (1984) *Cell* **39**, 27–38.
- Okayama, H. & Berg, P. (1983) *Mol. Cell. Biol.* **3**, 280–289.
- Gluzman, Y. (1981) *Cell* **23**, 175–182.
- Horowitz, M., Cepko, C. L. & Sharp, P. A. (1983) *J. Mol. Appl. Genet.* **2**, 147–159.
- Gorman, C. (1985) in *DNA Cloning*, ed. Glover, D. M. (IRI, Oxford), pp. 143–190.
- Tolleshang, H., Goldstein, J. L., Schneider, W. & Brown, M. S. (1982) *Cell* **30**, 715–724.
- Laemmli, U. K. (1970) *Nature (London)* **227**, 680–685.
- Vitetta, E. S., Krolick, K. A. & Uhr, J. W. (1982) *Immunol. Rev.* **62**, 159–183.
- McCracken, A. A. & Fishman, N. F. (1986) *J. Biol. Chem.* **261**, 508–511.
- Lappi, D. A., Kapmeyer, W., Beylaur, J. M. & Kaplan, N. O. (1978) *Proc. Natl. Acad. Sci. USA* **75**, 1096–1100.
- Houston, L. L. (1982) *J. Biol. Chem.* **257**, 1532–1537.
- Cushley, W., Muirhead, M. J., Silva, F., Greathouse, J., Tucker, T., Uhr, J. W. & Vitetta, E. S. (1984) *Toxicol.* **22**, 265–277.
- Vitetta, E. S., Krolick, K. A., Miyama-Inaba, M., Cushley, W. & Uhr, J. W. (1983) *Science* **219**, 644–650.
- Fulton, R. J., Blakey, D. C., Knowles, P. P., Uhr, J. W., Thorpe, P. E. & Vitetta, E. S. (1986) *J. Biol. Chem.* **261**, 5314–5319.
- Montfort, W., Villafranca, J. E., Monzingo, A. F., Ernst, S. R., Katzin, B., Rutenber, E., Xuong, N. H., Hamlin, R. & Robertus, J. D. (1987) *J. Biol. Chem.* **262**, 5398–5403.

Major structural differences between pokeweed antiviral protein and ricin A-chain do not account for their differing ribosome specificity

John A. CHADDOCK¹, Arthur F. MONZINGO², Jon D. ROBERTUS², J. Michael LORD¹ and Lynne M. ROBERTS¹

¹ Department of Biological Sciences, University of Warwick, Coventry, UK

² Department of Chemistry and Biochemistry, University of Texas, Austin, TX USA

(Received 4 September/26 October 1995) – EJB 95 1447/3

Pokeweed antiviral protein (PAP) and the A-chain of ricin (RTA) are two members of a family of ribosome-inactivating proteins (RIPs) that are characterised by their ability to catalytically depurinate eukaryotic ribosomes, a modification that makes the ribosomes incapable of protein synthesis. In contrast to RTA, PAP can also inactivate prokaryotic ribosomes. In order to investigate the reason for this differing ribosome specificity, a series of PAP/RTA hybrid proteins was prepared to test for their ability to depurinate prokaryotic and eukaryotic ribosomes. Information from the X-ray structures of RTA and PAP was used to design gross polypeptide switches and specific peptide insertions. Initial gross polypeptide swaps created hybrids that had altered ribosome inactivation properties. Preliminary results suggest that the carboxy-terminus of the RIPs (PAP 219–262) does not contribute to ribosome recognition, whereas polypeptide swaps in the amino-terminal half of the proteins did affect ribosome inactivation. Structural examination identified three loop regions that were different in both structure and composition within the amino-terminal region. Directed substitution of RTA sequences into PAP at these sites, however, had little effect on the ribosome inactivation characteristics of the mutant PAPs, suggesting that the loops were not crucial for prokaryotic ribosome recognition. On the basis of these results we have identified regions of RIP primary sequence that may be important in ribosome recognition. The implications of this work are discussed.

Keywords: ribosome-inactivating proteins; pokeweed antiviral protein; ricin; ribosome recognition; *N*-glycosidase.

Many plants, fungi and bacteria produce ribosome-inactivating proteins (RIPs) which can attack and catalytically inactivate eukaryotic ribosomes and thereby inhibit protein synthesis. The physiological role of these proteins is unknown although it is widely believed that plant RIPs play roles in defence, e.g. as potential antiviral or antifungal agents (Lord et al., 1991). RIPs are characterised by their ability to remove an invariant adenine base from a conserved loop in 28S rRNA (Endo and Tsurugi, 1987). This loop is involved in binding elongation factors and its depurination leads to irreversible inactivation of the 60S ribosomal subunit and the cessation of protein synthesis.

Classically, RIPs have been categorised into two families based on their structural characteristics. Pokeweed antiviral protein (PAP) from *Phytolacca americana* is a representative of the type 1 family of RIPs, all of which are single chain *N*-glycosidases with molecular mass around 30 kDa. In addition to the type 1 class of RIPs, some plants produce heterodimeric proteins termed type 2 RIPs. These have an A chain that appears to be structurally and functionally related to the type 1 RIPs, disulfide

linked to a sugar-binding B chain. The majority of the type 2 RIPs, as exemplified by the castor oil seed toxin ricin, are potent cytotoxins owing to the cell binding ability of the B chain which promotes the obligatory first step in toxin uptake. The type 1 RIPs, in contrast, are not cytotoxic since they lack a means of initially binding to the surface of cells. If introduced into cells by an alternative carrier then cytotoxicity is observed. Unusually, two type 2 RIPs have been shown to exhibit extremely poor cytotoxicity but *in vitro* protein synthesis inhibition is equivalent to other type 2 RIPs (Girbes et al., 1993a,b).

A surprising finding in recent years has been that several type 1 RIPs, including PAP, show activity towards not only eukaryotic ribosomes but also prokaryotic ribosomes (Hartley et al., 1991). To date, no type 2 RIPs have been shown to inactivate prokaryotic ribosomes. Depurination of *Escherichia coli* 23S rRNA occurs at A2660, in a functionally equivalent position to the target adenine of eukaryotic 26/28S rRNA (A4324 in rat liver). The location of the target adenine within the rRNA structure is equivalent in both eukaryotic and prokaryotic ribosomes and was shown by Endo et al. (1987) to lie in a highly conserved 14-base purine-rich sequence (α -sarcin loop). Studies of the kinetics of RTA-catalysed depurination have determined the K_m and k_{cat} for eukaryotic ribosomes to be approximately 1 μ M and 1500 min⁻¹ respectively (Endo and Tsurugi, 1987). Although RTA is inactive towards intact prokaryotic ribosomes, depurination of naked 23S rRNA by RTA has been described (Endo and Tsurugi, 1987). Since the prokaryotic rRNA can serve as a sub-

Correspondence to L. M. Roberts, Department of Biological Sciences, University of Warwick, Coventry, West Midlands, United Kingdom, CV4 7AL.

Fax: +44 1203 523701

Abbreviations. ID₅₀, concentration of protein for 50% depurination; PAP, pokeweed antiviral protein; RTA, ricin A-chain; RIP, ribosome inactivating protein.

Enzyme. *N*-glycosidase (EC 3.5.1.52).

strate for RTA-dependent N-glycosidase activity when stripped of ribosomal proteins, and the rRNA target sequence is conserved, the molecular basis of this difference in RIP specificity is intriguing.

Studies have also shown that the three-dimensional structural alignments of PAP and ricin A chain are very similar and the organisation of the putative active-site region is highly conserved. However, a small number of polypeptide regions were identified as having sufficiently different tertiary structure to warrant investigation as possible ribosome-specificity determinants (Monzingo et al., 1993). It has been suggested that regions of RIP protein structure, possibly quite distinct from the active site, may determine ribosome specificity. The aim of this present study is to investigate this possibility by using RTA and PAP as model proteins for RIPs that are only active against eukaryotic ribosomes (RTA) or have activity against both eukaryotic and prokaryotic ribosomes (PAP). Gross polypeptide swaps and specific peptide swaps have been generated to create RTA/PAP hybrid proteins for examination of their ability to inactivate ribosomes.

MATERIALS AND METHODS

Construction of polypeptide hybrids. Hybrids were constructed using the PAP template described previously (Chaddock et al., 1994) which has a TGA codon inserted after the codon for Thr262 and a deletion of the sequence coding for the 29-amino-acid C-terminal extension. Nucleotide and amino acid numbering are derived from the previously reported PAP cDNA (Lin et al., 1991) and ricin cDNA (Lamb et al., 1985) sequences, with numbering initiated at the first codon of the mature protein sequence. Site-specific mutagenesis was performed using the T7-GEN *in vitro* mutagenesis system.

In order to construct templates for the polypeptide swaps, M13 clones were prepared by ligation of a pET *Xba*I–*Bam*HI fragment from pETPAPSTOP and pETRTA into M13mp18. Clones were initially created in M13, sequenced and the *Xba*I–*Bam*HI fragment isolated for ligation into similarly cut pET11d. Swap 1 clones (i.e. the N-terminal portions) were constructed from PAP and RTA templates mutated to create a *Nhe*I site at base 192 (PAP). Mutant M13 was cleaved with *Nhe*I/*Hind*III and the small DNA fragments swapped. In addition to the desired mutation, this strategy resulted in the mutation Met65 → Ala in PAP. Swap 2 clones (i.e. central region) were created from templates having *Nhe*I and *Csp*45 sites inserted at base positions 192 and 379, respectively. The respective *Nhe*I–*Csp*45 DNA fragments were swapped. This strategy resulted in the mutation Leu126 → Phe in both swap 2 hybrids. Swap 3 clones (i.e. C-terminal region) were created using templates mutated to introduce *Csp*45 sites at base 654, resulting in secondary mutants Ala218 → Ser (PAP) and Glu220 → Asp (RTA). *Hind*III–*Csp*45 small DNA fragments from these mutated templates were swapped to construct the swap 3 series.

Construction of peptide swap mutants. Three peptide swaps (PAP80, PAP110 and PAP122) were constructed using the following procedures. pET80 was created by insertion of a double-stranded oligonucleotide linker into a PAP template which had been mutagenised to insert two restriction sites. Two mutated M13PAPSTOP templates with a *Nru*I site at base position 232 and a *Kpn*I site at 260 (M13JAC1 and M13JAC2, respectively) were prepared. A linker oligonucleotide (created by hybridisation of GCTGGAAATTCGTAC with GAATTC-CAGC) was ligated to a 661-bp M13JAC2 *Kpn*I–*Bam*HI fragment. The hybrid was ligated to a 6672-bp M13JAC1 *Bam*HI–*Nru*I fragment, transformed into *E. coli* TG2 and sequenced.

Clone 110 was constructed using a PCR method. A 485-bp PAP sequence, amplified using oligonucleotide TTAACGTGATGTT-CAAAATAGTAAAAACAT and JACEND (Chaddock et al., 1994), was digested with *Bam*HI and ligated to *Bam*HI/AflII-cut M13JAC5 (containing an *Afl*II site mutated into the PAP sequence at base 315). The PCR fragment/M13 hybrid was treated with mungbean nuclease to blunt the *Afl*II site, then ligated to form M13110. M13122 was constructed by mutagenesis of M13PAPSTOP with the T7-GEN system and the mutagenic oligonucleotide AACATAAACTTTGGTGGTAATTATGATAGATTGGAATCAAAAG. All M13 clones were sequenced fully before mutant DNA was cloned into pET11d by digestion of the M13 clone with *Xba*I/*Bam*HI.

Northern blotting. Northern Blotting of rRNA onto Hybond-N membrane was performed essentially as described by Sambrook et al. (1989) using Pharmacia VacuGene XL apparatus. Hybridisation of ³²P-end-labelled oligonucleotide probes (75 pmol, approximately 2×10⁶ dpm) specific to the 3' end of the 28S and 23S rRNA was performed overnight in fresh hybridisation solution (0.015 M NaCl, 0.0015 M sodium citrate, pH 7, 0.3% SDS) at 37°C/42°C respectively. Filters were washed twice for 30 min with 0.03 M NaCl, 0.003 M sodium citrate, 0.1% SDS prior to exposure to X-ray film at –70°C.

Miscellaneous methods. All clones were transformed into *E. coli* BL21(DE3)pLysS and were maintained as glycerol stocks at –70°C. Protein expression and prokaryotic rRNA extraction are described elsewhere (Chaddock et al., 1994). Protein purification, N-glycosidase assay, and *in vitro* transcription/translation techniques were essentially as previously described (Chaddock and Roberts, 1993). Other standard laboratory methods were as in Sambrook et al. (1989).

RESULTS

Polypeptide switches. Hybrids were constructed with the potential to encode large regions switched in polypeptide content to investigate their contribution to ribosome specificity. The validity of such an approach was confirmed with the later observations from X-ray structure analysis of PAP and RTA demonstrating the highly conserved tertiary structure. These gross changes were made by introduction of specific restriction enzyme sites into the PAP and RTA DNA sequences, digestion of mutant DNA, and cloning DNA fragments into the respective partner. Restriction sites were chosen to minimise codon mutations. Sequences between PAP residues 1–63, 64–126, and 219–262 were exchanged with RTA equivalents 1–71, 72–126, and 222–267 to investigate the contribution to ribosome recognition of these gross changes.

The first swap representing amino acids 1–63 was designed to investigate the N-terminal region, which is relatively low in conservation between PAP and RTA and has previously been implicated in having potential ribosome-interactive properties (Watanabe and Funatsu, 1986; Misra et al., 1993). The second region (64–126) was changed to investigate several phenomena. These include the effects of altering a substantial amount of the β -sheet structure on one side of the active site but not affecting the key catalytic residues, and investigating the importance of the putative RNA recognition motif present in residues 78–84 in RTA and 70–76 in PAP identified by primary sequence similarity in a maize RIP by Bass et al. (1992). In addition, swap 2 contained the peptide regions of loops 80 and 110 that were later individually mutated (see below). The third swap assessed the contribution of the C-terminal region of the protein, leaving all the major catalytic residues untouched. The C-termini of PAP and RTA constitute a region of low secondary structure and are

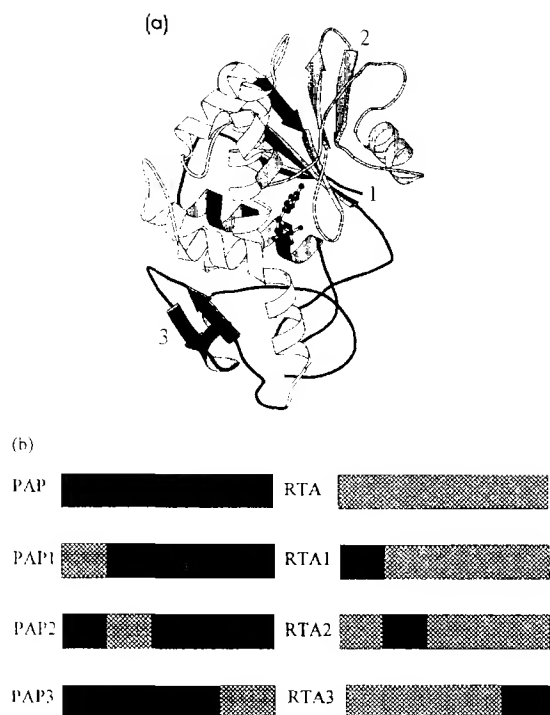


Fig. 1. Polypeptide swap structure. Three PAP mutants, PAP1 (1–63), PAP2 (64–126) and PAP3 (219–262) were created by substitution of the PAP residues indicated by the equivalent RTA residues. (a) Location of polypeptide swaps in PAP tertiary structure. The swapped regions in PAP1, PAP2 and PAP3 are highlighted in dark grey, light grey and black respectively. (b) Schematic representation of swap constructs. PAP-derived polypeptide is highlighted in black and RTA-derived polypeptide in hatching.

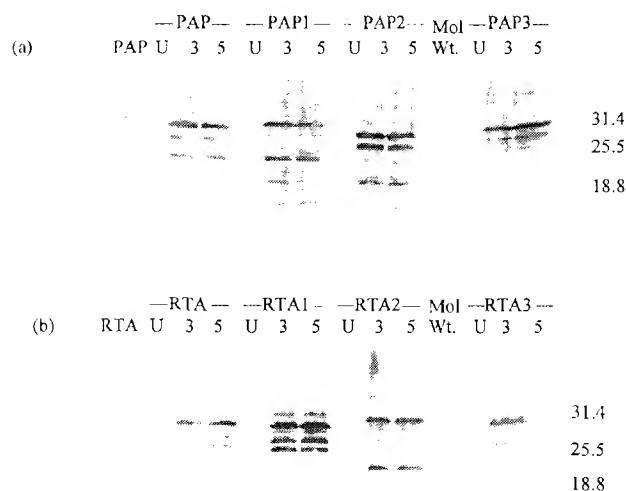


Fig. 2. Expression of polypeptide swap mutants in *E. coli* and analysis by Western blotting. Samples of expression culture were removed prior to induction (U), 3 h post-induction (3) and 5 h post-induction (5) and analysed by SDS/PAGE and Western blotting with anti-PAP antibodies (a) or anti-RTA antibodies (b). In both cases 100 ng recombinant wild-type protein was blotted as control. Approximate molecular masses (in kDa) are indicated on the right.

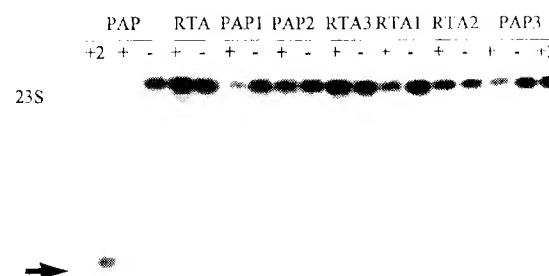


Fig. 3. N-glycosidase activity of PAP and RTA mutants during *E. coli* expression. rRNA from expression-culture ribosomes was isolated and 4 µg was treated (+) or not treated (–) with aniline. Samples were electrophoresed on agarose/formamide gels prior to Northern blotting onto nylon membrane. The 3' fragment of the 23S rRNA was identified by hybridisation to a specific oligonucleotide probe. Fragments of 23S rRNA released by aniline cleavage of depurinated RNA are indicated by an arrow. Increased amounts of rRNA were loaded in lanes identified as +2 for ease of visualisation.

poorly conserved. This may reflect the fact that RTA has a requirement to bind to ricin B-chain, whereas the type 1 RIP PAP does not. Alternatively, the C-terminal region may have the characteristics to interact with prokaryotic ribosomes which have been lost by the type 2 RIPs during evolution of the A-chain/B-chain interface. Fig. 1a indicates the location of the swap regions in the tertiary structure of PAP and Fig. 1b shows a schematic of the primary structure. Nomenclature of these hybrids is based on the name of the majority protein content of the hybrid followed by the domain swap number. For example, PAP with the amino-terminal peptide from RTA would be termed PAP1, while that contains the C-terminal peptide from RTA would be PAP3; PAP2 would be the 'central' swap.

Hybrids were constructed in M13mp18 for convenient sequencing and the subcloned into pET11d for *in vitro* and *in vivo* expression. This expression system is tightly regulated and has previously been used to express highly toxic proteins with success (Studier and Moffatt, 1986). *In-vitro*-generated transcripts were translated in a wheat germ cell-free system and were shown to give products of the expected molecular mass (data not shown). The DNAs were transformed into BL21(DE3)pLysS for expression experiments, and the expression of full length hybrids was assessed by Western blotting of crude *E. coli* lysates using anti-PAP and anti-RTA sera. Fig. 2 shows that, in all cases, protein was expressed following isopropyl β -D-thiogalactopyranoside induction, though there was a certain amount of proteolytic activity that lead to some specific degradation of hybrids. Mutants were expressed to similar levels and there was no observable difference in the culture growth rates (data not shown).

The ability of the hybrids to inactivate prokaryotic and eukaryotic ribosomes was investigated. rRNA was isolated from bacterial ribosomes extracted from the hybrid expression system both before and after a 3-h induction with isopropyl β -D-thiogalactopyranoside. This rRNA was treated with aniline and depurination assessed. Fig. 3 shows a Northern blot of such an experiment. Northern blotting and radioactive probing was necessary to visualise and confirm depurination. Protein was expressed to equivalent levels from all the constructs as ascertained by Western blot analysis of culture after 3-h induction. Depurination of host ribosomes was observed with PAP and PAP3 but not in the cases of PAP1, PAP2, RTA1, RTA2 or RTA3. This suggests that PAP1 and PAP2, both predominantly PAP-like, had either reduced or no ability to inactivate prokaryotic ribosomes.

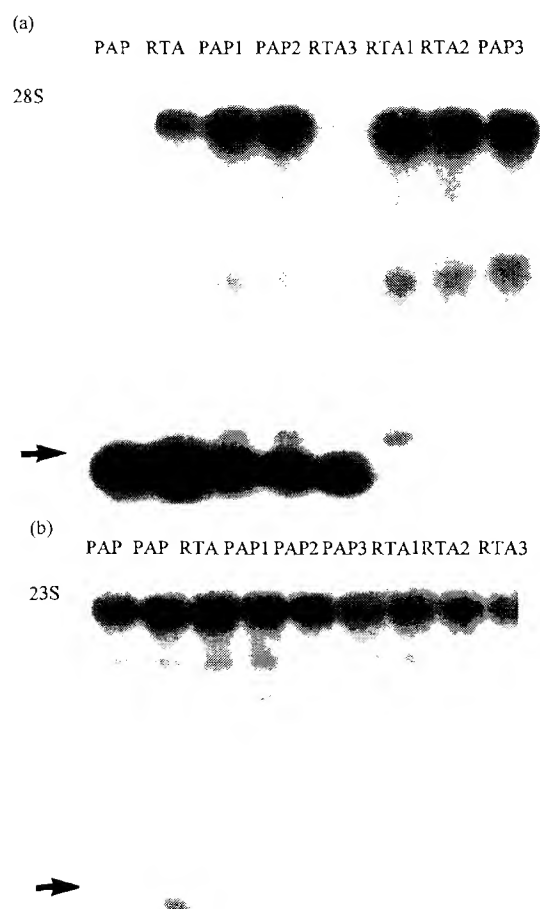


Fig. 4. N-glycosidase activity of PAP and RTA mutants toward eukaryotic and prokaryotic ribosomes in a non-translating *in vitro* system. Soluble protein was prepared from *E. coli* sonicates and equivalent amounts assessed for depurination ability. Northern blots of aniline-treated rRNA were probed with specific probes for the 3' termini of the eukaryotic 28S rRNA (a) and prokaryotic 23S rRNA (b). The RIP-specific RNA fragment released following aniline cleavage is indicated by an arrow.

In order to test if the proteins expressed in this system retained N-glycosidase activity toward isolated eukaryotic ribosomes, crude sonicates were prepared after induction of expression for 3 h. Subsequent 100000×g centrifugation prepared a soluble fraction of each hybrid which was used to test for the ability to inactivate reticulocyte ribosomes *in vitro*. Equivalent amounts of soluble protein from each mutant was analysed. As indicated in Fig. 4, only constructs PAP1, PAP2, RTA3, RTA and PAP showed activity in this assay. Northern blot analysis was performed to increase the sensitivity of RNA visualisation, and this analysis confirmed that only the hybrids identified above were active. The data for PAP3 were not consistent with its observed activity towards prokaryotic ribosomes during expression. When proteins including PAP3 were extracted from *E. coli* and added to isolated prokaryotic ribosomes *in vitro*, only wild-type PAP depurinated rRNA (Fig. 4). A summary of these domain swap results is shown in Table 1.

Peptide swaps. Comparison of the tertiary structures of PAP (Monzingo et al., 1993) and RTA (Katzin et al., 1991) led to the identification of three peptide regions that were noticeably

dissimilar between RTA and PAP. They were located within the polypeptide swaps that had altered properties and therefore were potentially important. These regions were named 80, 110 and 122 to describe the approximate amino acid positions in PAP. Loops 80 (Asp78–Arg86) and 110 (Cys106–Val113) are located in the regions between β -strands d and e and between α -helix B and β -strand f, respectively, whereas loop 122 (residues Asp120–Thr125) forms a 'lid' structure at the entrance of the active site, displaying a different structure and charge distribution between PAP and RTA. To investigate if activity towards prokaryotic ribosomes could be reduced, as had been seen with PAP1 and PAP2, the respective RTA sequences were inserted into the PAP backbone to create mutant PAP proteins. The positions of the peptide swaps in the tertiary structure are indicated in Fig. 5 and the amino acid changes are shown in the accompanying legend.

Conversion of the PAP-like motifs to the equivalent RTA-like motifs was performed by DNA manipulation as described and constructs were prepared in the *E. coli* expression vector pET11d. All three mutants were shown to express equivalent quantities of protein after induction with isopropyl β -D-thiogalactopyranoside (Fig. 6a). No significant differences in growth characteristics were observed following induction of toxic and non-toxic proteins, therefore monitoring the absorbance during expression did not provide a good indicator of relative activities of the hybrids. An improved indication of activity was provided by *E. coli* cell viability, as measured by a plating assay. Viability was reduced to less than 0.1% of the pre induction levels after 3 h of PAP expression (data not shown). Ribosomal RNA from the expression cultures of the three mutants was isolated and checked for depurination. In all cases the ribosomes had been depurinated indicating that the protein was active to the host ribosomes during expression (data not shown). In order to assess activity more accurately, the mutant proteins were purified by cation-exchange chromatography. PAP80 (Fig. 6b) and PAP122 were successfully purified to homogeneity as assessed by silver staining samples following SDS/PAGE. PAP110 was not obtained fully pure using similar techniques but was highly enriched. The concentration of PAP110 within the semi-purified sample could be estimated from densitometry of stained SDS/polyacrylamide gels, as was done also for the fully purified mutant proteins PAP80 and PAP122.

Mutant proteins were assayed for activity toward isolated rabbit reticulocyte ribosomes and isolated *E. coli* ribosomes *in vitro*. *E. coli* ribosomes have previously been shown to be approximately 100–500-fold less sensitive to RIPs than eukaryotic ribosomes (Hartley et al., 1991). Assays were performed in Endo buffer in the absence of additional factors. Appropriate concentrations of toxin were incubated with 1 μ g/ μ l ribosomes for 30 min at 30°C. rRNA was extracted and the amount of depurination estimated by densitometry of ethidium-bromide-stained gels (Chaddock and Roberts, 1993). Since it was not the intention of this analysis to prepare kinetic parameters for each mutant, but rather to investigate their relative activities toward the two ribosome types, these assay conditions were satisfactory. Fig. 7 shows a titration of purified recombinant PAP versus PAP80 and clearly demonstrates that the mutant PAP80 protein does not have reduced activity towards prokaryotic ribosomes. For each mutant toxin a similar titration was performed and the amounts of depurination assessed. Comparison of the activities of the toxins was made possible by estimating the ID_{50} (concentration of toxin for 50% depurination) from graphical analysis of the amount of depurination resulting from various toxin concentrations. For each measurement of hybrid activity, a control experiment was performed using purified wild-type PAP and an ID_{50} calculated. The mutant ID_{50} was then compared to the wild-

Table 1. Summary of activity assessments of polypeptide swaps.

Ribosomal substrate	Depurination activity of protein							
	RTA	PAP	PAP1	PAP2	PAP3	RTA1	RTA2	RTA3
Eukaryotic <i>in vitro</i> (non-translating)	yes	yes	yes	yes	no	no	no	yes
Prokaryotic <i>in vitro</i> (non-translating)	no	yes	no	no	no	no	no	no
Prokaryotic host (translating)	no	yes	no	no	yes	no	no	no

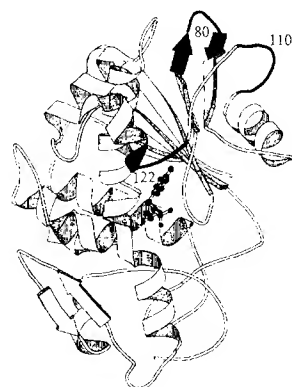


Fig. 5. The location of peptide loop swaps in the tertiary structure of PAP. Mutant PAP proteins were created by replacement of peptide regions by the RTA equivalent sequences. Proteins were termed PAP80, PAP110 and PAP122 for D⁷⁸PFETNKR⁸⁶ to AGNS, C¹⁰⁶PNANSRV¹¹³ to TDVQN and D¹²⁰SRYPT¹²⁵ to GGNVDR respectively. The location of the proposed active site at the centre of the figure is shown by the position of the formycin 5'-monophosphate ring structure.

type and the N-glycosidase activity of the mutants calculated as a percentage of wild-type activity (Table 2).

From the analysis it is apparent that RTA sequences inserted into PAP had not significantly affected the ability of the mutant proteins to inactivate prokaryotic or eukaryotic ribosomes. In all three cases, the activity of the mutant was within one order of magnitude of wild-type PAP during these assays. Since RTA is not active towards *E. coli* ribosomes at concentrations up to 10000-fold greater than concentrations needed to inactivate reticulocyte ribosomes (Ready et al., 1991), we can assume that the mutant PAP hybrids are not greatly affected in prokaryotic ribosome depurination. Clearly, the swapped peptide regions alone do not account for the prokaryotic ribosome specificity of PAP.

DISCUSSION

Although the key catalytic residues present in the active site of RIPs are always conserved, and the target adenine residue they remove from rRNA is present in an absolutely conserved base sequence, the target ribosome specificity for different RIPs can vary dramatically. The work presented here represents an initial attempt to determine whether the structural features of RIPs govern their ribosome specificity. It was decided to use RTA and PAP to investigate their documented differences in inactivation of bacterial (prokaryotic) and rabbit reticulocyte (eukaryotic) ribosomes. The availability of cDNA clones and the later information derived from the tertiary structures of PAP and RTA were deciding factors in the choice of RIPs. Many workers have described the specificity of RIPs in relation to their ability to inactivate self and non-self ribosomes, and have attempted to

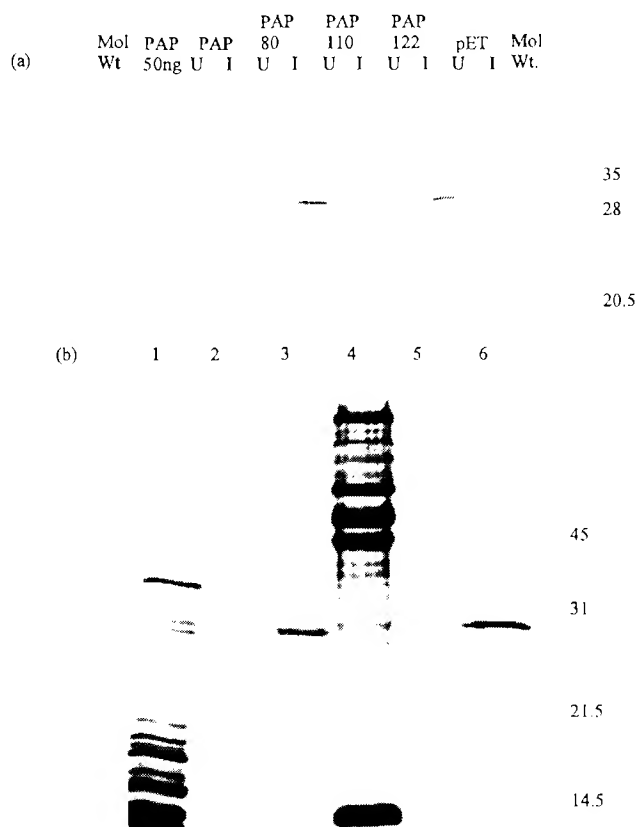


Fig. 6. Expression and purification of PAP peptide loop mutants. (a) Analysis of PAP peptide loop mutants expressed in BL21(DE3)pLysS by SDS/PAGE and Western blotting with anti-PAP antibodies. 1-ml samples of culture were removed prior to (U) and 3 h post-induction (I) with isopropyl- β -D-thiogalactopyranoside, centrifuged at 13000 \times g for 5 min, and samples prepared for electrophoresis. Samples were also taken from *E. coli* transformed with the expression vector alone (pET). (b) Purification of PAP80 by cation-exchange chromatography. Samples of *E. coli* culture (lane 1), 100 ng PAP protein from *Physolacca americana* (lanes 2 and 5), purified recombinant PAP80 (lane 3) and purified recombinant PAP (lane 6) were visualised by silver staining following SDS/PAGE. Molecular mass markers are shown in lane 4 and approximate molecular masses (in kDa) are indicated on the right.

explain why RIPs have evolved a specificity for ribosomes (Prestle et al., 1992; Taylor et al., 1994; Wong et al., 1995). However, little work has been described where the features necessary for ribosome recognition and interaction have been investigated. Rather, most mutagenesis experiments have concentrated on the determination of the catalytic mechanism (Kim and Robertus, 1992; Chaddock and Roberts, 1993). A recent study by Morris and Wool (1994) described the effects of deletions on helix D in RTA and concluded that none of the residues in this region (Asn141–Tyr152) were involved in ribosome recogni-

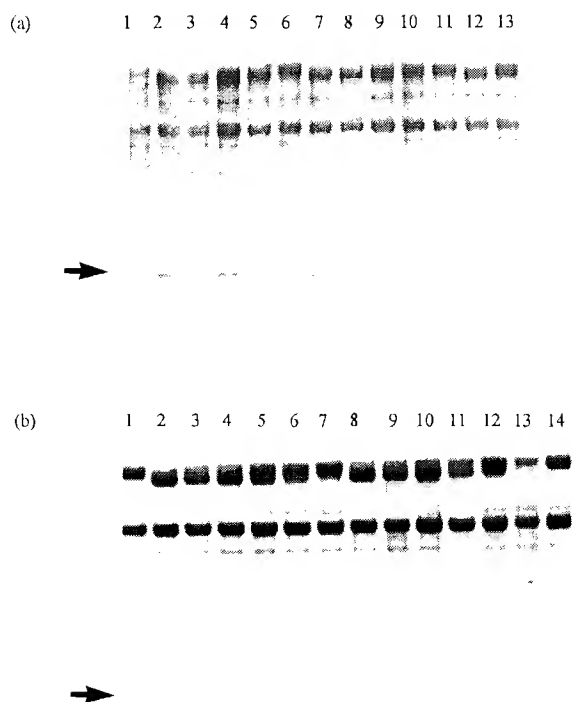


Fig. 7. Assessment of the N-glycosidase activity of purified PAP and PAP80 towards eukaryotic and prokaryotic ribosomes. (a) 30 μg isolated rabbit reticulocyte ribosomes were treated with PAP (lanes 2–6) and PAP80 (lanes 7–11) for 30 min at 30°C, RNA isolated and the aniline-treated RNA visualised following electrophoresis by ethidium bromide staining of agarose/formamide gels. Final toxin concentrations of 10 ng/μl (lanes 2 and 7), 5 ng/μl (lanes 3 and 8), 1 ng/μl (lanes 4 and 9), 0.1 ng/μl (lanes 5 and 10) and 0.01 ng/μl (lanes 6 and 11) were used. Lanes 1 and 13 show non-aniline-treated samples of 10 ng/μl PAP and 10 ng/μl PAP80 respectively. Lane 12 shows depurination resulting from incubation of 3.3 ng/μl RTA. (b) 30 μg isolated *E. coli* ribosomes were treated with PAP (lanes 2–7) and PAP80 (lanes 8–13) as above. Final toxin concentrations of 10 ng/μl (lanes 2 and 8), 6.7 ng/μl (lanes 3 and 9), 5 ng/μl (lanes 4 and 10), 3.3 ng/μl (lanes 5 and 11), 1.7 ng/μl (lanes 6 and 12) and 0.8 ng/μl (lanes 7 and 13) were used. Lanes 1 and 14 show non-aniline-treated samples of 10 ng/μl PAP and 10 ng/μl PAP80, respectively. The rRNA fragment released is indicated by an arrow.

Table 2. N-glycosidase activity of purified PAP80, enriched PAP110 and purified PAP122 relative to wild-type PAP.

Ribosome substrate	N-glycosidase activity of		
	PAP80	PAP110	PAP122
	% wild-type PAP		
Eukaryotic (non-translating)	100	14	26
Prokaryotic (non-translating)	100	30	13

tion or catalysis. Habuka et al. (1992), investigating the properties of active-site mutants of *Mirabilis* antiviral protein, showed that certain mutants do have a reduced ability to inactivate prokaryotic ribosomes. In addition, it was recently suggested that

the electrostatic potential of the residues surrounding the active site was important in determining ribosome interaction (Ago et al., 1994). However the study did not go further to investigate whether this charge distribution determined ribosome specificity.

We (Katzin et al., 1991; Monzingo et al., 1993), and others (Husain et al., 1994; Weston et al., 1994), have taken the view that the recognition of substrate may involve residues distant from the active site in regions of the protein that may interact with ribosomal proteins to determine specificity. There are several lines of evidence to support this hypothesis. First, the key active-site residues of all RIPs studied are conserved, as are their positions in the active site. Second, the ribosomal RNA sequences are highly conserved in the target area leading to little differences in the RNA substrate. Third, *E. coli* rRNA is depurinated by RTA, albeit poorly, after removal of ribosomal proteins (Endo & Tsurugi, 1987) suggesting that, in the absence of ribosomal-proteins, prokaryotic rRNA does indeed adopt a conformation, possibly RTA-induced, suitable for depurination. Since RTA possesses the correct active-site structure to depurinate *E. coli* rRNA, we hypothesise that the deciding factor for depurination *in vivo* is the presence of ribosomal proteins and their relative ability to interact with RIPs. It appears that certain RIPs have fortuitously evolved a surface compatible for the interaction with prokaryotic ribosomes.

In order to address the question of ribosomal specificity, a series of polypeptide and peptide swaps between PAP and RTA were constructed. A random mutagenesis approach was not adopted here since we rationalised that single-residue changes brought about by a random approach may not be sufficient to determine substrate recognition. Further, such an approach would generate mostly structural and active site mutants which would be laborious to distinguish from mutants of interest. Rather, it seemed more likely that a patch of residues may create a suitable recognition determinant. Polypeptide swap hybrids were prepared in order to transfer larger patches of potential surface-interactive zones to test this hypothesis.

The results obtained for the polypeptide changes were interesting. Of the polypeptide switch mutants, only PAP3 was active towards prokaryotic ribosomes during expression in *E. coli*. However, no activity against ribosomes from *E. coli* or rabbit reticulocyte was observed following isolation of PAP3 from the expression culture and *in vitro* activity assessment. This implies that PAP3-dependent depurination during expression may be a transient activity that could only be observed briefly after translation before aberrant folding and loss of activity. It was shown that, although soluble PAP3 could be recovered, the hybrid was very sensitive to proteinase K digestion (in contrast to PAP and RTA) suggesting poor/alttered folding properties (data not shown). The complementary hybrid RTA3 was active toward eukaryotic ribosomes but was not active to prokaryotic ribosomes as one would expect of a hybrid protein that was predominantly RTA. The results from RTA3 and PAP3 suggest that the C-terminus of PAP does not contain crucial prokaryotic ribosome recognition determinants.

In contrast to PAP3, PAP1 and PAP2 did not inactivate prokaryotic ribosomes, either during translation in *E. coli* or in an *in vitro* assay. However, they exhibited substantial eukaryotic ribosome inactivation properties *in vitro*, suggesting that the active-site co-ordination was intact. Therefore, it appears that these mutants have been altered in prokaryotic ribosome recognition, suggesting that interactive zones lie within the first 126 residues of the protein. Since these swapped regions are non-overlapping, the possibility exists that each region, when mutated separately, affects just a component of the recognition zones. It may be that only when both components are intact can prokaryotic ribosomes be depurinated. Alternatively, it is pos-

sible that the conversion of one region has had a deleterious effect on crucial recognition residues present in the second, such that the observed effect is the same.

RTA1 and RTA2, complementary swaps to PAP1 and PAP2, were inactive in both the eukaryotic and prokaryotic assay systems tested, suggesting that, although soluble protein could be prepared, these proteins were non-functional. PAP1 and PAP2 were active against reticulocyte ribosomes, suggesting that the PAP backbone may have an inherently greater ability to accept changes in its structure compared to RTA. Deletion mutagenesis performed previously by Morris and Wool (1992) suggested that RTA has the ability to accept primary sequence perturbation in many positions without affecting *in vitro* N-glycosidase activity during translation. Insertion of large polypeptide regions will impose a different constraint to deletions, and it may be that PAP is better equipped to accommodate these replacements.

In order to examine further the results obtained for PAP1 and PAP2, a series of peptide swaps were created using information from the X-ray structures of PAP and RTA. Analysis of the tertiary structures revealed striking differences between the PAP and RTA tertiary structures within the potentially important N-terminal region. Loops 80 and 110 are noticeably less pronounced in RTA and do not project to solvent as clearly in the case of PAP. Under suitable conditions these loop structures in PAP are disulfide-bonded together, though this is not essential for activity. Examination of the modelled three-dimensional structure of *Mirabilis* antiviral protein (from *Mirabilis jalapa*), a protein also shown to be active against bacterial ribosomes, had amino acid extensions in these areas, suggesting that they could be important in prokaryotic recognition. These regions were therefore strong candidates for ribosome specificity determinants. The proteins were otherwise highly conserved at the level of the α -carbon backbone. However, directed switching of specific peptide loop regions in PAP to the equivalent residues in RTA did not abolish ribosome inactivation (Table 2). Therefore, it must be concluded that these regions are not involved in the determination of prokaryotic ribosome specificity and that other features of the swapped polypeptides in PAP1 and PAP2 are responsible. The reason for the existence of these polypeptide loop extensions is therefore unclear.

Examination of the X-ray structure in the light of these peptide and polypeptide swap experiments has revealed two peptide regions of interest that correlate with the ability of the hybrids to inactivate prokaryotic ribosomes. Regions 48–55 and 95–101 in PAP are surface-located towards the outer face of the active-site cleft and are both present in hybrids that are active toward prokaryotes. If either or both are replaced by the equivalent RTA sequence then prokaryotic depurination is lost, hence PAP1, PAP2, RTA1, RTA2 and RTA3 were not active, whereas PAP3, PAP80, PAP110 and PAP122 are active. In this region, the α -carbon positions in PAP and the equivalent atoms in RTA are observed as different surface loop structures, with the RTA loops being slightly more extended than PAP. This altered backbone structure affects the organisation and orientation of the side chains. In the case of RTA, the side chain of Arg48 could form an ion pair with the side chain of Glu99. The acidic side chains of Asp75, Asp100 and Glu102 probably remain unpaired in this region. With PAP, the side chain of Lys48 may ion pair with Asp100; and Glu97 may form an ion pair with Arg67, whereas Asp92 probably remains unpaired. Comparison of the electrostatic surfaces of PAP and RTA using GRASP (Nicholls et al., 1991) indicated that the charge organisation on the surface of these RIPs is different, particularly in the 48–55 and 95–101 area. Examination of the electrostatic potential of X-PLOR energy minimised models (Brunger, 1988) of the various PAP-RTA hybrids revealed that only PAP3, which was active toward pro-

karyotic ribosomes, has a virtually identical charge pattern to PAP in this area. It is unclear at present whether the backbone structure and subsequent side-chain organisation or the charge differences alone are important. Further experimental work will be required to investigate if these regions are involved in recognition and to decide whether the charge characteristic is the major factor.

This work represents an initial attempt to define regions of RIP structure that may determine ribosome specificity. Future work will focus on the specific areas speculated above to investigate any contribution to ribosome recognition. The increasing number of reported crystal structures for RIPs will greatly assist this exercise since more accurate comparisons can then be made. Additional activity data for RIP activity will prove to be invaluable in studies of this type. In the longer term, it is hoped that a greater understanding of RIP-ribosome recognition will allow the creation of hybrid RIPs with defined specificities for use in the fields of therapeutics, plant-pathogen defence and ribosomal structural studies.

We are grateful to Ed Marcotte for valuable assistance with the preparation of figures. Work at Warwick was supported by the Agricultural and Food Research Council (grant PG88/520) and the Biotechnology and Biological Sciences Research Council (grant 88/T02035). Work at Texas was supported by grants GM 30048 and GM 35989 from the National Institutes of Health and by grants from the Foundation for Research and the Welch Foundation.

REFERENCES

- Ago, A., Kataoka, J., Tsuge, H., Habuka, N., Inagaki, E., Noma, M. & Miyano, M. (1994) X-ray structure of a pokeweed antiviral protein, coded by a new genomic clone, at 0.23-nm resolution. *Eur. J. Biochem.* **225**, 369–374.
- Bass, H. W., Webster, C., O'Brian, G. R., Roberts, J. K. M. & Boston, R. S. (1992) A maize ribosome-inactivating protein is controlled by the transcriptional activator *Opauc-2*. *Plant Cell* **4**, 225–234.
- Brunger, A. T. (1988) Crystallographic refinement by simulated annealing, in *Crystallographic computing 4: Techniques and new technologies* (Isaacs, N. W. & Taylor, M. R., eds) Clarendon Press, Oxford.
- Chaddock, J. A. & Roberts, L. M. (1993) Mutagenic and kinetic analysis of the active site Glu177 of ricin A-chain. *Protein Eng.* **6**, 425–431.
- Chaddock, J. A., Lord, J. M., Hartley, M. R. & Roberts, L. M. (1994) Pokeweed antiviral protein (PAP) mutations which prevent *E. coli* growth do not eliminate catalytic activity towards prokaryotic ribosomes. *Nucleic Acids Res.* **22**, 1536–1540.
- Endo, Y. & Tsurugi, K. (1987) The RNA N-glycosidase activity of ricin A-chain: The characteristics of the enzymatic activity of ricin A-chain with ribosomes and with rRNA. *J. Biol. Chem.* **263**, 8735–8739.
- Endo, Y., Mitsui, K., Motizuki, M. & Tsurugi, K. (1987) The mechanism of action of ricin and related toxic lectins on eukaryotic ribosomes. *J. Biol. Chem.* **262**, 5908–5912.
- Girbes, T., Citores, L., Iglesias, R., Ferreras, J. M., Munoz, R., Rojo, M. A., Arias, E. J., Garcia, J. R., Mendez, E. & Calonge, M. (1993a) Ebulin 1, a nontoxic novel type 2 ribosome-inactivating protein from *Sambucus ebulus* L. leaves. *J. Biol. Chem.* **268**, 18195–18199.
- Girbes, T., Citores, L., Ferreras, M., Rojo, M. A., Iglesias, R., Munoz, R., Arias, E. J., Calonge, M., Garcia, J. R. & Mendez, E. (1993b) Isolation and partial characterisation of nigrin b, a non-toxic novel type 2 ribosome-inactivation protein from the bark of *Sambucus nigra* L. *Plant Mol. Biol.* **22**, 1181–1186.
- Habuka, N., Miyano, M., Kataoka, J., Tsuge, H. & Noma, M. (1992) Specificities of RNA N-glycosidase activity of *Mirabilis* antiviral protein variants. *J. Biol. Chem.* **264**, 6629–6637.
- Hartley, M. R., Legname, G., Osborn, R., Chen, Z. & Lord, J. M. (1991) Single-chain ribosome-inactivating proteins from plants depurinate *Escherichia coli* 23S ribosomal RNA. *FEBS Lett.* **290**, 65–68.

- Husain, J., Tickle, I. J. & Wood, S. P. (1994) Crystal structure of momordin, a type 1 ribosome-inactivating protein from the seeds of *Momordica charantia*. *FEBS Lett.* 342, 154–158.
- Katzin, B. J., Collins, E. J. & Robertus, J. D. (1991) Structure of ricin A-chain at 2.5 Å. *Protein Struct. Funct. Genet.* 10, 251–259.
- Kim, Y. & Robertus, J. D. (1992) Analysis of several key active site residues of ricin A chain by mutagenesis and X-ray crystallography. *Protein Eng.* 5, 775–779.
- Lamb, I., Roberts, L. M. & Lord, J. M. (1985) Nucleotide sequence of cloned cDNA coding for preproricin. *Eur. J. Biochem.* 148, 265–270.
- Lin, Q., Chen, Z. C., Antoniwi, J. F. & White, R. F. (1991). Isolation and characterisation of a cDNA clone encoding the anti-viral protein from *Phytolacca americana*. *Physiol. Mol. Plant Pathol.* 42, 237–247.
- Lord, J. M., Hartley, M. R. & Roberts, L. M. (1991) Ribosome inactivating proteins of plants. *Sem. Cell Biol.* 2, 15–22.
- Misna, D., Monzingo, A. F., Katzin, B. J., Ernst, S. & Robertus, J. D. (1993) Structure of recombinant ricin A chain at 2.3 Å. *Protein Sci.* 2, 429–435.
- Monzingo, A. F., Collins, E. J., Ernst, S. R., Irvin, J. D. & Robertus, J. D. (1993) The 2.5 Å structure of pokeweed antiviral protein. *J. Mol. Biol.* 233, 705–715.
- Morris, K. N. & Wool, I. G. (1992) Determination by systematic deletion of the amino acids essential for catalysis by ricin A-chain. *Proc. Natl Acad. Sci. USA* 89, 4869–4873.
- Morris, K. N. & Wool, I. G. (1994) Analysis of the contribution of an amphiphilic α -helix to the structure and to the function of ricin A chain. *Proc. Natl Acad. Sci. USA* 91, 7530–7533.
- Nicholls, A., Sharp, K. & Honig, B. (1991) Protein folding and association: Insights from the interfacial and thermodynamic properties of hydrocarbons. *Protein Struct. Funct. Genet.* 11, 281–293.
- Prestle, J., Schonfelder, M., Adam, G. & Mundry, K. W. (1992) Type 1 ribosome-inactivating proteins depurinate plant 25S rRNA without species specificity. *Nucleic Acids Res.* 20, 3179–3182.
- Ready, M. P., Kim, Y. & Robertus, J. D. (1991) Site-directed mutagenesis of ricin A-chain and implications for the mechanism of action. *Protein Struct. Funct. Genet.* 10, 270–278.
- Sambrook, J., Fritsch, E. F. & Maniatis, T. (1989) *Molecular cloning: a laboratory manual*, 2nd edn. Cold Spring Harbor Laboratory Press, Cold Spring Harbor NY.
- Studier, F. W. & Moffatt, B. A. (1986) Use of bacteriophage T7 RNA polymerase to direct selective high-level expression of cloned genes. *J. Mol. Biol.* 189, 113–130.
- Taylor, S., Massiah, A., Lomonosoff, G., Roberts, L. M., Lord, J. M. & Hartley, M. R. (1994) Correlation between the activities of five ribosome-inactivating proteins in depurination of tobacco ribosomes and inhibition of tobacco mosaic virus infection. *Plant J.* 5, 827–835.
- Watanabe, K. & Funatsu, G. (1986) Involvement of arginine residues in inhibition of protein synthesis by ricin A-chain. *FEBS Lett.* 204, 219–222.
- Weston, S. A., Tucker, A. D., Thatcher, A. D., Derbyshire, D. J. & Paupit, R. A. (1994) X-ray structure of recombinant ricin A-chain at 1.8 Å resolution. *J. Mol. Biol.* 244, 410–422.
- Wong, R. N. S., Mak, N. K., Choi, W. T. & Law, P. T. W. (1995) Increased accumulation of trichosanthin in *Trichosanthes kirilowii* induced by micro-organisms. *J. Exp. Bot.* 46, 355–358.

Purification, characterization and molecular cloning of trichoanguin, a novel type I ribosome-inactivating protein from the seeds of *Trichosanthes anguina*

Lu-Ping CHOW*, Ming-Huei CHOU*, Cheng-Ying HO*, Chyh-Chong CHUANG†, Fu-Ming PAN†, Shih-Hsiung WU† and Jung-Yaw LIN*¹

*Institute of Biochemistry, College of Medicine, National Taiwan University, No. 1, Section 1, Jen-Ai Road, Taipei, Taiwan, Republic of China, and

†Institute of Biological Chemistry, Academia Sinica, Nankang, Taipei, Taiwan, Republic of China

The seeds of the plant *Trichosanthes anguina* contain a type I ribosome-inactivating protein (RIP), designated trichoanguin, which was purified to apparent homogeneity by the combined use of ion-exchange chromatographies, i.e. first with DE-52 cellulose and then with CM-52 cellulose. The protein was found to be a glycoprotein with a molecular mass of 35 kDa and a pI of 9.1. It strongly inhibits the protein synthesis of rabbit reticulocyte lysate, with an IC_{50} of 0.08 nM, but only weakly that of HeLa cells, with an IC_{50} of 6 μ M. Trichoanguin cleaves at the A4324 site of rat 28 S rRNA by its N-glycosidase activity. The cDNA of trichoanguin consists of 1039 nt and encodes an open reading frame coding for a polypeptide of 294 amino acid residues. The first 19 residues of this polypeptide encode a signal peptide sequence and the last 30 residues comprise an extension at its C-terminus. There are four potential glycosylation sites, located at Asn-51, Asn-65, Asn-201 and Asn-226. A comparison of the amino acid sequence of trichoanguin with those of RIPs such as trichosanthin, α -momorcharin, ricin A-chain

and abrin A-chain reveals 55%, 48%, 36% and 34% identity respectively. Molecular homology modelling of trichoanguin indicates that its tertiary structure closely resembles those of trichosanthin and α -momorcharin. The large structural similarities might account for their common biological effects such as an abortifacient, an anti-tumour agent and anti-HIV-1 activities. Trichoanguin contains two cysteine residues, Cys-32 and Cys-155, with the former being likely to be located on the protein surface, which is directly amenable for conjugation with antibodies to form immunoconjugates. It is therefore conceivable that trichoanguin might be a better type I RIP than any other so far examined for the preparation of immunotoxins, with a great potential for application as an effective chemotherapeutic agent for the treatment of cancer.

Key words: inhibition of protein synthesis, N-glycosidases, ribosome-inactivating proteins, Cucurbitaceae.

INTRODUCTION

Ribosome-inactivating proteins (RIPs) are ubiquitous in the plant kingdom, with great abundance found in some plant families, such as the Cucurbitaceae [1]. RIPs inhibit protein synthesis by cleaving the N-glycosidic bond of adenine at position 4324 of rat liver 28 S rRNA and preventing the binding of elongation factor 2 [1]. The single adenine residue is removed from a highly conserved loop structure in the ribosomal RNA that render its 5'- and 3'-phosphodiester bonds very susceptible to acid-aniline cleavage and release the diagnostic RNA fragment of 420 nt [1]. RIPs are classified into two subgroups on the basis of their structures and functions: type I proteins consist of a single polypeptide chain of molecular masses ranging between 28 and 35 kDa and alkaline isoelectric points (pI) of pH 8–10 with or without carbohydrates [2]; type II RIPs consist of a catalytically active A chain linked to a cell-binding B chain. The B chain, possessing lectin properties, binds to the D-galactose moieties of the cell surface, leading to endocytosis and delivery of the A chain into the cell, where the latter can attack ribosomes enzymically [3,4]. Among type II RIPs, the cDNA species of ricin from *Ricinus communis* and abrin from *Abrus precatorius* have been cloned [5,6] and expressed in an *Escherichia coli* system [7,8].

Several type I RIPs have been purified and characterized from plants, e.g. pokeweed antiviral protein (PAP; *Phytolacca*

americana) [9], momordin (*Momordica charantia*) [10], jufin (*Luffa cylindrica*) [11], bryodin (*Bryonia dioica*) [12] and dianthin (*Dianthus caryophyllus*) [13]. Trichosanthin (*Trichosanthes kirilowii*), α -momorcharin (*Momordica charantia*), saporin (*Sapornaria officinalis*), PAP and bryodin have also been shown to have abortifacient activities [14].

Trichosanthin and α -momorcharin have been shown to be effective against T cells and macrophages infected with HIV-1 [15,16]. Clinical trials on trichosanthin also showed a decrease in the p24 antigen and an increase in CD4-positive cells in some patients [16,17]. There is great interest in their potential application as immunotoxins that can be selectively targeted to a particular cell type, such as cancer cells [18]. Here we describe the purification, characterization and molecular cloning of a new RIP from seeds of *T. anguina* in the Cucurbitaceae family, and study three-dimensional molecular models of it, based on the tertiary structure of trichosanthin and α -momorcharin.

EXPERIMENTAL

Materials

The seeds of snake gourds (*T. anguina*) were purchased from a local store. Restriction enzymes and T4 DNA ligase were obtained from New England Biolabs (Beverly, MA, U.S.A.). The

Abbreviations used: PAP, pokeweed antiviral protein; RACE, rapid amplification of cDNA ends; RIP, ribosome-inactivating protein.

¹ To whom correspondence should be addressed (e-mail: lupin@ha.mc.ntu.edu.tw).

The nucleotide sequence data reported will appear in DDBJ, EMBL and GenBank Nucleotide Sequence Databases under the accession number AF055086.

Trizol kit for RNA extraction was obtained from Life Sciences (Petersburg, FL, U.S.A.). Oligo(dT)-cellulose was purchased from Pharmacia (Uppsala, Sweden). The Marathon™ cDNA amplification kit was from Clontech (Palo Alto, CA, U.S.A.). Deoxyribonucleotide primers were synthesized by the phosphoramidite method with an Applied Biosystems (Foster City, CA, U.S.A.) automated DNA synthesizer. *Taq* DNA polymerase, pGEM-T vector, rabbit reticulocyte lysate and L-[³H]leucine were obtained from Promega (Madison, WI, U.S.A.). The AmpliTag FS Prism Ready Reaction Cycle sequencing kit was from Applied Biosystems. Abrin A-chain was isolated and purified as described previously [6]. Other chemicals were of analytical grade.

Purification of trichoanguin

All purification procedures were performed at 4 °C. *T. anguina* seeds were homogenized with a Waring blender by using 10 mM sodium phosphate buffer, pH 7.2. A floating layer of solidified fat was removed with cheesecloth. After centrifugation of the suspension at 15000 g for 30 min, solid (NH₄)₂SO₄ was added to the supernatant to 95% saturation. After being left for 1 h, the precipitates were collected by centrifugation, dissolved in 10 mM sodium phosphate buffer, pH 7.8, and dialysed against the same buffer. After dialysis the clear supernatant was applied to a DE-52 cellulose column (2.2 cm × 10 cm) pre-equilibrated with the buffer. The flow-through fractions were collected and applied to a CM-52 cellulose column (2.2 cm × 10 cm) pre-equilibrated with 10 mM sodium acetate buffer, pH 5.0. The column was eluted with a linear gradient of 0–0.4 M NaCl in the same buffer. Fractions with inhibitory activity towards protein synthesis were pooled, dialysed extensively against distilled water and freeze-dried. The purified fraction was analysed by SDS/PAGE.

Gel filtration

Gel filtration of trichoanguin was performed with a Superose 12 column HR 10/30 (Pharmacia), which was eluted with 50 mM sodium phosphate buffer, pH 6.8, containing 150 mM NaCl; the flow rate was 0.4 ml/min. The column was calibrated with the following molecular mass markers: BSA (67 kDa), ovalbumin (45 kDa) and chymotrypsinogen (25 kDa).

Electrophoresis

Active fractions isolated from each purification step were analysed by SDS/PAGE [12.5% (w/v) gel], as described by Laemmli [19]. The protein bands were revealed by being stained with Coomassie Brilliant Blue R-250. Carbohydrate-containing bands were detected with periodic acid/Schiff reagent [20]. The pI of trichoanguin was estimated from isoelectric focusing electrophoresis performed with a pH 3.5–10 gel with a Pharmacia Multiphor II system.

Protein sequence analysis

The N-terminal amino acid sequence of trichoanguin was determined by using the automated Edman degradation method with an Applied Biosystems model 477 A protein sequencer and an on-line phenylthiohydantoin analyser. The C-terminal residues were determined by using the method of Kamo and Akira [21]. The reaction was performed by carboxypeptidase A digestion in 0.1 M pyridine/acetate/collidine buffer, pH 8.2, at

37 °C for 6 h, and the reaction products were dried and analysed directly with an A-5500 amino acid analyser (Irica, Kyoto, Japan).

Cell-free inhibition of protein synthesis

Assay of inhibition of protein synthesis *in vitro* was performed as described [22], with a cell-free rabbit reticulocyte lysate (Promega). Various amounts of toxin were added to the reaction mixture, and the reaction was performed at 30 °C for 1 h. The trichloroacetic acid-insoluble products were collected on a glass fibre disc by filtration with Whatman GF/C, then processed for liquid-scintillation counting. Each inhibition point is calculated as the mean for three individual tests.

Cytotoxicity assays

HeLa cells were grown in RPMI 1640 medium supplemented with 4 mM non-essential amino acids, streptomycin (100 i.u./ml), penicillin (100 µg/ml) and 10% (v/v) fetal calf serum. Cells were plated in 24-well plates at a concentration of 10⁵ cells per well and incubated at 37 °C under CO₂ for 24 h. The medium was then replaced by serum-free RPMI 1640 medium containing various amounts of toxin. Cells were further incubated at 37 °C for 18 h; protein synthesis was measured by incubating the cells for 1 h in serum-free, leucine-free RPMI 1640 containing 0.5 µCi/ml L-[³H]leucine. The radioactivity incorporated into protein was determined as described previously [23]. Each point is the mean for triplicate assays.

RNA N-glycosidase activity

Rat liver ribosomes were prepared by the method of Wettstein et al. [24]; the ribosomes were incubated for 15 min with abrin A-chain or trichoanguin (10 nM) at 37 °C in a final volume of 100 µl of reaction buffer [113 mM KCl/10 mM MgCl₂/0.05% (v/v) β-mercaptoethanol/2 units of RNasin]. The reaction was terminated by the addition of 0.5% SDS; the reaction products were extracted with phenol, precipitated with alcohol and then treated with 0.8 M aniline to cleave 28 S rRNA selectively at the depurinated site by β-elimination. The reaction products were analysed by using 7 M urea/3.5% (w/v) PAGE; the gels were stained with ethidium bromide [25].

Sequencing of trichoanguin cDNA

Total RNA was extracted from the maturing seeds of *T. anguina* in late summer with the Trizol reagent kit [26]. Poly(A)-rich RNA species were purified with a oligo(dT) column (Pharmacia). mRNA (1 µg) was reverse-transcribed with the Marathon™ cDNA amplification kit (Clontech), and the double-stranded cDNA species were ligated to Marathon™ cDNA adaptors. Two degenerate primers were synthesized based on the N-terminal and internal conserved sequences of trichoanguin: 5' primer A, encoding the first eight residues (DVSFDLST), and 3' primer B, encoding the highly conserved amino acids [EAARY(F)KYI] (Table 1), were used, and the reactions were subjected to 30 cycles of heat denaturation at 94 °C for 1 min, annealing the primers to the DNAs at 50 °C for 1 min, and DNA chain extension with *Taq* polymerase at 72 °C for 2 min, followed by a final extension at 72 °C for 10 min.

Rapid amplification of cDNA ends (RACE) on the 3' end was performed with the Marathon™ cDNA amplification kit by using the flanking primer AP-1 and gene-specific primer C (Table 1). The 5' end was amplified by 5' RACE in essentially the same

Table 1 Oligonucleotide primers used for the isolation and cloning of trichoanguin cDNA

Technique	Primer	Sequence
Cloning	5' Primer A	5'-GATGTTAGCTTCGATTTGTCGAC-3'
	3' Primer B	5'-ATATATTATACCTTGCAGCTTC-3'
RACE	Adaptor AP-1	5'-CCATCCTAATACGACTCAGTATAGGGC-3'
	Primer C	5'-GGCCTCTTGTACTCATTGAGTGT-3'
	Primer D	5'-ATCATTAATTACCGAATAAGGAAG-3'

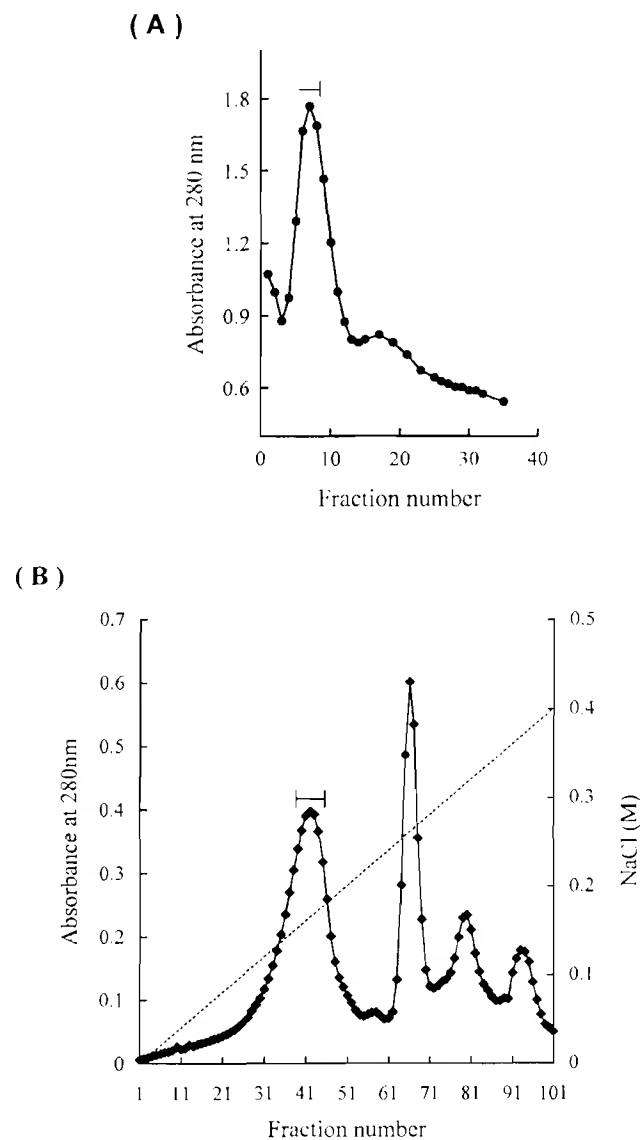
manner as that for the 3' end, by using the flanking primer AP-1 and the gene-specific primer D [27] (Table 1). All PCR products were subcloned into the pGEM-T vector (Promega), then transformed into *E. coli* strain JM109. DNA sequencing was performed with the Tag dye primer cycle sequencing kit (Perkin Elmer) and subjected to electrophoresis on a 373 A Stretch ABI DNA sequencer.

Molecular modelling of trichoanguin protein

A sequence search against the SCOP [28] database revealed the high degree of similarity of the trichoanguin protein sequence to those of RIPs. In the RIP superfamily, several three-dimensional structures have been solved by X-ray crystallography. Four sequences from RIPs, α -trichosanthin (PDB code 1TCS [29]), α -momorcharin (PDB code 1MGR [30]), abrin A chain (PDB code 1ABR [31]), and ricin A chain (PDB code 1RTC [32]), were obtained from the PDB for pairwise sequence alignment, and were compared with the trichoanguin sequence by using the GAP and BESTFIT programs of the GCG package.

The three-dimensional model of trichoanguin was built by using the X-ray structures of α -trichosanthin and α -momorcharin as templates. The multiple sequence alignments generated from the PILEUP program were checked manually and then used in the comparative homology modelling process because of their great similarity. Starting with the alignment, a method of automatic comparative modelling by means of satisfying spatial constraints as implemented in the MODELLER (version 4.0) program [33] was used to produce a trichoanguin model containing all main chains and side chain atoms without further manual intervention. First, MODELLER was used to derive many distance and dihedral angle restraints on the trichoanguin sequence from its alignment with the template RIP structures. Then the spatial restraints and CHARMM energy [34] terms enforcing the proper stereochemistry were combined into an objective function. The variable target function procedures, employing the methods of conjugate gradients and molecular dynamics with simulated annealing, were used to obtain three-dimensional models by optimizing the objective function. Twenty slightly different three-dimensional models of trichoanguin were calculated by varying the initial structure. The structure with the lowest value of the objective function was selected as the representative model. Assessment of the reliability of the model was performed residue by residue. The deviation from the standard geometry and atomic overlap was determined and evaluated more rigorously, residue by residue, with the PROCHECK program [35]. PROSAII [36] and Profile-3D [37,38] were used to test the suitability of the derived three-dimensional

conformation for the amino acid sequence of trichoanguin and to develop an energetic profile of the modelled structure. Secondary structures of the trichoanguin model were calculated with the DSSP program [39]. Graphics were displayed by the InsightII package from MSI/Biosystem Technologies (San Diego, CA, U.S.A.) and the MOLMOL program [40].

**Figure 1** Purification of trichoanguin by ion-exchange chromatography

(A) Elution profile of trichoanguin from a DE-52 cellulose column. After precipitation by $(\text{NH}_4)_2\text{SO}_4$ and dialysis against equilibrium buffer (10 mM sodium phosphate buffer, pH 7.8), the supernatant of the dialysate was applied to a DE-52 cellulose column and eluted with equilibrium buffer. The A_{280} of each fraction was measured. Fractions showing activity in the inhibition of protein synthesis were pooled (as indicated by the horizontal bar). (B) Elution profile of trichoanguin from a CM-52 cellulose column. Fractions containing protein synthesis inhibitory activity from (A) were applied to a CM-52 cellulose column previously equilibrated with 10 mM sodium acetate buffer, pH 5.0. The protein was eluted with a linear gradient of 0–0.4 M NaCl with the same eluting buffer. The A_{280} of each fraction was measured. Fractions with inhibitory activity in a cell-free rabbit-reticulocyte system were collected (as indicated by the horizontal bar).

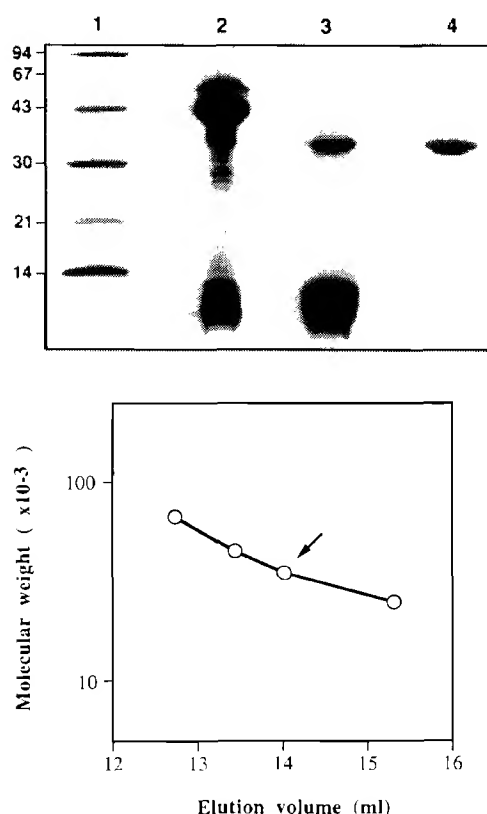


Figure 2 Molecular masses of the purified fractions

Upper panel: SDS/PAGE of various purified fractions. Lane 1, molecular mass markers; lane 2, crude extract; lane 3, active fractions from DE-52 cellulose column chromatography; lane 4, active fractions from CM-52 cellulose column chromatography. The gel was stained with Coomassie Brilliant Blue R-250. The positions of molecular mass standards (in kDa) are shown at the left. Lower panel: estimation of apparent molecular mass of native protein by gel filtration. Approx. 0.2 mg of trichoanguin was subjected to gel filtration on a Superose 12 column (Pharmacia) equilibrated and eluted at a flow rate of 0.4 ml/min with 50 mM sodium phosphate buffer, pH 6.8, containing 150 mM NaCl. Each collected fraction was 0.2 ml. The column was calibrated with the following molecular mass standards: BSA (67 kDa), ovalbumin (45 kDa) and chymotrypsinogen (25 kDa). The elution of the proteins was monitored by measuring A_{280} . The logarithm of protein molecular mass was plotted against elution volume. The arrow indicates the elution volume of trichoanguin.

Table 2 Purification of trichoanguin from *T. anguina* seeds

The preparation was from 250 g of *T. anguina* seeds as described in the Experimental section. One unit is defined as the amount of enzyme necessary to inhibit protein synthesis by 50% in 1 ml of rabbit reticulocyte lysate reaction mixture.

Preparation	Total protein (mg)	Total activity (10^3 units)	Specific activity (10^3 units/mg)	Yield (%)
Crude extract	2851	81	29	100
DE-52 cellulose	315	45	143	55
CM-52 cellulose	31	14.8	477	18

RESULTS

Isolation of trichoanguin from *T. anguina*

Trichoanguin was purified to homogeneity from seeds of *T. anguina* by two simple steps. One major peak obtained in the first step of DE-52 cellulose chromatography exhibited the protein

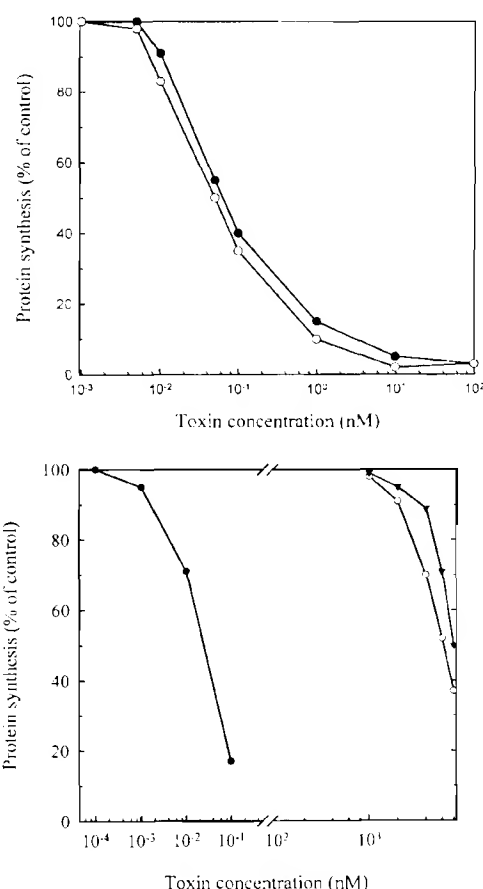


Figure 3 Effects of trichoanguin on protein synthesis

Upper panel: inhibitory effect of varying the concentration of trichoanguin on protein synthesis in a cell-free rabbit reticulocyte lysate system. The incorporation of radioactivity in ^3H leucine into protein was measured; each point denotes the mean for triplicate assays. Symbols: ●, trichoanguin; ○, abrin A chain. Lower panel: inhibition of protein synthesis in HeLa cells. Various concentrations of toxin were incubated with HeLa cells and the incorporation of ^3H leucine into cellular proteins was subsequently determined. Each value is the mean for triplicate samples. Symbols: ○, trichoanguin; ▼, abrin A chain; ●, abrin.

synthesis inhibitory activity (Figure 1A). In this fraction, a major protein of 35 kDa and a minor protein of 10 kDa were present, as revealed by SDS/PAGE analysis. The 10 kDa protein was removed in the second step by CM-52 cellulose chromatography (Figure 1B), resulting in a protein fraction (the first peak) with a subunit molecular mass of 35 kDa and apparent homogeneity (Figure 2, upper panel). The protein thus obtained was characterized and designated 'trichoanguin'. The fraction containing purified trichoanguin was analysed further by size-exclusion chromatography. Trichoanguin was eluted as a single chain of 35 kDa under non-denaturing conditions (Figure 2, lower panel). A pI of 9.1 was estimated with the Pharmacia Multiphor II system (results not shown), in agreement with the alkaline property of most type I RIPs. The inhibitory activity and relative yields in the various steps of purification are summarized in Table 2. Trichoanguin showed a positive reaction to staining with periodic acid/Schiff reagent (results not shown), indicating its glycoprotein nature. Trichoanguin strongly inhibited the incorporation of labelled amino acids into the rabbit reticulocyte lysate cell-free system, and the degree of inhibition was com-

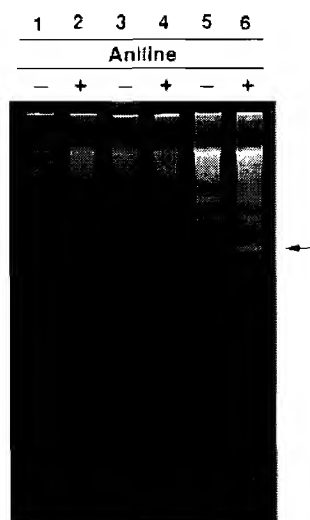


Figure 4 Analysis by gel electrophoresis of N-glycosidase activity

Rat liver ribosomes were used in each assay. Extracted RNA from those ribosomes treated with aniline (+) or untreated (—) were separated by electrophoresis on a denaturing polyacrylamide gel. Lanes 1 and 2, samples in the absence of toxin; control; lanes 3 and 4, samples treated with 10 nM trichoanguin; lanes 5 and 6, samples treated with 10 nM abrin A chain. The arrow indicates the position of the RNA fragment generated by aniline treatment of the ribosomal RNA.

parable with that of abrin. As shown in Figure 3 (upper panel), the IC_{50} values of trichoanguin and abrin A-chain were determined as 0.8 and 0.06 nM respectively.

Cytotoxicity

The addition of trichoanguin to cultures of HeLa cells resulted in the weak inhibition of protein synthesis, with an IC_{50} of 6 μ M (Figure 3, lower panel). At relatively high concentrations, trichoanguin causes a moderate decrease in protein synthesis. Abrin,

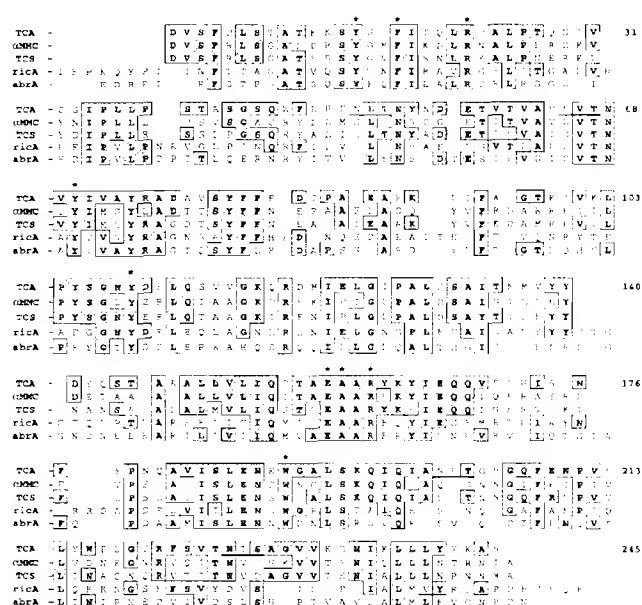


Figure 6 Sequence comparison of trichoanguin (TCA) and other RIPs

Sequence alignment was performed with the PILEUP program of GCG by using published sequences of α -momorcharin (xMMC) [30], trichosanthin (TCS) [29], ricin A chain (rita) [32] and abrin A chain (abra) [31]. The numbering system is based on the sequence of trichosanthin as reference. Gaps have been introduced for optimal alignment and maximum similarity between all compared sequences. Identical amino acids are shown in shaded boxes. The highly conserved and consensus amino acid residues involved in the active site are indicated by asterisks. Potential N-glycosylation sites are underlined.

```

1      c taa ttc atg gca ctc tcc ttt ttc ttc ctc ggc atc tct ctt ggc tct cct act gcc att ggt gat gtt agc 22
1      c taa ttc atg gca ctc tcc ttt ttc ttc ctc ggc atc tct ctt ggc tct cct act gcc att ggt gat gtt agc 73
23  f d l s t a t k x s y s f i t q l r d a l p t q 47
74  ttc gat ttg tgc aca gct act aaa aaa tcc tat tca tct ttc atc aca caa ctc agg gat gct ctt cca act caa 148
45  g t v c g i p l l f s t a s g s q w f r f f n l t 72
149  ggc aca ttg tgc ggc att cca ttg ctg cct tcc acc gca tcc ggc tca caa tgg ttc aga ttc ttc aat ctt acc 223
73  m y n d e t v t v a v n v t n v t i v a y r a d a 97
224  aat tat aac gat gaa acc gtc acc gtc gct gta aat gta acc aat gtc tac atc ttg ggc tat ggt gcc gat gct 298
98  v s y f f e d t p a e a f k l i f a g t k t v k l 122
299  gta tcc tac ttt ttt gaa gac act cca gct gaa gct ttc gca ggt act aag acg gta aaa ctt 373
123  f y s g n y d k l q s v v g k q r d m i e l g i p 147
374  cct tat tgc ggt aat tat gat aag ctt caa agt gta gta ggc aaa caa aga gat atg att gag ctt gga atc ccg 448
148  a l s s a i t n m v y y d y q s t a a a l l v l i 172
449  gct tta agc agt gcc att acg aac atg gtt tat tac gac tac caa agt act gca gcc ggc ctt ctt gta ctc att 523
173  q c t a e a a r t k y i e q q v s s h i s s n f y 197
524  cag tct act gca gaa gct gca agg tat aaa tat att gag caa caa gtt tct tca cat att acc tct aat ttt tat 598
198  f n q a v i s l e n k w g a l s k q i q i a n r t 222
599  cca aat caa gca gtc ata agc tta gaa aac aag tgg ggt gct ctt tcc aaa caa atc cag ata gca aat ago acc 673
223  g h g q f e n p v e l y n p d g t r f s v t n t s 247
674  gga cat gga caa ttc gaa aac cct gtt gag cta tat aac cct att ggc aca cga ttt agt gta acc aat act tgg 748
248  a g v v k g n i k l l l y y k a s v g s e y d i p 272
749  gct gga gtt gta aaa ggc aat atc aaa ctc cta cta tac aaa gcc agt gtt ggt agt gaa tat gat atc cct 823
273  t t i l h p g a m c g n q n y v t m f t p 294
824  act aca atc ttg cac cct gga gct atg gga atc ctt cac aat cag aat gga aat tat gtt aca atg tga ctt tta 898
899  att ctc aca gct ctg cct tgg gtt caa cac cca cgc ata gat tta agg cat tgt tca tag tca ccc atg ttg tga 973
974  atg tgc ttt att tca tta aat aaa taa gta tgg aat ctt ttc cgc caa aaa aaa aaa aaa aaa 1039

```

Figure 5 Nucleotide and amino acid sequences encoding trichoanguin

The nucleotides and the predicted amino acid residues are numbered at the right and at the left. The mature protein sequence is numbered from 20 to 264; the signal peptide runs from 1 to 19, and the additional extension region at the C-terminus extends from 265 to 294. The regions encoding the polyadenylation signal (AATAAA) and the poly(A) tail are underlined.



Figure 7 Superposition of three-dimensional models for homologous proteins

Comparison of trichoanguin (thick line) and its closest structurally known homologous R.I.P.s, α -momorcharin (medium line) and trichosanthin (thin line).

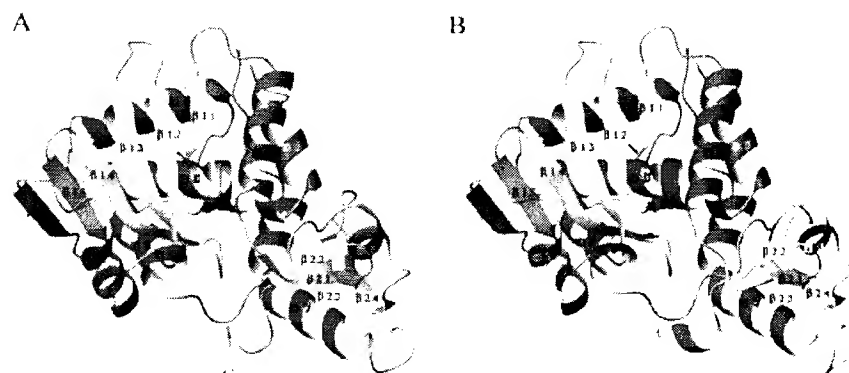


Figure 8 Ribbon representations of trichosanthin (A) and trichoanguin (B) molecules

The N-terminus and C-terminus of each secondary structure region are labeled. The helices are labelled $\alpha 1$ to $\alpha 8$ along the chain, the β -sheets are labelled $\beta 1.1$ to $\beta 2.2$. The computer program MOLMOL was used to generate these diagrams.

N-glycosidase activity

The N-glycosidase activity of trichoanguin was examined by incubating ribosomes with various amounts of trichoanguin or abrin A-chain, and the extracted rRNA was analysed by gel electrophoresis. As shown in Figure 4, when the rRNA from trichoanguin-treated ribosomes was treated with aniline at acidic pH, a cleaved fragment of approx. 420 nt was obtained, similar to that found in abrin A chain/aniline-treated ribosomes.

Molecular cloning and sequence analysis of trichoanguin

PCR amplification of total cDNA mixtures prepared from seeds of *T. anguina* with the Marathon™ cDNA amplification protocol coupled with designed primers for 5' RACE and 3' RACE achieved the amplification of a full-length cDNA fragment of approx. 1000–1100 nt encoding trichoanguin. Sequence analysis

of the cDNA clone revealed that it is 1039 nt in length, a cDNA sequence containing an open reading frame of 882 nt, corresponding to a polypeptide of 294 residues with a calculated molecular mass of 27066 Da (Figure 5).

In most cases, type I RIPs are cleaved post-translationally to yield the mature form. The deduced polypeptide chain of trichoanguin contains a segment of 19 residues at the N-terminus coding for a signal peptide. The C-terminal residues were identified as Ala-Ser by carboxypeptidase A digestion. The cDNA sequence also contained a 30-residue extension at the C-terminus, followed by a translation termination codon (TGA) and a 105 nt 3'-untranslated sequence with an AATAAA polyadenylation site.

There are four potential glycosylation sites at residues 51, 65, 201 and 226 (Figure 6); the presence of carbohydrate might account for the discrepancy observed between the actual coding

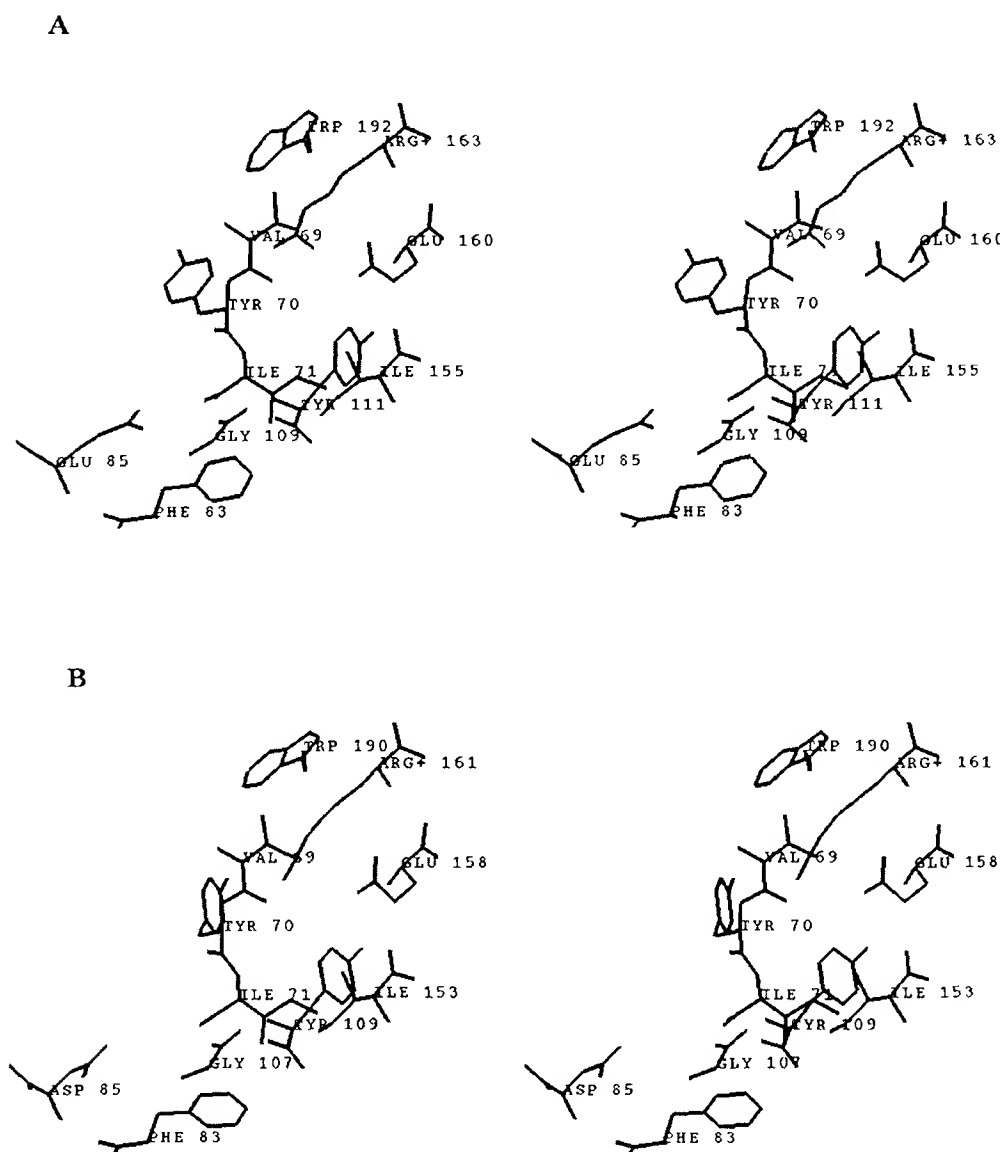


Figure 9 Stereo diagrams of the active site in trichosanthin (A) and trichoanguin (B)

The diagrams show the amino acid residues involved in the binding of adenine and the residues associated with the surroundings of the active site.

molecular mass and that estimated by SDS/PAGE. Unlike trichosanthin and α -momorcharin, trichoanguin contained two free cysteine residues, one located at residue 32 and the other at residue 155.

Sequence similarity and comparison between various RIPs

A comparison of the amino acid sequence of trichoanguin with sequences of trichosanthin and other RIPs (Figure 6) revealed that there is a high degree of similarity between them. A number of gaps and insertions have been made in the sequences to optimize the alignment, and the percentages of identity between trichoanguin and trichosanthin, α -momorcharin, ricin A-chain and abrin A-chain were found to be 55%, 48%, 36% and 34% respectively. There are several major regions of high sequence

similarity in these RIPs, i.e. regions of matching amino acids: residues 4–25, 66–85, 104–134, 146–166 and 182–190 of trichoanguin, with the last four regions clustering around the putative active-site cleft. In these regions, absolutely conserved amino acids are: Tyr-14, Phe-17, Arg-22, Tyr-70, Gly-107, Tyr-109, Ala-146, Glu-158, Ala-159, Arg-161, Glu-187, Asn-188 and Trp-190 in trichosanthin. It is interesting to note that the conserved residues Tyr-70, Tyr-109, Glu-158, Ala-159, Arg-161, Glu-187 and Trp-190 are clustered together around the proposed active-site cleft in the three-dimensional crystal structure of trichosanthin. The aromatic amino acids (Tyr-14, Phe-17, Tyr-70, Tyr-109 and Trp-190) are highly conserved in RIPs, and these aromatic residues are important in stabilizing the interactions between the bases of RNA and trichoanguin, which are involved in the N-glycosidase activity.

Molecular modelling of trichoanguin

The trichoanguin sequence was modelled with the coordinates of trichosanthin and α -momorcharin because these two proteins exhibited the highest sequence identity (55% and 48%) in the sequence comparison with trichoanguin [30]. Figure 7 shows that the α -carbon backbones of trichoanguin and α -momorcharin can be superimposed on the backbone of trichosanthin. The root-mean-square difference for aligned α -carbon positions between trichosanthin and trichoanguin was 0.520 Å, whereas that between α -momorcharin and trichosanthin was 0.502 Å. However, positional differences between the individual side chain positions might be substantially larger, particularly for the less constrained residues on the molecular surface. A schematic ribbon drawing of the known structure of trichosanthin is shown in Figure 8. To facilitate the discussion of the modelling of trichoanguin in relation to this structure, the secondary structural elements are numbered as described previously [30]. The model contains eight α -helices and a six-stranded β -sheet with a left-handed twist similar to that found in trichosanthin.

In Figure 8, trichoanguin was divided into two domains in accordance with the structural description of trichosanthin [30]. The main differences between trichoanguin and trichosanthin in domain 1 are located in the middle portion and in the loops connecting the secondary structural elements. Internally, there are differences at two residues between the two: deletions of residues 89 and 98 of trichosanthin. The first deletion removes one residue from helix 2 in trichosanthin. Because this helix is located on the molecular surface, the deletion is easily accommodated in trichoanguin. The second deletion shortens a surface loop connecting helix 2 and β -sheet 1.6 by the four-residue loop. It implies that this region might not be specifically crucial to the structure or function of trichoanguin. Trichoanguin has an insertion of one residue, Arg-202, in a loop connecting helix 7 and β -sheet 2.1. The antiparallel β -sheets (β 2.1 and β 2.2) of trichoanguin in C-terminal regions differ slightly from those in trichosanthin. The C-terminal part of trichoanguin is one residue shorter than that of trichosanthin and is predicted to be a 3_{10} helix.

Trichoanguin contains two free thiol groups: one, Cys-32, is located at the surface loop region; the other, Cys-155, located adjacent to the active site, seems to interfere with disulphide linkage formation. The four putative N-glycosylation sites Asn-51, Asn-65, Asn-201 and Asn-226 are located at the solvent-exposed surface or flexible loop in the modelled structure.

It has been suggested that amino acid residues lining the active site cleft are generally conserved within the RIP family, which might be important for substrate binding and catalysis (Figure 9). Eleven residues were found to be highly conserved in trichosanthin and trichoanguin: five of them, Tyr-70, Tyr-109, Glu-158, Arg-161 and Trp-190, directly form the major cleft in the crystal structure of trichosanthin, whereas the others, including Val-69, Ile-71, Phe-83, Asp-85, Gly-107 and Ile-153, are also located at the active-site cleft and are highly conserved between various RIPs.

DISCUSSION

In the present study it was found that the 19 residues at the N-terminal extension and the extra 30 residues at the C-terminal end of trichoanguin are removed post-translationally to yield the mature form. The 19-residue leader segment is a secretory signal sequence containing a higher content of hydrophobic amino acids, which is expected to direct transport of the nascent polypeptide chain across the endoplasmic reticulum membrane into the endoplasmic reticulum lumen [41]. Similar post-translational

processing mechanisms of a C-terminal extension for these RIPs were recently observed for the precursors of trichosanthin [42] and saporin-6 [43]. Four putative N-glycosylation sites, Asn-51, Asn-65, Asn-201 and Asn-226 (Figure 6), occur along the amino acid sequence of trichoanguin. In the modelled structure, all of these are located on the exposed surface of trichoanguin and are thus expected to be glycosylated (Figure 7).

It is noteworthy that modelling studies of these proteins have allowed us to visualize the prominent cleft, which has been suggested to comprise the active site of various RIPs [30]. The presence of conserved residues of similar amino acids around the proposed active-site cleft among trichoanguin, trichosanthin and α -momorcharin was clearly identified and confirmed. This similarity strengthens the notion that there could be a strong preservation of three-dimensional structure in these proteins with similar catalytic functions, with critical amino acid residues being conserved especially in the region of the active site.

Figure 9 shows a close-up view of the active centres of trichoanguin and trichosanthin. The residues constituting the active site of trichosanthin (Tyr-70, Tyr-111, Glu-160, Arg-163 and Trp-192) are fully conserved in trichoanguin. In trichosanthin, the key active-site residues, including Glu-160 and Arg-163, are directly involved in catalysis, whereas Tyr-70 and Tyr-111 have a crucial role in binding the rRNA loop. Trichoanguin possesses the same residues at its catalytic site and the rRNA loop-binding site. Most RIPs contain an acidic amino acid residue at position 85, which might provide a proton for protonating adenine. In trichosanthin, the N-7 atom of the adenine is protonated by Glu-85, which is replaced by Asp in trichoanguin and the abrin A-chain.

Many immunoconjugates of RIPs and specific antibodies have been evaluated *in vitro* and *in vivo* as potential therapeutic agents for the treatment of cancer and autoimmune diseases. When trichosanthin was conjugated to a hepatoma-associated antibody, the resultant immunotoxin was 500-fold more cytotoxic than free trichosanthin and only one order of magnitude less cytotoxic than free ricin [44]. By linking monoclonal anti-Thy1.1 antibodies to PAP or ricin A-chain through a disulphide bond, both conjugates were shown to specifically inhibit protein synthesis of Thy1.1-positive target leukaemic cells [45]. Cross-linking of saporin to an anti-CD4 antibody leads to effective killing of CD4⁺ cells [46]. Bryodin conjugated with anti-CD40 antibody was shown to be potently cytotoxic against CD40-expressing B-lineage non-Hodgkin's lymphoma and multiple myeloma cells [47]. Furthermore a conjugate of PAP with the anti-CD4 antibody was found to be very effective in inhibiting HIV-1 production [48].

From the above examples of immunotoxins applied to therapeutic uses, an important consideration for immunoconjugate assembly is the nature of the linkage between antibody and RIP. A disulphide linkage is usually thought to be essential for maximal cytotoxicity. Most type I RIPs do not have any free cysteine residues, which necessitates the modification of both antibody and RIP with chemical agents to produce the disulphide bond. Fortunately, trichoanguin contains two cysteine residues, one of which is located at the surface loop and can directly form a disulphide bond with an activated antibody thiol group via a disulphide-exchange reaction. Therefore trichoanguin is a novel free-cysteine-containing RIP, which might be ideal for the preparation of immunoconjugates with great potential as a chemotherapeutic agent for the treatment of various cancers or AIDS.

We thank Professor S.-H. Chiou (Institute of Biochemical Sciences, National Taiwan University, Taipei, Taiwan) for critical reading and comments on the manuscript. This

work was supported by grant NSC-87-2314-B-002-026 (to L.-P.C.) from the National Science Council, Taipei, Taiwan.

REFERENCES

- 1 Stirpe, F. and Barbieri, L. (1986) *FEBS Lett.* **195**, 1–8.
- 2 Stirpe, F., Gasperi-Campani, A., Barbieri, L., Falasca, A., Abbondanza, A. and Stevens, W. A. (1983) *Biochem. J.* **216**, 617–625.
- 3 Barbieri, L. and Stirpe, F. (1982) *Cancer Surv.* **1**, 489–520.
- 4 Stirpe, F., Barbieri, L., Battelli, M. G., Soria, M. and Lippi, D. A. (1992) *Biotechnology* **10**, 405–412.
- 5 Lamb, F. J., Roberts, L. M. and Lord, J. M. (1985) *Eur. J. Biochem.* **148**, 265–270.
- 6 Hung, C. H., Lee, M. C., Lee, T. C. and Lin, J. Y. (1993) *J. Mol. Biol.* **229**, 263–267.
- 7 Pataki, M., Lane, J. A., Lard, W., Bjorn, M. J., Wang, A. and Williams, M. (1998) *J. Biol. Chem.* **263**, 4837–4843.
- 8 Hung, C. H., Lee, M. C., Chen, J. K. and Lin, J. Y. (1994) *Eur. J. Biochem.* **219**, 83–87.
- 9 Irvine, J. D. (1975) *Arch. Biochem. Biophys.* **169**, 522–528.
- 10 Barbieri, L., Zamboni, M., Lorenzoni, E., Montanaro, L., Sperti, S. and Stirpe, F. (1980) *Biochem. J.* **186**, 443–452.
- 11 Kishida, K., Masuko, Y. and Hara, T. (1983) *FEBS Lett.* **153**, 209–212.
- 12 Stirpe, F., Barbieri, L., Battelli, M. G., Falasca, A. L., Abbondanza, A., Lorenzoni, E. and Stevens, W. A. (1986) *Biochem. J.* **240**, 659–665.
- 13 Stirpe, F., Williams, D. G., Ghyon, L. J., Legg, R. F. and Stevens, W. A. (1987) *Biochem. J.* **195**, 399–405.
- 14 McGrath, M. S., Hwang, K. M., Caldwell, S. E., Gaston, J., Luk, K. C., Wu, P., Ng, V. L., Crowe, S., Daniels, J., Marsh, J. et al. (1989) *Proc. Natl. Acad. Sci. U.S.A.* **86**, 2844–2848.
- 15 Huang, S. L., Huang, P. L., Nara, P. L., Chen, H. C., Kung, H. F., Huang, P., Huang, H. T. and Huang, P. L. (1990) *FEBS Lett.* **272**, 12–18.
- 16 Byers, V. S., Levin, A. S., Malkino, A., Waters, L., Robins, R. A. and Baldwin, R. W. (1994) *AIDS Res. Hum. Retroviruses* **10**, 413–420.
- 17 Kahn, J. O., Gorelick, K. J., Gatti, G., Arri, C. J., L'Esch, J. D., Gambertoglio, J. G., Bestrom, A. and Williams, R. (1994) *Antimicrob. Agents Chemother.* **38**, 260–267.
- 18 Lambert, J. M., Blattler, W. A., Monty, G. D., Goldmacher, V. S. and Scott, Jr., C. F. (1993) *Cancer Treat. Res.* **37**, 175–209.
- 19 Laemmli, U. K. (1970) *Nature (London)* **227**, 680–685.
- 20 Zacharous, R. M., Zeil, T. E., Morrison, J. H. and Woodlock, J. J. (1969) *Anal. Biochem.* **30**, 148–152.
- 21 Kato, M. and Akira, T. (1987) *J. Biochem. (Tokyo)* **102**, 243–246.
- 22 Thorpe, P. E., Brown, A. N. F., Ross, W. C. J., Cumber, A. J., Dittre, S. I., Edwards, D. C., Davies, A. J. S. and Stirpe, F. (1981) *Eur. J. Biochem.* **116**, 447–454.
- 23 Oda, T., Aizono, Y. and Funatsu, G. (1984) *J. Biochem. (Tokyo)* **96**, 377–384.
- 24 Wettstein, F. O., Staehelin, T. and Noll, H. (1963) *Nature (London)* **197**, 430–435.
- 25 May, M. J., Hartley, M. R., Roberts, L. M., Krieg, P. A., Osborn, R. W. and Lord, J. M. (1989) *EMBO J.* **8**, 301–308.
- 26 Chomczynski, P. and Sacchi, N. (1987) *Anal. Biochem.* **162**, 156–159.
- 27 Frohman, M. A., Dush, M. K. and Martin, G. R. (1986) *Proc. Natl. Acad. Sci. U.S.A.* **85**, 8998–9002.
- 28 Hubbard, T. J. P., Munir, A. G., Brenner, S. E. and Chothia, C. (1997) *Nucleic Acids Res.* **25**, 236–239.
- 29 Xiong, J. P., Xia, Z. X. and Wang, Y. (1994) *Nat. Struct. Biol.* **1**, 695–700.
- 30 Huang, Q. C., Lu, S. P., Jin, Y. Q. and Wang, Y. (1995) *Biochem. J.* **309**, 285–298.
- 31 Tanrov, T. H., Lu, T. H., Liaw, Y. C., Chen, Y. L. and Lin, J. Y. (1995) *J. Mol. Biol.* **250**, 354–367.
- 32 Mishra, D., Monzingo, A. F., Katzin, B. J., Ernst, S. and Robertus, J. D. (1993) *Protein Sci.* **2**, 429–435.
- 33 Sak, A. and Blundell, T. L. (1993) *J. Mol. Biol.* **234**, 779–815.
- 34 Brooks, B. R., Brucoleri, R. E., Olafson, B. D., States, D. J., Swaminathan, S. and Karplus, M. (1983) *J. Comp. Chem.* **4**, 187–217.
- 35 Laszowski, R. A., MacArthur, M. W., Moss, D. J. and Thornton, J. M. (1993) *J. Appl. Crystallogr.* **26**, 283–291.
- 36 Spoel, M. J. (1993) *Proteins* **17**, 355–362.
- 37 Bowie, J. U., Luthy, R. and Eisenberg, D. (1991) *Science* **253**, 164–170.
- 38 Luthy, R., Bowie, J. U. and Eisenberg, D. (1992) *Nature (London)* **356**, 83–85.
- 39 Kabach, W. and Sander, C. (1983) *Biopolymers* **22**, 2577–2537.
- 40 Koradi, R., Billeter, M. and Wuthrich, K. (1996) *J. Mol. Graphics* **14**, 51–55.
- 41 Butterworth, A. G. and Lord, J. M. (1983) *Eur. J. Biochem.* **137**, 57–65.
- 42 Chow, T. P., Feldman, R. A., Lovett, M. and Pataki, M. (1990) *J. Biol. Chem.* **265**, 8570–8574.
- 43 Benatti, L., Nitti, G., Solinas, M., Valsasina, B., Vira, A., Cerotti, A. and Soria, M. R. (1991) *FEBS Lett.* **291**, 285–288.
- 44 Wang, Q. C., Ying, W. B., Xie, H., Zhang, Z. C., Yang, Z. H. and Ling, L. Q. (1991) *Cancer Res.* **51**, 3353–3355.
- 45 Ramakrishnan, S. and Houston, L. L. (1984) *Cancer Res.* **44**, 1389–1404.
- 46 Ramakrishnan, S., Fryxell, D., Mohanra, D., Olson, M. and Li, B. M. (1992) *Annu. Rev. Pharmacol. Toxicol.* **32**, 579–621.
- 47 Francisco, J. A., Gawlak, S. L. and Siegfalt, C. B. (1997) *J. Biol. Chem.* **272**, 24165–24169.
- 48 Zarling, J. M., Moran, P. A., Haffar, O., Sas, J., Richman, D. D., Soria, C. A., Meyers, D. E., Kuebebeck, V., Ledbetter, J. A. and Ukun, F. M. (1990) *Nature (London)* **347**, 92–95.

Received 7 September 1998/20 October 1998; accepted 30 November 1998

Characterization of a saporin isoform with lower ribosome-inhibiting activity

M. Serena FABBRINI[✉], Emilia RAPPOCCIOLO^{*}, Daniela CARPANI^{*}, Michela SOLINAS[‡], Barbara VALSASINA[‡], Umberto BREME[‡], Ugo CAVALLARO^{*}, Anders NYKJAER[§], Ermanna ROVIDA^{*}, Giuseppe LEGNAME^{||} and Marco R. SORIA^{*}

^{*}Department of Biological and Technological Research – Dibit, San Raffaele Scientific Institute, via Olgettina 58, 20132 Milano, [†]Istituto Biosintesi Vegetali del Consiglio Nazionale delle Ricerche, via Bassini, 15, 20133 Milano, [‡]Biotechnology Department, Pharmacia & Upjohn, via Giovanni XXIII 20014 Nerviano, Italy, [§]Department of Medical Biochemistry, University of Aarhus, Ole Worms Alle, DK-800 Aarhus C, Denmark, and ^{||}Italfarmaco Research Center, via dei Lavoratori 54, 20092 Cinisello Balsamo, Milano, Italy

We have expressed in *Escherichia coli* five isoforms of saporin, a single-chain ribosome-inactivating protein (RIP). Translation inhibition activities of the purified recombinant polypeptides *in vitro* were compared with those of recombinant dianthin 30, a less potent and closely related RIP, and of ricin A chain. Dianthin 30, and a saporin isoform encoded by a cDNA from leaf tissue (SAP-C), both had about one order of magnitude lower activity in translation inhibition assays than all other isoforms of saporin tested. We recently demonstrated that saporin extracted from seeds of *Saponaria officinalis* binds to α 2-macroglobulin receptor (α 2MR; also termed low density lipoprotein-receptor-related-protein), indicating a general mechanism of interaction of plant RIPs with the α 2MR system [Cavallaro, Nykjaer, Nielsen and Soria (1995) *Eur. J. Biochem.*

232, 165–171]. Here we report that SAP-C bound to α 2MR equally well as native saporin. However, the same isoform had about ten times lower cytotoxicity than the other saporin isoforms towards different cell lines. This indicates that the lower cell-killing ability of the SAP-C isoform is presumably due to its altered interaction with the protein synthesis machinery of target cells. Since saporin binding to the α 2MR is competed by heparin, we also tested in cell-killing experiments Chinese hamster ovary cell lines defective for expression of either heparan sulphates or proteoglycans. No differences were observed in cytotoxicity using native saporin or the recombinant isoforms. Therefore saporin binding to the cell surface should not be mediated by interaction with proteoglycans, as is the case for other α 2MR ligands.

INTRODUCTION

Plants synthesize toxic ribosome-inactivating proteins (RIPs), that are *N*-glycosidases (EC 3.2.2.22) recognizing a specific adenine (A4324 in the rat) located in a universally conserved stem-loop region of 28S ribosomal RNA. The most representative RIP is ricin, which in addition to the catalytic A-chain subunit contains a B-chain that allows it to attach to and enter the cells. Conversely, single-chain or type I RIPs, like saporin, lack the B-chain [1]. RIPs might have great therapeutic potential as chimaeric toxins, obtained with either genetic [2] or biochemical manipulations, such as immunotoxins [3] or toxin conjugates [4,5]. Thus they are useful for treating cancer and autoimmune diseases and also against HIV infection [6]. By virtue of their antiviral properties, type I RIPs might also be used to improve defence mechanisms of transgenic plants of interest [7,8].

Saporin extracted and purified from seeds of *Saponaria officinalis* (SAP-S) was found initially to be heterogeneous at two amino acid positions, i.e. residues 48 (Asp or Glu) and 91 (Arg or Lys) ([9,10]; G. P. Nitti, unpublished work). This predicted the existence of at least four seed isoforms and, indeed, several different genomic clones were successively identified, confirming the existence of a multigene saporin family [11]. In addition, a leaf cDNA clone had been found to encode a saporin precursor, giving rise to a mature polypeptide of 253 amino acids that differed from SAP-S at 13 amino acid residues [12,13]. In contrast with type II RIPs, type I RIPs are active not only against

eukaryotic but also against prokaryotic ribosomal RNA [14]. Initial attempts to express dianthin 30 [15], as well as other type I RIPs in *Escherichia coli*, did not involve tightly controlled systems of expression and were unsuccessful, as reported for Mirabilis antiviral protein [16], pokeweed antiviral protein (PAP) [17] and saporin [11]. Thus presumably type I RIPs are all toxic to *E. coli* ribosomes to various extents, whereas type II RIPs are not [14]. In addition, all RIPs display different specificities for ribosomes from different sources [1]. Indeed, RIPs must first interact with the complex structure of the ribosomes in order to recognize and then depurinate target rRNA. Therefore steps towards elucidating structure, function relationships among type I and type II RIPs would be highly desirable in order to engineer highly selective cytotoxins.

EXPERIMENTAL

Plasmids, strains and DNA manipulations

BL 21 (DE3) pLysS (Novagen) strain was used for expression of recombinant proteins. The pET-11d plasmid (Novagen) was used in all the constructs. A single *Nco*I site (CCATGA) provides the translational starting codon. A *Sac*II–*Eco*RI fragment from sequence 3 DNA [11] was ligated to pET-11d DNA digested with *Eco*RI and *Nco*I in the presence of a linker-adaptor containing *Nco*I–*Sac*II sites. The pET-11d SAP-3 construct was sub-

Abbreviations used: RIP, ribosome-inactivating protein; SAP, saporin isoform; α 2MR, α 2-macroglobulin receptor; PAP, pokeweed antiviral protein; RP–RP, reversed-phase HPLC; 3D, three-dimensional; TFA, trifluoroacetic acid; TCA, trichloroacetic acid; CHO, Chinese hamster ovary; RAP, receptor-associated protein; LpL, lipoprotein lipase; RNP, ribonucleoprotein.

✉ To whom correspondence should be addressed.

sequently engineered by substituting the original *Bam*HI-*Eco*RI fragment with 690 bp purified *Bam*HI-*Eco*RI genomic fragments from sequences 1, 4 and 6 genomic clones. This yielded pET-11d SAP-1, pET-11d SAP-4 and pET-11d SAP-6 respectively. With sequence 6, an *Ssp*I restriction site allowed selection of recombinant clones. An *Xba*I restriction site could be used instead to select recombinants for the other saporin clones, since sequence 3 lacks this site. The saporin-coding leaf cDNA [12] was mutated to introduce a stop codon before the encoded C-terminal propeptide [13]. The resulting construct, pET-11d-SAP-C, was then fully sequenced to confirm that no changes were introduced during the amplification step. DNA sequencing was performed using the Pharmacia (Uppsala, Sweden) T7 sequencing kit. Oligonucleotides were synthesized with a 380B automatic DNA synthesizer (Applied Biosystems).

Expression and purification of recombinant saporin isoforms

Induction of expression of the toxic genes was essentially following manufacturer's instructions (Novagen). A single-step purification by ion-exchange chromatography was performed, loading soluble fractions of protein onto a Mono S[®] HR 5/5 FPLC[®] column as described [18]. Total *E. coli* extracts and fractions from column chromatography purifications were loaded onto 12.5% and 15% (w/v) polyacrylamide gels respectively. For Western blot analysis, proteins transferred onto nitrocellulose were probed with a rabbit anti-saporin antiserum at a 1:1000 dilution, and detected with goat anti-rabbit-horseradish peroxidase-conjugate antiserum [11]. Polyclonal rabbit antibodies directed against native saporin were generously given by D. A. Lappi, Advanced Targeting Systems, San Diego, CA, U.S.A.

Protein content in the peak fractions from ion-exchange chromatography purifications was determined with the Bio-Rad Protein Assay. Bovine serum albumin (Bio-Rad) and native saporin were utilized as standards.

Reversed-phase HPLC (RP-HPLC) and electrospray mass analysis

Native seed-extracted saporin, and all the recombinant isoforms were subjected to RP-HPLC on a Hewlett Packard 1090M apparatus (Wilmington, DE, U.S.A.) using a 1 × 250 mm, 218 TD C18 Vydac column (The Separation Group, Hesperia, CA, U.S.A.). Mobile phases A and B were respectively 0.1% trifluoroacetic acid (TFA) in Milli-Q grade water and 0.078% TFA in acetonitrile. Elutions were carried out with a linear gradient of buffer B from 25% to 79% in 25 min at a flow rate of 0.085 ml/min. Separations were performed at 50 °C and elution profiles were monitored with a Hewlett Packard 1040A Diode array detector at the wavelength of 215 nm.

On-line RP-HPLC/electrospray mass spectrometry was performed with samples of SAP-S, SAP-6 and SAP-C (a saporin isoform encoded by a cDNA from leaf tissue) on a Hewlett Packard 5989S MS-Engine single quadrupole instrument equipped with a Hewlett Packard 59987A electrospray interface. Eluates from the RP-HPLC were directly injected into the ion source of the mass spectrometer. The electrospray potential was approx. 6 kV. The quadrupole mass analyser was set to scan over a mass-to-charge ratio (*m/z*) from 1000 to 1700, at 2 s per scan for a total time of 10–12 s. The sum of data acquired over this time constituted the final spectrum. Molecular masses were calculated from several multiply-charged ions within coherent series. Mass calibrations were performed with horse skeletal muscle myoglobin (Sigma).

N-terminal sequence analysis

For protein sequence analysis, samples of SAP-3, SAP-4 and SAP-C after SDS/PAGE were electroblotted onto polyvinylidene difluoride membranes (Fluorotrans) at 300 mA for 45 min using 10 mM 3-(cyclohexylamino)-1-propanesulphonic acid (pH 11) in 10% (v/v) methanol as transfer buffer. The membrane was stained for 1 min in Coomassie Blue R250/methanol/acetic acid (1:400:100, by vol.) and destained in 50% methanol for 5 min. Bands were excised from the membrane and arranged in the cartridge block of the sequencer. Automated Edman degradation was performed on a pulsed-liquid-phase Sequencer, model 477 (Applied Biosystems) equipped with a Mod. 120 A HPLC instrument for detection of phenylthiohydantoin amino acids.

Biological assays of ribosome-inhibiting activities

Serial log dilutions ranging from 40 nM to 0.4 pM final concentration of each isoform in phosphate-buffered saline (PBS) were assayed in duplicate, dispensing 2 µl of each dilution in Eppendorf tubes on ice. A reaction mixture containing 2.5 µCi of tritiated leucine (L-[4,5-³H]leucine, 45–85 Ci/mmol, Amersham International), 250 ng of bromine mosaic virus RNA and 0.053 mM amino acid mixture without leucine was added in 3 µl samples. Nuclease-treated rabbit reticulocyte lysate (10 µl; Promega, Madison, WI, U.S.A.) thawed on ice was added to the assay tubes. Samples of 15 µl final volume were incubated at 30 °C for 60 min. The SAP-C dilutions tested range from 700 nM to 7 pM final concentration. At the end of incubations, samples were chilled on ice, brought to 0.1 mg/ml final concentration of ribonuclease A then further incubated at 23 °C for 20 min. To quantify the amount of radioactivity incorporated into translated protein, spots were made in triplicate on 3MM Whatman filter paper cut into small pieces. The filters were washed four times, 10 min each with 5% ice-cold trichloroacetic acid (TCA; 5 ml/filter), then boiled for 1 min in 5% TCA and washed with ice-cold 95% ethanol twice. Filters were dried at 65 °C for 30 min and then radioactivity was measured by liquid scintillation counting. Recombinant dianthin-30 mature polypeptide was also assayed for comparison, as well as recombinant ricin A chain (kindly supplied by J. Michael Lord, University of Warwick, U.K.). The concentration inhibiting translation by 50% (*IC*₅₀) was 200 pM for recombinant ricin A chain when tested in these assays. The program MacALLFIT was used to process and evaluate the data from SAP-C, SAP-3, SAP-4 and SAP-S inhibition assays. Saporin RIP activities were also tested in rabbit reticulocyte lysates measuring inhibition of luciferase mRNA translation. Light emission of translated luciferase was measured in a Berthold LB Lumat luminometer. Inhibition of translation was reported as a decrease of light emission, i.e. as a percentage of control luciferase translated in the absence of saporin, which corresponds to 100% of light emitted. Negative translation controls in the presence of the same concentrations of non-toxic proteins (carbonic anhydrase or bovine serum albumin) were identical with the control (results not shown). The *IC*₅₀ of SAP-C was 125 pM whereas that of recombinant ricin A chain was 80 pM in these assays.

Cytotoxicity experiments

At least two independent cell-killing experiments were performed using each of the following cell lines: murine LB6, treated as described in [5], the human permanent cell line EA.hy 926, obtained by fusing human umbilical vein endothelial cells with

the tumour cell line A549 [19] and treated as in [20]. Three Chinese hamster ovary (CHO) cell lines: CHO-K1, the parental control cell line, and the two defective cell lines CHO-745 [21] proteoglycan-deficient, and CHO-677 [22] heparan sulphate-deficient, were kindly provided by J. Esko, University of California, La Jolla, CA, U.S.A. All three CHO cell lines were cultured in Ham's F12 medium (ICN, Costa Mesa, CA, U.S.A.) supplemented with 7.5% fetal bovine serum, 100 units/ml penicillin, 0.1 mg/ml streptomycin sulphate and plated at a density of 3.75×10^4 cells per ml in 80 μ l/well. Briefly, cells were plated on gelatin-coated 96-well plates (Costar, Cambridge, MA, U.S.A.) 16–18 h before the experiments, and treated for either 24 h (LB6) or 48 h (CHO and EA.hy 926) in the absence or in the presence of serial log dilutions (ranging from 1 nM to 1000 nM final in 100 μ l/well) of either native saporin or the recombinant isoforms SAP-3 and SAP-C. Each point was tested in quadruplicate. At the end of the incubations in the presence of toxins, cells were washed with PBS then pulse-labelled for 2 to 4 h with L-[4,5- 3 H]leucine (45–85 Ci/mmol, Amersham International) at 0.5 μ Ci/well. Total incorporation of radioactivity into protein was measured by harvesting cells on glass fibre filters and liquid scintillation counting. Cytotoxicity was calculated measuring the ID_{50} .

Binding of 125 I-labelled α 2-macroglobulin receptor (α 2MR) to immobilized saporin

Wells of microtitre plates (Polysorp, Nunc, Denmark) were coated with 1 μ g (100 μ l of 10 μ g/ml) of either native or recombinant saporin isoforms in 50 mM NaHCO₃, pH 9.6, for 2 h to provide about 80 ng (2.7 pmol) of immobilized saporin/well. After blocking with binding buffer (10 mM Hepes/140 mM NaCl/2 mM CaCl₂/1 mM MgCl₂, pH 7.8) containing 2% Tween-20 for 2 h at 20 °C, microtitre wells were washed three times and incubated with 5–10 pM 125 I-labelled α 2MR in binding buffer containing 0.2% BSA for 16 h at 4 °C. Following a wash with binding buffer, bound radioactivity was eluted in 10% SDS and counted in a Packard (Meriden, CT, U.S.A.) gamma-counter. In the absence of immobilized saporin, binding of 125 I-labelled α 2MR (blank value) amounted to less than 0.2%. All values have been corrected accordingly. For competition assays, 125 I-labelled α 2MR (10 pM) was added to the wells in the presence of either 400 nM receptor-associated protein (α 2MRAP) or 800 nM lipoprotein lipase (LpL, Sigma L-2254), which was dialysed overnight against binding buffer.

Multiple alignments, prediction of saporin secondary structure and three-dimensional (3D) structure comparisons

The sequences of saporin, trichosanthin, PAP, momorcharin and ricin used for our alignments were obtained from release 29 of the Swissprot sequence database. Multiple alignments were performed using the program PILEUP of the WISCONSIN package, version 8.0, based on the progressive alignment method [23] followed by manual adjustment. Co-ordinates of PAP (code IPAG), α -momorcharin (IAHB) and ricin A chain (Irtc) were obtained from the Brookhaven structure data bank [24]. The superposition of the known 3D structures was performed within the QUANTA (Molecular Simulations) molecular modelling package using a least-squares fitting algorithm [25]. For the secondary structure prediction of saporin, the method PHD [26] was used. The overall three-state accuracy was improved by up to 72% [26].

RESULTS

Construction and selection of clones coding for mature saporin isoforms

Figure 1 is a schematic representation of the strategy used to subclone the sequences coding for the mature polypeptides of the different saporin isoforms in the pET-11d expression vector. The isoform encoded by the sequence 3 genomic clone [11], coding for the isoform termed SAP-3, was previously expressed in *E. coli* fused to a bacterial signal sequence. Almost all the recombinant saporin was expressed intracellularly in an insoluble form, although some was exported to the periplasmic space. N-terminal sequencing of purified osmotic shock extracts indicated that part of the plant-encoded signal peptide was still present in the recombinant product. Yet the RIP activity of the recombinant saporin was 20 pM, almost identical with that of SAP-S [11]. Therefore the DNA of the genomic clone sequence 3 was digested with *Sac*II and *Eco*RI to remove the encoded leader peptide of saporin. Purified DNA was ligated to *Nco*I/*Eco*RI-cut pET-11d DNA in the presence of a specific adapter bearing *Nco*I and *Sac*II sites and restoring the missing coding sequence of mature SAP-3. Since all the differences in amino acid residues present

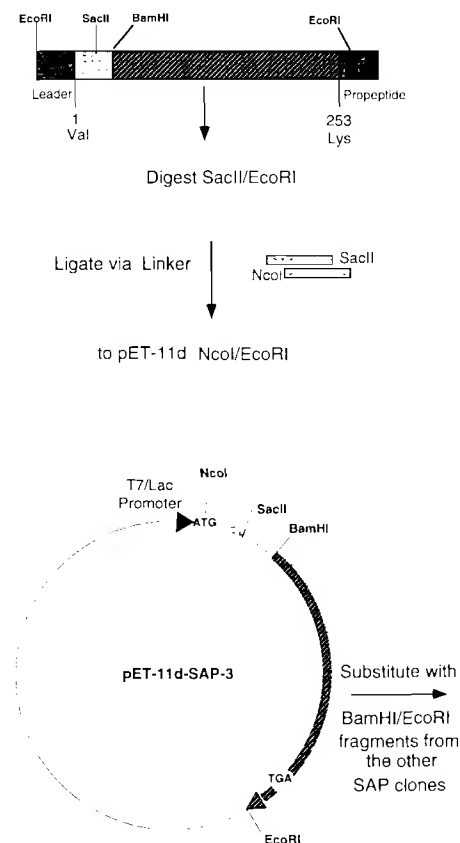


Figure 1 Schematic representation of the saporin-coding region and details of the pET-11d expression constructs

The N-terminal leader sequence and the C-terminal propeptide of preprosaparin (upper part of the Figure) are shown together with the first and the last amino acid residue found in mature saporin. The light grey box corresponds to the common N-terminal part of mature saporin. Restriction enzyme sites used for cloning the mature saporin-coding portions are also indicated.

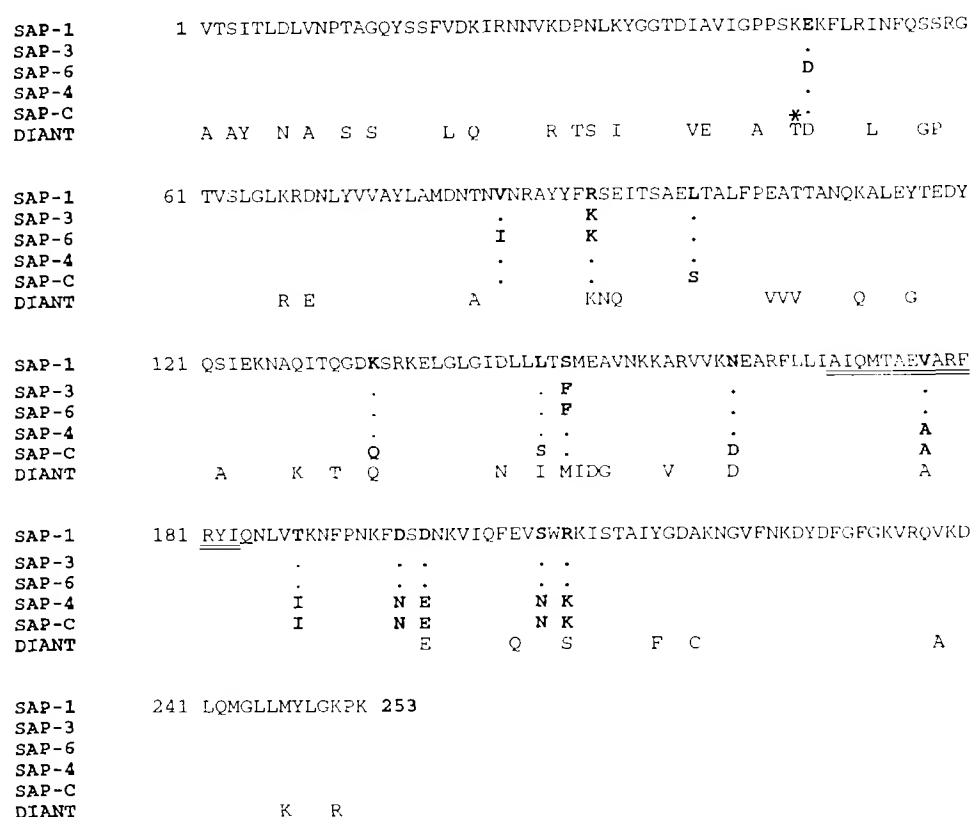


Figure 2 Protein sequence alignment of the saporin isoforms expressed in *E. coli*

The complete amino acid sequence of SAP-1 is shown. Dots identify conserved residues among SAP-1 and the other saporin isoforms, whereas variations in amino acid residues are indicated with bold type. Underlined is the ribosomal inactivating active site signature. The dianthin 30 (DIANT) sequence is also compared and aligned, and only the residues differing from SAP-1 are shown. The asterisk indicates that after Thr¹⁸¹ a second threonine is found in dianthin 30 which has been omitted to optimize the alignment.

among the other encoded isoforms are contained within a DNA stretch between two unique restriction sites, *Bam*HI and *Eco*RI. pET-11d-SAP-3 was used to obtain all subsequent constructs, substituting the original *Bam*HI–*Eco*RI fragment with those encoding the other isoforms (for details, see Experimental section). Thus only the ATG start codon is present before the sequence coding for the various mature saporin isoforms.

Expression and purification of saporin isoforms

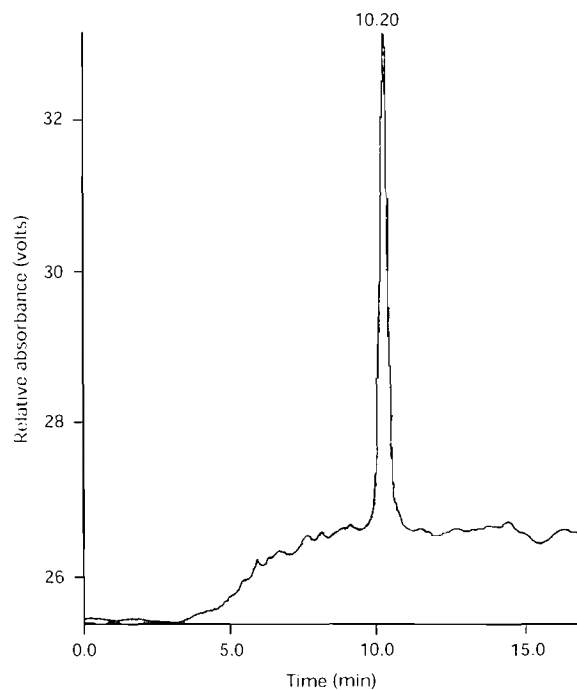
In Figure 2 the aligned amino acid sequences of the recombinant mature saporins are shown. We have expressed the mature saporin polypeptides, termed SAP-1 and SAP-3 following the numbering of the respective genomic coding sequences [11], as well as the isoform termed SAP-6, as three representatives of seed-type isoforms. SAP-1 has one of the four possible seed-type amino acid patterns at residues 48 and 91; however, instead of having Phe⁴⁹, which is present in the two other seed-type isoforms, it has Ser⁴⁹, like the SAP-C isoform (Figure 2). In addition, SAP-6 has Ile⁹¹, instead of Val, which is present in all the other isoforms; however, we cannot exclude the possibility that this variant might be an artifact due to the DNA amplification step. We also expressed a polypeptide closely resembling SAP-C, herein referred to as SAP-4, encoded by DNA sequence 4 [11]. Thus SAP-C and SAP-4 differ from all the other saporin isoforms only in a few residues, mainly located in a region of

saporin close to the adenylate-binding site [11,27]. The protein sequence of dianthin 30 is also shown for comparison. When dianthin 30 was expressed in *E. coli* with the same host-vector system that we used here, the IC₅₀ observed in cell-free inhibition assays was the same as that of native dianthin, i.e. about 300 pM [18]. SAP-C differs from SAP-4 in four residues (Figure 2), two of them being shared only with dianthin 30, i.e. Gln¹⁸¹ and Asp¹⁸².

Tightly controlled conditions are required for efficient expression of the saporin and dianthin 30 genes in *E. coli*, since these recombinant RIPs are quite toxic to the bacterial host [14]. Non-induced or induced bacteria were lysed, sonicated and cell lysates were ultracentrifuged as described [18]; soluble and insoluble protein fractions were then analysed by SDS/PAGE, followed by immunoblot analysis using rabbit anti-saporin antiserum. No leaky expression of toxic saporin genes was observed before induction of T7 RNA polymerase. After induction, bacteria expressing the SAP-C isoform were growing at a faster rate than those expressing the other saporin isoforms, such that higher protein yields would be obtained both in the soluble and in the insoluble fractions. Yields of soluble recombinant seed-type saporin isoforms were between 1 and 3 mg/litre of culture, similar to those of recombinant PAP expressed using the same host-vector system described here [17]. However, yields were lower than those of the SAP-C isoform and of recombinant mature dianthin 30 (up to 10 mg/litre of culture

Table 1 HPLC-separated peak fractions of recombinant isoformsExpected M_r values do not take into account the N-terminal methionine

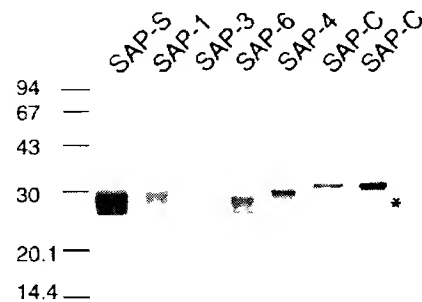
	Expected M_r	Mono-S* retention time (min)	RP-HPLC retention time (min)
SAP-1	28 560	9.37	20.45
SAP-3	28 592	9.92	21.54
SAP-6	28 592	9.92	21.61
SAP-4	28 555	8.63	19.83
SAP-C	28 505	10.20	19.65

**Figure 3** Ion-exchange chromatography purification of a saporin isoform

The elution profile of SAP-C is shown as representative of an HPLC purification performed after loading of *E. coli* soluble extracts; x-axis, time in min ($\times 10^3$); y-axis, UV monitoring expressed as differential of potential. Retention time (min) corresponds to the SAP-C elution peak.

[18]), suggesting that the latter RIPs possessed lower *E. coli* host toxicity (results not shown).

In all the extracts analysed, the soluble fraction contained the vast majority (90%) of recombinant protein, and was therefore used for purifying the different isoforms. A single-step purification was performed by ion-exchange HPLC, exploiting the high isoelectric point of saporin. All the isoforms eluted as single peaks around 150 mM NaCl, as did recombinant, mature dianthin 30 purified using the same procedure [18]. They also had similar retention times (Table 1), ranging from 8.63 min for SAP-4 to 10.20 min for SAP-C, whose elution profile is shown in Figure 3. The peak fractions from ion-exchange chromatography were analysed by SDS/PAGE followed by Coomassie Blue staining (Figure 4). The recombinant proteins had the expected relative molecular mass (M_r) of approx. 29000 as SAP-S. The three recombinant seed-type isoforms SAP-1, SAP-3 and SAP-6 behave

**Figure 4** SDS/PAGE analysis of the recombinant, purified saporin isoforms

Equivalent amounts of the peak fractions (approx. 1.2 μ g) from column chromatography purifications were run on a 15% polyacrylamide gel, then stained with Coomassie Brilliant Blue, with the exception of SAP-S and SAP-C (3 μ g). The asterisk in the right most lane identifies a faster migrating band in SAP-C. Markers ($10^3 \times M_r$) are also indicated.

similarly, showing electrophoretic patterns most resembling that of non-recombinant, native saporin extracted and purified from seeds (SAP-S). The presence of a diffuse band, almost appearing as two bands with a smear between them, was always observed with SAP-S, and was suggested to be an artifact due to the isoelectric point of 10.5 measured for native saporin [28]. Conversely, both SAP-C and SAP-4 isoforms migrated as a sharper band with slightly lower electrophoretic mobility (Figure 4). However, their theoretical pIs cannot account for their different mobilities. By increasing the amount of SAP-C loaded onto the gels, a faint faster-migrating band can also be detected (Figure 4, asterisk). Interestingly, it has been reported that leaf-extracted saporins show on SDS/PAGE an M_r higher than the seed-extracted protein by approx. 1500–2000 [29].

Biochemical characterization of recombinant saporin isoforms

To assess the purity of the peaks from our ion-exchange chromatography purifications, the recombinant isoforms were also subjected to RP-HPLC. A single peak was eluted in each case, as shown for SAP-C (Figure 5, top). Retention times obtained with each recombinant isoform are summarized in Table 1.

In addition, the M_r was accurately estimated by electrospray analysis of SAP-C and SAP-6 isoforms. For comparison, native seed-extracted saporin was also analysed. The mass spectrum of SAP-S was centred on the value of M_r 28 560 when directly injected in the ionization chamber. However, since SAP-S is known to be heterogeneous, the mass spectrum analysis was performed with SAP-S previously subjected to RP-HPLC purification. Figure 5 (bottom) shows that three peaks were eluted by RP-HPLC, having retention times of 19.83, 20.44 and 21.65 min. The two main peaks accounted for about 35% and 60% of the total protein respectively. Mass spectra of peak A were resolved to three values of M_r 28 546, 28 555 and 28 557. Peak B yielded a single value of M_r 28 557. The same analysis was performed with the recombinant isoforms SAP-C and SAP-6, coupling RP-HPLC separation to electrospray mass analysis. The single RP-HPLC peak of SAP-C was resolved into two mass values of 28 502.4 and 28 617.6, representing respectively 46% and 54% of the total. A similar situation was observed with SAP-6. The RP-HPLC peak was resolved into two mass values of 28 574 and 28 715 representing respectively 24% and 76% of the total. Therefore, in the case of the recombinant isoforms, the

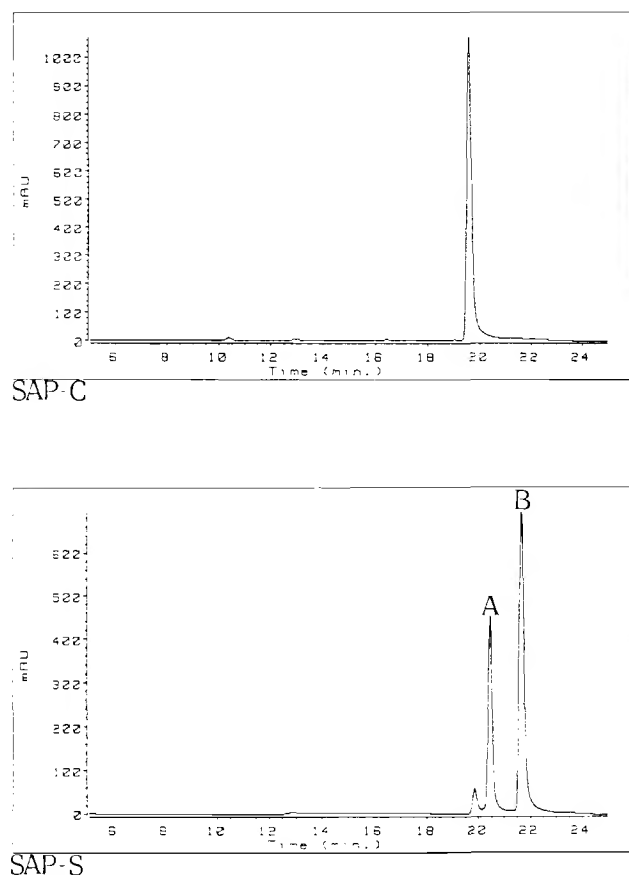


Figure 5 RP-HPLC analysis of SAP-S and SAP-C

(Top panel) The elution profile of SAP-C is shown as a representative example. All recombinant isoforms were loaded onto a C18 Vydac column and eluted using a linear gradient from 25 to 75% v/v acetonitrile at 50 °C. A single peak was obtained in each case. (y-axis) UV monitoring expressed as differential of potential. (Bottom panel) For comparison, elution profile of native seed-extracted saporin.

Table 2 Comparison between SAP-3 and SAP-C RIP activities

*Means \pm S.E.M. of at least two experiments each counted in triplicate. †Means \pm S.D. of one representative experiment performed in quadruplicate. N.D. = not determined

	SAP-3	SAP-C	SAP-S
Cell-free IC_{50} (pM)	17 ± 4	157 ± 27	12 ± 5
Cell lines IC_{50} (pM)			
EA.hy 926	20 ± 5	200 ± 30	N.D.
LB6	50 ± 15	500 ± 50	N.D.
CHO-K1	150 ± 30	> 1000	90 ± 10
CHO-745	150 ± 30	> 1000	100 ± 20
CHO-677	150 ± 25	> 1000	150 ± 30

presence of two mass spectra should be solely related to either the presence or the absence of an N-terminal methionine. The accuracy of mass determinations was 99.9% (Table 1).

The RP-HPLC coupled to electrospray mass analysis of recombinant seed-type isoform SAP-I (which correspond to the same batch of preparation of the protein loaded onto the SDS/PAGE) revealed the presence of a single mass of 28683.

Table 3 Binding of SAP-C to the $\alpha 2$ MR

Binding of 125 I-labelled $\alpha 2$ MR was measured as described in the Experimental section and is expressed as the percentage of added tracer. Data are means \pm S.D. of a representative experiment performed in triplicate. N.D. = not determined.

	125 I-labelled $\alpha 2$ MR bound (%)	
	SAP-C	SAP-S
Total binding	12.42 ± 1.8	11.89 ± 2.3
+ EDTA (5 mM)	3.67 ± 0.22	3.81 ± 0.62
+ heparin (10 IU/ml)	0.92 ± 0.34	1.68 ± 0.30
+ LpL (800 nM)	0.88 ± 0.11	N.D.
+ RAP (400 nM)	1.40 ± 0.53	N.D.

thus corresponding to 100% of polypeptide still bearing the initiator Met. The electrophoretic pattern shows, however, two migrating bands as observed with the native seed-extracted saporin.

The isoforms SAP-3, SAP-4 and SAP-C were further characterized by N-terminal sequencing. After PVDF-blotting either the smeared band of SAP-3 or those corresponding to SAP-4 and SAP-C were excised and microsequenced. Each isoform had either Met or Val as first amino acid residue, as detected by automated Edman degradation of the purified polypeptides. The relative percentages of Met and Val were respectively 52% and 48% for SAP-3, and 60% and 40% for both SAP-4 and SAP-C.

Ribosome-inactivating activity of recombinant saporin isoforms

The specific ribosome-inhibiting capabilities of the natural and of the recombinant proteins were compared using a cell-free translation system (Experimental section), assaying activities of these RIPs in serial log dilutions. The saporin isoforms SAP-1, SAP-6, SAP-4 and SAP-3 all had IC_{50} values of approx. 10–20 pM, like that of SAP-S, as previously observed [11]. In contrast, SAP-C showed an IC_{50} of 175 pM in the range of activity of the less potent RIP dianthin 30. Processing these data using a statistical program, MacALLFIT, yielded the IC_{50} s for SAP-3, SAP-C and SAP-S shown in Table 2.

We next compared the cytotoxicity of the recombinant proteins in cell-killing experiments, testing LB6 murine cells and the human hybrid permanent cell line EA.hy 926. In two independent experiments, SAP-3 was equally cytotoxic with SAP-S on both LB6 [5] and EA.hy 926 [20] cells, whereas SAP-C had lower cytotoxicity (approx. 10-fold less than that of SAP-3) with both LB6 and EA.hy 926 (Table 2) cells.

Great efforts are currently ongoing to identify sequential events starting from cell-surface toxin binding to the final step, taking place in the cytosol, of ribosome depurination. Most of these studies have been carried out on the internalization pathway of the ricin holotoxin [30]. We previously demonstrated that saporin entry into the cells is not a passive mechanism as was generally believed, but is mediated by a large and widespread receptor, the $\alpha 2$ MR [31]. $\alpha 2$ MR is a multifunctional endocytic receptor bearing multiple binding sites [32]. Therefore we performed solid-phase binding experiments to $\alpha 2$ MR, comparing SAP-S with the recombinant SAP-3 and SAP-C isoforms. In this assay, SAP-3 was able to bind to $\alpha 2$ MR as efficiently as SAP-S (A. Nykiaer, unpublished work). In addition, SAP-C also bound equally well to $\alpha 2$ MR (Table 3). Binding could be inhibited by EDTA, heparin and both the competitors LpL and RAP, as

previously shown for SAP-S [31]. This confirms the specificity of α 2MR binding (Table 3).

Finally, since heparin competed with the binding of saporin isoforms to α 2MR, we compared the cytotoxicities of SAP-S, SAP-3 and SAP-C in CHO cell lines defective in proteoglycan biosynthesis [22]. We tested mutant 745, which lacks one of the first acting enzymes, xylosyltransferase; therefore, assembly of both heparan sulphate and chondroitin sulphate does not take place. This mutant has less than 15% proteoglycans compared with wild-type CHO cells. Conversely, mutant 677 is defective specifically in heparan sulphate biosynthesis but makes about three times as much chondroitin sulphate as the wild-type cell line. When we tested either SAP-S or the recombinant isoforms on these CHO cell lines, no differences could be observed in specific cytotoxicity between wild-type and mutant CHO cells (Table 2).

DISCUSSION

Plants express several RIP isoforms in a tissue-dependent [33,34] and season-dependent fashion [1,35], but the reason for such wide heterogeneity remains unclear. This might represent a plant defence mechanism. Indeed, depurination of tobacco ribosomes catalysed by several RIPs correlates, for instance, with their antiviral activity in the infected plants [8]. Moreover, ribosomes from several species of dicotyledonous plants are sensitive to their own RIP, including PAP [36], dianthin 32 [37] and saporin [2].

In this study we have expressed several saporin isoforms in *E. coli* and compared their RIP activities, as a first step to determining whether amino acid variations present among them could reflect different specificities or catalytic properties. Three seed-type (SAP-1, SAP-3, SAP-6) as well as two closely related isoforms termed SAP-C and SAP-4 were selected for expression.

After purification of the recombinant isoforms, we observed that seed-type isoforms migrated on SDS-PAGE with a pattern similar to that of native saporin, whereas SAP-C and SAP-4 showed a different electrophoretic behaviour. However, by RP-HPLC only one single peak was eluted on loading each of the recombinant isoforms, while SAP-S was confirmed to be heterogeneous. Although the electrophoretic mobility of SAP-C is altered, accurate mass analysis showed that SAP-C has an M_r consistent with its theoretical one. Therefore the reason for the heterogeneity in the electrophoretic mobilities of our saporin isoforms remains unclear. Similarly aberrant electrophoretic mobilities had been observed previously, e.g. a decrease in mobility after removal of a protein's signal peptide [38]. Also, the relative mobility of a mutant G-protein was affected by a single amino acid change [39].

The specific inhibitory activity of the saporin isoforms was compared with that of seed-extracted saporin and of recombinant dianthin 30. Only the recombinant highly expressed leaf isoform, SAP-C, showed similar potency to dianthin 30, whereas all the other recombinant isoforms had similar RIP activity to the seed-extracted saporin. Saporin isoforms extracted from leaves of *S. officinalis* showed almost one order of magnitude lower inhibitory activity in rabbit reticulocyte lysates, when compared with seed isoforms extracted from the same plants [34]. However, only the N-terminal sequences of these isoforms were determined and none of them matches the recombinant isoforms expressed in our work [34].

A truncated saporin lacking the first 28 residues of the mature peptide had virtually no depurinating activity [40]. Indeed, Tyr¹⁶ and Arg²⁴ are invariant residues, present in saporin and dianthin as well, which are thought to play a crucial role in stabilizing a

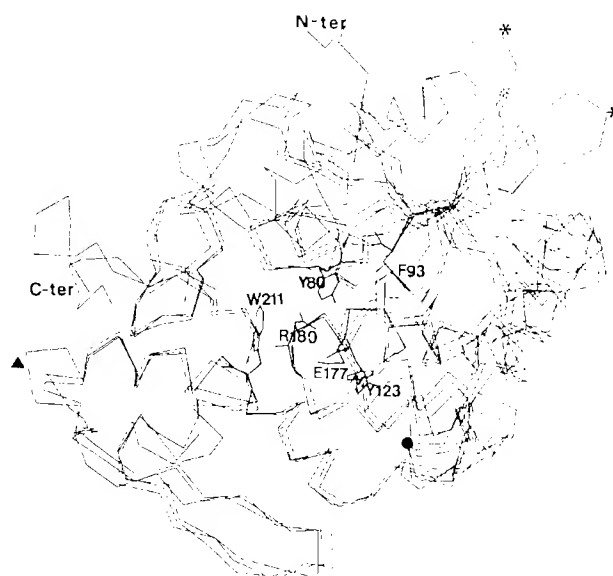


Figure 6 Superposition of C α traces

C α traces of superposed X-ray structures of ricin A chain, PAP and momorpharin are shown. The N-terminus and the prominent loop at the C-terminus of ricin A chain are indicated together with the position of key active site residues. The asterisks identify the loops (80–85) and (107–111) protruding from the PAP structure, and the solid triangle corresponds to a loop (203–205) in momorpharin. The solid circle marks the putative position of the saporin exposed residue Lys¹²⁶, which is substituted by Gln in SAP C-ter. terminus.

helix bend, allowing the two catalytic residues Glu¹⁷⁷ and Arg¹⁸⁰ of ricin to interact [41]. Also, it was demonstrated that aromatic and charged residues in the first α -helix of ricin A chain, at the N-terminus, are necessary for ricin activity [42]. Iodination of extractive saporin at Tyr residues results in protein aggregation and, presumably, in an inactive RIP (U. Cavallaro, unpublished work). Thus arginine and tyrosine residues at the N-terminus might be involved in correct saporin folding as well. In this work, N-terminal sequencing of recombinant SAP-C confirmed that no degradation at the N-terminus was present. The presence of the initiator methionine should not affect the catalytic RIP activity of either recombinant saporin isoform and might simply reflect a low efficiency in its removal by the *E. coli* methionyl-amino-peptidase. Mis-folding of the SAP-C isoform was ruled out because SAP-C was expressed at high level in soluble form and was resistant to protease degradation to the same extent as SAP-S (M. S. Fabbrini, unpublished work). Far-UV circular dichroism (CD) analysis showed that the CD spectra of SAP-4 and SAP-C were almost indistinguishable and accounted for an $\alpha + \beta$ -type architecture, as found in ricin A chain (G. Fossati, unpublished work).

Ricin A-chain and crystallized type 1 RIPs share the same overall tri-dimensional folding pattern, despite sharing only about 30% sequence similarity [43]. However, all residues in the catalytic active-site cleft of ricin A chain are conserved among type 1 and type 2 RIPs (Figure 6). Therefore mutation of these same key catalytic residues in other RIPs always results in a drastic loss of activity, as recently demonstrated for the type 2 RIP abrin [44].

To identify regions involved in substrate recognition and binding, we aligned several RIP sequences with their corresponding X-ray-structure-derived secondary structures. A pre-

diction of the secondary structure of seed-type saporin was obtained by multiple alignment using the neural network system PHD. Structurally conserved regions among the RIPs correspond to regions of high local amino acid similarity. However, major structural differences between PAP and ricin A-chain do not seem to account for their differing ribosome specificity [45]. Molecular electrostatic potential distribution, calculated for residues close to the adenylate-binding site, mapped onto the solvent surface, indicating that there is considerable variation between ricin, PAP and dianthin 30. This could account for the differences in ribosome specificity exhibited by these RIPs [46]. Thus exposed residues at putative RNA-binding domains might be likely candidates responsible for the heterogeneity observed between RIP activities.

Proteins binding RNA contain one or more copies of a putative RNA-binding domain consisting of two ribonucleoprotein (RNP) consensus motifs: a hydrophobic hexapeptide stretch, RNP-2, and an octapeptide motif, RNP-1 [47]. A RNP-like structural motif was identified in ricin A chain [42] that shows similarity to the recently solved 3D structure of the RNP motif of U1A spliceosomal protein [48]. This motif overlaps with a RNP domain tentatively identified in the RIPs we examined, including a putative hydrophobic RNP-2 found in the core β -sheet that contains the active-site residue Tyr⁹⁰ involved in sandwiching together with Tyr¹²³ the formycin monophosphate analogue at the adenylate-binding site. Within this RNP-2 like motif, the first three positions are conserved among saporin and other RNA-binding proteins [49]. Conserved residues in the RNP-1- and RNP-2-like motifs might be critical for the RIP's association with rRNA, whereas exposed residues in the most variable regions, especially in unstructured loops, may account for differences in specificity. From our putative model of saporin structure, we predict that Lys¹³¹ of the saporin sequence (which is substituted by Gln¹³¹ in SAP-C and dianthin-30) is located at a conserved surface loop found in the putative RNA-binding domain (Figure 6). Therefore we postulate that the difference in SAP-C activity might be due to impaired RIP-ribosome interaction.

To test this hypothesis, SAP-C was assayed in cytotoxic experiments. If steps from receptor binding and internalization to retrograde transport along the endomembrane system, to toxin translocation to the cytoplasm, were as efficient for SAP-C as for native saporin and only ribosome recognition was impaired, we would expect to observe a similar difference in potency between SAP-C and the seed-type isoforms, as found in the cell-free inhibition assays. Indeed, SAP-C was about ten-fold less cytotoxic irrespective of the cell line tested. Since SAP-C was able to bind efficiently to the putative receptor mediating saporin internalization, our data clearly support this hypothesis. Conversely, the polymorphism of saporin seed-type isoforms, involving residues at positions 48 and 91 that are also located in loop regions, presumably did not affect substrate recognition and activity, at least in reticulocyte lysates. The three other SAP-C substitutions compared with SAP-4 are found in α -helix structures. Although we cannot exclude the possibility that they contributed to the observed lower ribosome-inhibiting activity, these residues are presumably not accessible to the solvent surface.

Finally, to further investigate the role of proteoglycans in saporin internalization, we tested mutant CHO cell lines in cell-killing experiments. The same extent of loss of potency was obtained again when comparing the cytotoxicity of SAP-C with that of SAP-3 and SAP-S. However, since no significant differences in cytotoxicity were observed among seed-type saporin isoforms against the mutant CHO cells, heparan sulphate proteo-

glycans do not seem to facilitate the concentration of saporins at the cell surface, as was shown for other α 2MR ligands [50,51].

This work is dedicated to the memory of Gianpaolo Nitti. We are grateful to Gaetano Orsini, Lucia Monaco, Vinod Singh and Douglas A. Lappi for helpful discussions and to Aldo Ceriotti and Luca Benatti for critical reading of the manuscript. We also thank Jan Malyszko for oligonucleotide synthesis and Gianluca Fossati for the circular dichroism spectroscopy data. This research was supported by Consiglio Nazionale delle Ricerche PF ACRO, Rome, the Associazione Italiana per la Ricerca sul Cancro, Milan, the Italian National AIDS Research Project, and Regione Lombardia.

REFERENCES

- Shine FJ, Barbieri L, Battelli M, G, Soria M, R and Lappi D A (1990) *Bio Technology* **10**, 405-412.
- Lappi D A, Ying W, Barthelmy J, Martineau D, Prieto J, Benatti L, Soria M and Bard A (1994) *J Biol Chem* **269**, 12552-12558.
- Falini B, Bolognesi A, Fienghi U, Tazzari P L, Broe M K, Stein H, Dierker H, Aversa F, Corneli P, Piccolo G, Barbatoletta G, Sabbatini E, Pileri S, Martelli M F and Stripe F (1992) *Lancet* **339**, 1195-1196.
- Cassese W, Lappi D A, Olwin B B, Wei C, Seghian M, Speir E H, Sasse J and Bard A (1992) *Proc Natl Acad Sci USA* **89**, 7159-7163.
- Cavaliere U, del Vecchio A, Lappi D A and Soria M R (1993) *J Biol Chem* **268**, 23185-23190.
- McGrath M S, Hwang K M, Caldwell S E, Gaston J, Luk K, Wu P, Ng V L, Crowe S, Daniels J, Marsh J, Denhart T, Lekas P V, Venkari C, Yeung H W and Lifson J D (1989) *Proc Natl Acad Sci USA* **86**, 2844-2848.
- Lodge J K, Kanewski W K and Turner N E (1993) *Proc Natl Acad Sci USA* **90**, 7089-7093.
- Taylor S, Massari A, Lemonssoff G, Roberts L M, Lord J M and Hartley M (1994) *Plant J* **5**, 827-835.
- Maras B, Cecchi R, De Luca E, Lendario E, Bellotti A, Barra D, Bossa F and Brunori M (1993) *Biochem Int* **21**, 631-638.
- Barra D, Maras B, Schinza E, Angelesio S and Bossa F (1991) *Biotechnol Appl Biochem* **13**, 48-53.
- Barthelmy J, Martineau D, Ong M, Matsumura R, Ling N, Benatti L, Cavaliere U, Soria M and Lappi D A (1993) *J Biol Chem* **268**, 6341-6348.
- Benatti L, Sabbatini M B, Dani M, Nitti G P, Sabbatini M, Lorenzetti R, Lappi D A and Soria M (1989) *Eur J Biochem* **183**, 465-470.
- Benatti L, Nitti G, Soria M, Vasasira B, Vitale A, Ceriotti A and Soria M R (1991) *FEBS Lett* **291**, 285-288.
- Hartley M R, Legname G, Osipov R, Chen Z and Lord J M (1991) *FEBS Lett* **290**, 65-68.
- Legname G, Gromo G, Lord J M, Montini N and Modena D (1993) *Biochem Biophys Res Commun* **192**, 1220-1237.
- Hataoka N, Murakami Y, Noma M, Kudo T and Horikoshi K (1989) *J Biol Chem* **264**, 6629-6637.
- Oraddock J C, Lord J M, Hartley M R and Roberts L M (1994) *Nucleic Acids Res* **22**, 1536-1540.
- Legname G, Fossati G, Montini N, Gromo G, Marcucci F, Mascagni R and Modena D (1995) *Biomol Pept Proteins Nucleic Acids* **1**, 61-68.
- Edge J C, McDonald C C and Graham J B (1983) *Proc Natl Acad Sci USA* **80**, 3734-3737.
- Cavaliere U, del Vecchio A, Tazzari P L, Massazza G and Soria M R (1993) *Drug Delivery* **1**, 119-124.
- Eske J D, Stewart T E and Taylor W H (1985) *Proc Natl Acad Sci USA* **82**, 3197-3201.
- Eske J D, Rostand K S and Wenke J L (1988) *Science* **241**, 1090-1095.
- Feng D F and Doolittle R F (1987) *J Mol Evol* **25**, 351-360.
- Bernstein L, Koetle T F, Williams G, Meyer E F, Brice M D, Rodgers J R and Kennard O (1977) *J Mol Biol* **112**, 535-542.
- Sutcliffe M J, Harrel J, Carrey D and Blundell T (1987) *Protein Eng* **1**, 377-384.
- Rost B and Sanders C (1994) *Proteins* **123**, 123-125.
- Ready M P, Katzin B J and Roberts J D (1988) *Proteins* **3**, 53-59.
- Lappi D A, Esch F, Barbieri L, Stripe F and Soria M (1986) *Biochem Biophys Res Commun* **129**, 934-942.
- Carcanga R, Sinclair L, Fordham-Skelton A P, Harris N and Gray R R D (1994) *Planta* **194**, 461-470.
- Lord J M, Roberts L M and Roberts J D (1994) *FASEB J* **8**, 201-208.
- Cavaliere U, Nykjaer A, Nilsen M and Soria M R (1995) *Eur J Biochem* **232**, 165-171.
- Moestrup S K (1994) *Biochim Biophys Acta* **1197**, 197-213.
- Reisbig R R and Bruland C (1983) *Arch Biochem Biophys* **224**, 700-705.

- 34 Ferreras, J. M., Barbieri, L., Girbes, T., Battelli, M. G., Rojo, M. A., Arias, F. J., Rocher, M. A., Schiano, F., Mendez, E. and Stirpe, F. (1993) *Biochim. Biophys. Acta* **1216**, 31–42.
- 35 Houston, L. L., Ramakrishnan, S. and Hermodson, M. A. (1983) *J. Biol. Chem.* **258**, 9601–9604.
- 36 Taylor, B. E. and Irvin, J. D. (1990) *FEBS Lett.* **273**, 144–146.
- 37 Prestie, J., Shorfeider, M., Adam, G. and Mundry, K. W. (1992) *Nucleic Acids Res.* **20**, 3179–3182.
- 38 Facchini, M. S., Valsasina, B., Nitti, G., Benatti, L. and Vitale, A. (1991) *FEBS Lett.* **286**, 91–94.
- 39 Machamer, C. E. and Rose, J. K. (1968) *J. Biol. Chem.* **263**, 5948–5954.
- 40 Fordham-Sketch, A. P., Taylor, P., Hartley, M. R. and Grey, R. (1991) *Mol. Gen. Genet.* **229**, 460–466.
- 41 Monfort, W., Vilafraanca, J. E., Monzingo, A. F., Ernst, S. R., Katzin, B., Rutenber, E., Xiong, N. H., Hamlin, R. and Robertus, J. D. (1967) *J. Biol. Chem.* **262**, 5398–5403.
- 42 Munshkin, A. and Wool, I. G. (1995) *J. Biol. Chem.* **270**, 33581–33587.
- 43 Monzingo, A. F., Collins, E. J., Ernst, S. R., Irvin, J. D. and Robertus, J. D. (1993) *J. Mol. Biol.* **233**, 705–715.
- 44 Hung, C. H., Lee, M. C., Chen, J. K. and Lin, J. Y. (1994) *Eur. J. Biochem.* **219**, 83–87.
- 45 Chaddock, J. A., Monzingo, A. F., Robertus, J. D., Lord, J. M. and Roberts, L. M. (1996) *Eur. J. Biochem.* **235**, 159–166.
- 46 Bravi, G., Laghame, G. and Chan, A. W. (1995) *J. Mol. Graphics* **13**, 83–88.
- 47 Bandaru, R. J., Swanson, M. S. and Dreyfuss, G. (1989) *Genes Dev.* **3**, 431–437.
- 48 Oubridge, C., Ito, N., Evans, P. R., Teo, C. H. and Nagai, K. (1994) *Nature (London)* **372**, 432–433.
- 49 Query, C. Q., Bentley, R. C. and Keene, J. D. (1989) *Cell* **57**, 69–101.
- 50 Mkhailenko, I., Kounnas, M. Z. and Strickland, D. K. (1995) *J. Biol. Chem.* **270**, 9543–9549.
- 51 Nykjaer, A., Nelsen, M., Locken, A., Meyer, N., Rogaard, H., Eberdt, M., Basiege, U., Olschona, G. and Glemann, J. (1994) *J. Biol. Chem.* **269**, 31747–31755.

Received 16 February 1996; 22 October 1996; accepted 12 November 1996

Momordin II, a ribosome inactivating protein from *Momordica balsamina*, is homologous to other plant proteins

Marcelo Ortigao and Marc Better

XOMA Corporation, 1545 17th Street, Santa Monica, CA 90404, USA

Submitted June 29, 1992

EMBL accession no. Z12175

Many plants produce ribosome inactivating proteins (RIP) which are potent inhibitors of eukaryotic protein synthesis. RIPs hydrolytically cleave the N-glycosidic bond of a specific adenine in a highly conserved region of the 28s rRNA. Plants of the genus *Momordica* produce a number of related Type I ribosome inactivating proteins known as momordins or momorcharins. The gene encoding one member of this family, momordin I, has previously been cloned (1), and the N-terminal protein sequence of three *Momordica* RIPs have been described (2–3).

Momordins are homologous to other plant RIPs, including the trichosanthins, a multigene family of RIPs produced by the related plant *Trichosanthis kirilowii* (4–5). Trichosanthin is an abortifacient agent and is also capable of inhibiting the growth of viruses such as HIV (6).

We have cloned momordin II from a cDNA library constructed from the mRNA of *M. balsamina* seeds (EMBL Accession number Z12175). The predicted amino acid sequence reveals a putative 23 amino acid leader sequence followed by a 263 amino acid protein. The first 27 amino acids of the putative mature protein match the determined amino acid sequence of momordin

II. The amino acid sequence of momordin II, after likely leader processing, is homologous with trichosanthin (57%) and momordin I (51%). The C-terminal 19 amino acids of some RIPs such as trichosanthin is processed, and by analogy processing may occur for both momordin I and II.

REFERENCES

1. Ho, W.K.K., Liu, S.C., Shaw, P.C., Yeung, H.W., Ng, T.B. and Chan, W.Y. (1991) *Biochem. Biophys. Acta* **1088**, 311–314.
2. Li, S.S.-L. (1986) *Experientia* **36**, 524–527.
3. Bolognesi, A., Barbieri, L., Carnicelli, D., Abbondanza, A., Cenini, P., Falasca, A.I., Dinota, A. and Stirpe, F. (1989) *Biochem. Biophys. Acta* **993**, 287–292.
4. Chow, T.P., Feldman, R.A., Lovett, M. and Piatak, M.J. (1990) *Biol. Chem.* **265**, 8670–8674.
5. Shaw, P.-C., Yung, M.-H., Zhu, R.H., Ho, W.K.-K., Ng, T.-B. and Yeung, H.-W. (1991) *Gene* **97**, 267–272.
6. McGrath, M.S., Hwang, K.M., Caldwell, S.E., Gaston, I., Luk, K.-C., Wu, P., Ng, V.L., Crowe, S., Daniels, J., Marsh, J., Deinhardt, T., Lekas, P.V., Vennari, J.C., Yeung, H.-W. and Lifson, J.D. (1989) *Proc. Natl. Acad. Sci. USA* **86**, 2844–2848.

	-23	+1
Momordin II	MVKCLLSFLIIAIFIGVPTAKG	DVNFDLSTATAKTYTKFIEDFRATLPFSHKVYDIPLLYSTIS
Momordin I	MSRFSVLSFLILAIFLGGSIVKG	DVSFRLSGADPRSYGMFIKDLRNALPFREKVYNIPLLPSVS
Trichosanthin	MIRFLVLSLLILTLFTTPAVEG	DVSFRLSGATSSSYGVFISNLRKALPNERKLYDIPLLRSSLP
	*	*
	50	100
Momordin II	DSRRFILLDLTSYAYETISVAIDVTNVYVYAYRTRDVSFFKESPE-AYNIFKGT-RKITLEPYT	
Momordin I	GAGRYLLMHLFNYDGKTTITVAVDVTNVYIMGYLADTTSYFFNEPAELASQYVFRDARRKITLPYS	
Trichosanthin	GSQRYALIHLTNYADETISVAIDVTNVYIMGYRAGDTSYFFNEASATEAAKYVFKDAMRKVTLPYS	
	.. *	*
	150	
Momordin II	GNYENLQTAHAKIRENIDLGLPALSSAITTLFYNAQSAPSALLVLIQTAEAAKFYIERHVAKY	
Momordin I	GNYERLQIAAGKPREKIPIGLPALDSAITLLHYDSTAAGALLVLIQTAEAAKFYIEQQIQR	
Trichosanthin	GNYERLQTAAGKIRENIPGLPALDSAITTLFYNNASAAALMVLIQSTSEAAKYFIEQQIGKR	
	****.***	*
	200	
Momordin II	VATNFKPNLAIISLENQWSALSQKIFLAQNQGGKFRNPVDLIKPTGERFQVTNVDSDDVVKGNIKLL	
Momordin I	AYRDEVP SLATISLENSWSGLSKQIQLAQNGGIFRTPIVLVNKGNRVQITNVTSKVVT SNIQLL	
Trichosanthin	VDKTFLPSLAIISLENSWSALSQKIQIASTNNGQFESPVLINAQNRVITNVDAAGVVT SNIALL	
	*
	250	
Momordin II	LNSR--ASTADENFITTMTLLGESVVN	
Momordin I	LNTRNIAEGDNGDVSTTHGFS--SY--	
Trichosanthin	LNRNMAAMD-DVPMTQSFSGCSYAI	
	** *	
	↑	

Figure 1. Comparison of the predicted momordin II amino acid sequence to those of momordin I (1) and trichosanthin (5). Residues that are well conserved are indicated with · while perfectly conserved residues are indicated with *. The arrow indicates the position of the last residue of mature trichosanthin after C-terminal processing.

Nucleotide sequence of cDNA coding for saporin-6, a type-1 ribosome-inactivating protein from *Saponaria officinalis*

Luca BENATTI¹, Maria Beatrice SACCARDO¹, Maria DANI¹, Gianpaolo NITTI¹, Marica SASSANO¹, Rolando LORENZETTI¹, Douglas A. LAPPI¹ and Marco SORIA^{1,2}

¹ Biotechnological Research, Farmitalia Carlo Erba, Milano

² School of Pharmacy, University of Milano

(Received March 13, 1989) – EJB 89 0294

We have isolated and sequenced partial cDNA clones that encode SO-6, a ribosome-inactivating protein from *Saponaria officinalis*. A cDNA library was constructed from the leaves of this plant and screened with synthetic oligonucleotide probes representing various portions of the protein. The deduced amino acid sequence shows the signal peptide and a coding region virtually accounting for the entire amino acid sequence of SO-6. The sequence reveals regions of similarity to other ribosome-inactivating proteins, especially in a region of the molecule where critical amino acid residues might participate in the active site.

The ribosome-inactivating proteins (RIPs) from various plant extracts inhibit protein synthesis of animal cells by rendering the 60S subunits of eukaryotic ribosomes unable to bind elongation factor II. A single adenine residue is removed from ribosomal RNA in a region that is highly conserved between species [1]. RIPs can be classified as type 1 and type 2 [2]. Type-2 RIPs (e.g. ricin, abrin, modeccin and viscumin) consist of an active A chain linked to a cell-binding B chain. The B chain binds to the sugar moieties of the cell surface, causing the A chain to enter the cell and enzymatically attack the ribosomes. Among type-2 RIPs, ricin, from *Ricinus communis*, is the most extensively studied. Its cDNA [3] and genomic DNA [4] have both been isolated and sequenced. Ricin is translated as a preproricin precursor containing a signal peptide and the A and B chains, separated by a linker peptide 12 amino acids long. The gene does not contain introns. The ricin A-chain gene was successfully expressed in *Escherichia coli* [5, 6].

Type-1 RIPs were identified in extracts from *Phytolacca americana*, *Phytolacca dodecandra*, *Dianthus caryophyllus*, *Geranium multiflorum*, *Momordica charantia*, *Saponaria officinalis*, and other plants [7]. These are single-chain RIPs lacking the ability to bind cells; thus, they are much less toxic, probably because they cannot penetrate into all cells.

Their molecular mass ranges over 28–31 kDa. Some RIPs are glycoproteins, some contain little or no carbohydrates. Structural differences can be present in RIPs isolated from different tissues of the same plant, like in pokeweed antiviral protein (PAP) from leaves or from seeds (PAP-S) of *Phytolacca americana* or in RIPs isolated at different stages of the life cycle (PAP-II, summer leaves) [8]. Both type-1 and type-

2 RIPs have been used extensively for the preparation of cell-specific immunotoxins [9–11].

Several type-1 RIPs were isolated from *Saponaria officinalis* [12]. Proteins with ribosome-inactivating activity were purified from seeds and leaves of the plant, and were shown to be structurally related. Among these, saporin-6 (SO-6) was the most active and abundant, representing 7% of total seed proteins. Other RIPs from seeds (SO-5) and leaves (SO-4, also named saporin-I or SO-I) of *Saponaria* also cross-reacted with an antiserum raised against SO-6 [13, 14]. SO-6 had 40% amino acid sequence similarity with the RIPs from *Phytolacca americana* (PAP) at its NH₂-terminal sequence, though immunologically distinct from them and several other RIPs [13]. SO-4, SO-5 and SO-6 were partially sequenced, showing some differences at their NH₂-terminal extremities [13, 15].

To date, no studies have yet been reported on the genomic organization and sequence of type-1 RIPs and their transcripts. As a first step towards this goal, we have isolated and characterized bacterial clones containing portions of a cDNA coding for the SO-6 RIP of *Saponaria officinalis*.

MATERIALS AND METHODS

Amino acid sequence of clostripain fragments of SO-6

SO-6 was purified as previously described [13]. For clostripain digestions, 200 mg SO-6 were dissolved in 50 mM ammonium bicarbonate pH 7.0, 4 M urea, 10 mM dithiothreitol, 10 mM CaCl₂. The enzyme was first activated for 1 h at room temperature in the same buffer without urea; then the digestion was carried out at room temperature overnight, with an enzyme/substrate ratio of approximately 1:50. The reaction was stopped by addition of 0.1% F₃CCOOH immediately before injection.

Sequence analysis was performed by Edman degradation as previously described [15] in a gas-phase sequencer (Applied Biosystems, Foster City, CA, USA). A full description of the purification and sequencing of SO-6 will be described elsewhere (G. P. Nitti et al., unpublished results).

Correspondence to M. Soria, Farmitalia Carlo Erba, Viale E. Bezzi 24, Milano, Italy

Abbreviations. RIP, ribosome-inactivating protein; SSC, standard saline citrate; PAP, pokeweed antiviral protein; SO-6, saporin-6.

Note. The nucleotide sequence data reported here will appear in the EMBL, GenBank and DDBJ Nucleotide Sequence Databases under the accession number X15655 (saporin 6)

RNA isolation and cDNA library construction

Total RNA from summer leaves of *Saponaria officinalis* was extracted by the guanidine/isothiocyanate method [16]. Poly(A)-rich RNA was isolated on a column of oligo(dT)-cellulose [17]. cDNA was synthesized essentially as described in [18] from 3 µg poly (A)-rich RNA using avian myeloblastosis virus reverse transcriptase (Amersham, UK), followed by second strand synthesis with DNA polymerase I (New England BioLabs, USA), yielding molecules ranging from 400 bases to several kb (data not shown). After treatment with T4 DNA polymerase (New England BioLabs, USA), addition of *Eco*RI linkers and *Eco*RI digestion, the cDNA was ligated to phage λ gt10 arms and packaged *in vitro*. The library was amplified using *E. coli* NM514 as host. The number of independent clones thus obtained was 3.3×10^{10} with a background of non-recombinant phages of 36%.

Preparation of oligonucleotide probes

To probe the *Saponaria* leaf cDNA library, we initially designed a 111-bp-long oligonucleotide, corresponding to the first 37 amino acids of the NH₂-terminus of SO-6 [13]. Eight different oligonucleotides, 19–28 bases long, were synthesized using an automatic DNA synthesizer (model 380B, Applied Biosystems Inc., Foster City, CA, USA), and assembled by ligation. The resulting double-stranded oligonucleotide was inserted into the *Sma*I site of M13mp8 and the correct sequence was verified by the Sanger method [19]. Codons for this oligonucleotide were chosen from the frequency of codons in the seed storage proteins present in sequence databases (GenBank, USA).

A mixture of 16 21-base oligonucleotides, corresponding to clostripain fragment 5 (see Fig. 1), was also synthesized. The mixture of short oligonucleotides was end-labeled using [γ -³²P]ATP and T4 polynucleotide kinase as described in [20]. The 111-bp oligonucleotide, inserted into the single-stranded DNA phage M13mp8, was labeled by annealing to a primer complementary to the adjacent M13 sequence followed by treatment with Klenow polymerase [18]. After *Eco*RI and *Bam*HI digestion to remove the oligonucleotide from the phage vector, the DNA was electrophoresed on a 3.5% polyacrylamide gel. After a very short autoradiographic exposure, the portion of the gel containing the probe was cut out and the oligonucleotide eluted overnight in water at 37 °C. The specific activity was about 5×10^8 cpm/µg DNA.

Screening of the *Saponaria* leaves cDNA library

About 200 000 recombinant phages were plated on a lawn of *E. coli* NM514 cells. The phages were then transferred to duplicate nitrocellulose filters, their DNA was denatured, neutralized and filters were baked under vacuum at 80 °C for 2 h and were prehybridized in $6 \times$ SSC, $5 \times$ Denhardt's, 0.1% SDS, 100 µg/ml salmon sperm DNA at 50 °C for 2 h and were then hybridized overnight at 50 °C in the same mixture, adding 1×10^6 cpm/ml of the 111-bp oligonucleotide. The filters were washed in $0.1 \times$ SSC, 0.1% SDS at 60 °C and autoradiographed. Positive phage plaques were isolated and screened again twice in order to isolate single clones.

The clones that hybridized to the 111-bp probe were plated and screened with the labeled short oligonucleotide mixture. The filters were prehybridized in the same reaction mixture used for the 111-bp oligonucleotide, but at 42 °C for 2 h. The filters were then hybridized overnight at 42 °C after addition

Table 1. Sequence of clostripain fragments

Fragment number	Sequence
1	Tyr Ile Gln Asn Leu Val Thr Lys
2	Asn Asn Val Lys Asp Pro Asn Leu Lys -Tyr Gly Gly Thr Asp Ile Ala Val Ile Gly -Pro Pro Ser Lys Glu Lys Phe Leu Arg
3	Ala Tyr Tyr Phe Arg
4	Asp Asn Leu Tyr Val Val Ala Tyr Leu -Ala Met Asp Asn Thr Asn Val Asn Arg
5	Gln Val Lys Asp Leu Gln Met Gly Leu -Leu Met Tyr Leu Gly Lys Pro Lys
6	Ile Asn Phe Gln Ser Ser Arg
7	Lys Ile Ser Thr Ala Ile Tyr Gly Asp Ala -Lys Asn Gly Val Phe Asn Lys Asp Tyr -Asp Phe Gly Phe Gly Lys Val Arg
8	Gly Thr Val Ser Leu Gly Leu Lys Arg

of 2×10^6 cpm/ml of the short oligonucleotide mixture. The filters were washed in $6 \times$ SSC, 0.1% SDS at 45 °C and autoradiographed. Only these clones giving positive results with both probes were selected for further characterization.

Recombinant phage preparations and DNA sequencing methods

The DNA of the positive clones was isolated by the LambdaSorb phage adsorbent method (Promega Biotec, USA), the insert was removed with *Eco*RI (Boehringer, FRG) and ligated to the *Eco*RI site of M13mp8 [21] in both directions of insertion. Sequencing was carried out on both strands by the Sanger procedure [19] with M13 sequencing primers (Amersham, UK), and subsequently with a series of synthetic oligonucleotide primers complementary to adjacent portions of sequenced cDNA (see Fig. 2).

Genomic blotting

Total chromosomal DNA was extracted [24] from seeds and leaves of *Saponaria officinalis*, digested with restriction endonucleases, separated by electrophoresis on a 0.8% agarose gel and transferred to nitrocellulose. Probes were labelled by the Multiprime system (Amersham, UK) according to the manufacturer's instructions. Filters were hybridized overnight in $5 \times$ SSC at 65 °C and washed in $0.1 \times$ SSC, 0.1% SDS at 65 °C. The molecular mass of fragments was determined using *Hind*III digests of phage λ DNA as markers.

RESULTS

Identification of cDNA clones

Eight clostripain fragments of SO-6 were sequenced by Edman degradation (Table 1), confirming and extending the

OLIGONUCLEOTIDE PROBES

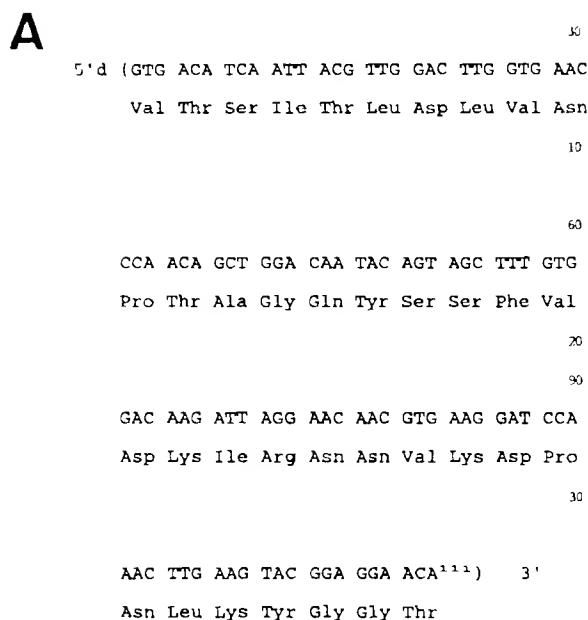
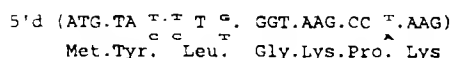
**B**

Fig. 1. Regions of SO-6 selected for the synthesis of oligonucleotide probes. The probes were designed to be complementary to the mRNA coding for amino acids 1–37 (A) and to seven amino acids from clostripain peptide 5 (B)

previously determined sequences [13, 15]. From this information, oligonucleotide probes were constructed (Fig. 1) to screen a cDNA library from the leaves of *Saponaria officinalis*. The library was constructed using λ gt10 and poly(A)-rich RNA from summer leaves (see Materials and Methods), yielding 1.2×10^6 independent clones after background subtraction. Inserts ranged in size between 600 bases and several kb (data not shown).

Initial efforts at screening the library with short mixtures of oligonucleotides derived from sequences at the NH₂-terminus were unsuccessful. Therefore, a 111-bp oligonucleotide (Fig. 1A) was assembled as described in Materials and Methods. We reasoned that complementary stretches in this probe should be sufficiently long for specific hybridization even in the presence of mismatches. Other genes were successfully isolated using this approach [22].

200000 plaques from insert-containing clones were screened with the labelled 111-bp oligonucleotide, yielding positive plaques that were isolated and successively rehybridized to the oligonucleotide mixture 21 A (Fig. 1B) to confirm our selection. Two such clones, pBL6 and pB6aj2 were selected for further analysis and were characterized by subcloning into *Eco*RI-digested M13mp8 in both directions of insertion.

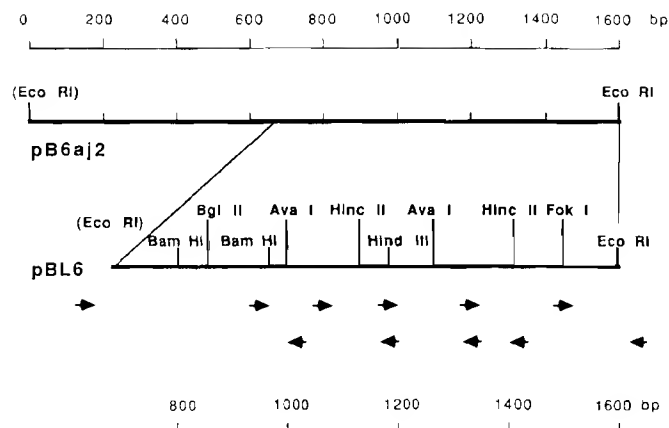


Fig. 2. Partial restriction map of cDNA and strategy of sequencing. Top: the 1600 bp cDNA clone pB6aj2. Bottom: the overlapping clone pBL6. *Eco*RI sites in parentheses result from addition of linkers to cDNA. Small arrows indicate the direction and positions of small oligonucleotide primers employed for sequencing. Grey arrows indicate M13 universal primers

Sequencing of clones

The partial restriction map and sequencing strategy of pBL6 and pB6aj2 shows that these clones overlap completely (Fig. 2). DNA sequencing in both directions resulted in only one base difference between the two clones in the 5'-noncoding region (Fig. 3). Comparing the NH₂-terminal amino acid sequence of *Saponaria* RIPs reported previously [13, 15] to that predicted by the coding portion of the cDNA, the start point of the amino acid sequence could be identified with the translation initiation site corresponding to a methionine codon, ATG, at nucleotide residues –72 to –70. The sequence further predicted an NH₂-terminal extension of 24 amino acids for the putative signal peptide, and a cleavage site in agreement with the –1, –3 rule of Von Heijne [23]. The length of the signal peptide is the same as that of preproricin [3], but no evident similarity in amino acid sequences is present.

Comparison of the NH₂-terminal sequences and of internal sequences from the clostripain fragments of SO-6 (Table 1) to the predicted amino acid sequence from the cDNA clones shows complete identity between these sequences at all but one amino acid residue along the molecule (Fig. 3). Both pBL6 and pB6aj2 ended with a natural *Eco*RI site at their 3' end, that is, a site not resulting from the addition of linkers to the cDNA. Thus, we could not identify a translation termination codon at the 3' end of these clones. At the protein level, positive identification of the COOH-terminal fragment of SO-6 was hindered by the resistance of this protein to treatment with some proteases, including carboxypeptidase (G. P. Nitti, unpublished observations) [12]. However, treatment of SO-6 with CNBr or pepsin yielded fragments with overlapping COOH-terminal sequences to that of clostripain fragment 5 (G. P. Nitti et al., unpublished results).

Genomic blot analysis

A *Hinc*II fragment encompassing the coding region of clone pBL6 (Fig. 2) was used as the radioactive probe for a Southern transfer of *Saponaria* genomic DNA. Digestion of seed DNA with *Bst*NI, a methylation-insensitive restriction enzyme, showed three hybridization bands of approximately



Fig. 3. Nucleotide sequence and deduced amino acid sequence of cDNA clones. Residues are numbered with the first residue of the codon specifying the amino-terminal residue of the SO-6-like protein numbered 1, and the nucleotides on the 5' side of residue 1 indicated by negative numbers. The predicted amino acid sequence is given below the nucleotide sequence. Amino acids are numbered from the amino-terminal residue of the protein and the preceding residues are indicated by negative numbers. The positions of amino acids confirmed by peptide sequencing are underlined. Differences with the sequences of the clostripain fragments (Table 1) are indicated beneath. The unique nucleotide differing in pB6aj2 is indicated above the sequence

1.4 kb, 2.9 kb and 3.6 kb, respectively (Fig. 4). Digestion of leaf DNA with the same enzyme, and of seed and leaf DNA with other restriction enzymes like *Eco*R1, *Bam*HI, *Bgl*II, *Pvu*II and *Sal*I, yielded partial restriction fragments, presumably due to protection of the corresponding sites on the DNA by methylation [24]. A prominent band of about 3.8 kb was present after digestion of leaf DNA with *Bgl*II, and a much weaker band of similar size was also present in *Bgl*II-digested

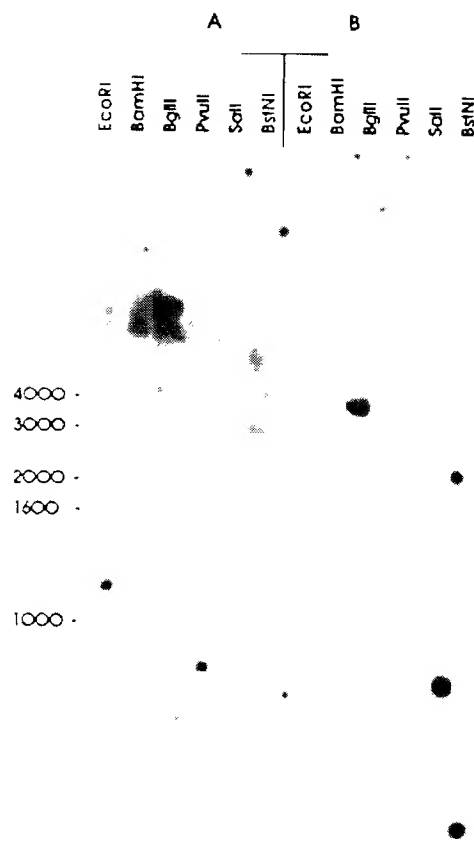


Fig. 4. DNA Southern blot analysis of the *Saponaria officinalis* genome. 10- μ g samples of seed and of leaf genomic DNA were digested with the indicated enzymes, electrophoretically separated on an agarose gel and transferred to nitrocellulose. Hybridization was carried out to a *Hinc*II fragment from the 3' end of clone pBL6 (Fig. 2) as described in Materials and Methods. A, seed DNA; B, leaf DNA

seed DNA. These bands are probably due to strong cross-hybridization with other *S. officinalis* genes of chloroplast origin in the leaf tissue, and of plastid origin in the seeds, such as those coding for ribosomal RNA (L. Benatti, unpublished) or RNA polymerase [25]. This interpretation is supported by recent findings on the discontinuous genetic system of ribosomal RNA in the mitochondrial DNA of *Chlamidomonas reinhardtii*, where large transcripts of scrambled rRNA have been found interspersed with protein coding sequences [26].

DISCUSSION

In this paper we report the first isolation and DNA sequence of cDNA clones encoding a type-1 RIP, the SO-6 RIP of *Saponaria officinalis*. In previous studies, we have shown that RIPs from the seeds and leaves of *Saponaria officinalis* possess varying levels of amino acid sequence similarity among themselves and with members of other plant families like the *Phytolaccaceae* [13, 15]. Besides similar functions, all these RIPs are present in different forms in the seeds or leaves of the plant, and are subject to seasonal variations in the same plant [8]. We have now extended our previous observations on the amino acid sequence of SO-6 to other parts of the protein after enzymatic fragmentation. Based on this information, we designed and synthesized a mixture of

oligonucleotides and used these as a probe to screen a cDNA library from summer leaves of *Saponaria officinalis*, in an attempt to isolate cDNA clones coding for RIPs present in leaf tissue. In this manner, the library was screened with two different probes corresponding to different regions of SO-6. This was necessary due to the abundance of cross-hybridizing, false-positive clones in the library, presumably of chloroplast origin [25].

The cDNA clones, pBL6 and pB6aj2, encode a protein showing high similarity to the RIPs of *Saponaria officinalis*. The NH₂-terminal sequence and the sequence of eight clostripain peptides of pure SO-6 covering a total of more than 100 amino acid residues were the same as the deduced cDNA sequence, providing unambiguous evidence that the cloned cDNAs derived from mRNA coding for SO-6 or an almost identical *Saponaria* RIP (Fig. 3). The few differences with the experimentally determined amino acid sequences of SO-6 (Table 1) [15] might be due to heterogeneity between seed varieties, or to different forms of such *Saponaria* RIPs present in the plant as in the case of PAP [8] and of ricin [3]. Whether such heterogeneity is a reflection of variability in the genetic system of *Saponaria* RIPs remains to be established. However, only three genomic DNA restriction fragments hybridized to a *Hinc*II fragment from one of the clones, suggesting that SO-6, like ricin, is a member of a small multi-gene family [4].

Since both pBL6 and pB6aj2 are partial cDNA clones, the missing portion of the cDNA for SO-6 might still code for a small COOH-terminal extension of the mature protein, followed by the stop codon(s) and polyadenylation signal. Alternatively, clostripain fragment 5 (Table 1) might be the COOH-terminal peptide of mature SO-6. If this were the case, SO-6 might derive by a processing mechanism from a longer protein precursor whose cDNA would extend beyond the 3' end of pBL6 and pB6aj2. Then, all the coding portion for the COOH-terminus of mature SO-6 would be contained in pBL6 and pB6aj2. Preliminary evidence suggesting this possibility derives from fragmentation studies of SO-6 with CNBr or pepsin, all yielding fragments terminating with an identical sequence to that of clostripain fragment 5 (G. P. Nitti et al., unpublished results). Similar post-translational processing mechanisms of a COOH-terminal extension were recently described in the precursors of γ -interferon [27] and of tobacco glucanase, a plant defense-related enzyme [28].

Complete amino acid sequences are now known for ricin A and B chains [3], for trichosanthin [29], for barley protein-synthesis inhibitor [30] and for *E. coli* Shiga-like toxin [31]. Considerable amino acid sequence similarity has been observed among these proteins, all sharing a similar mechanism of action [32]. In addition, high-resolution crystallographic studies of ricin allowed visualization of a prominent cleft in the A subunit, that was suggested to contain the active site of the RIP [33, 34]. Examination of similarity between these sequences and the protein sequence derived from the pBL6 clone reveals the presence of similarly conserved residues around the proposed active-site cleft (Fig. 5). This similarity strengthens the notion that there could be a strong retention of three-dimensional structure among these proteins having similar catalytic functions, with critical amino acid residues conserved, especially in the region of the active site [34].

The SO-6 RIP from *S. officinalis* has yielded very promising results as a candidate partner for the synthesis of immunotoxins. It has been suggested that its characteristic high pI [35] contributes to form compact immunoconjugates in the circulation by electrostatic interaction of SO-6 with the nega-

```

a 169I Q S T S E A A R Y K F I . . . L E N S L W L A L S K R 206
b 172I Q M I S E A A R F Q Y I . . . L E N S - W G R L S T A 217
c 172I Q M T A E A A R F R Y I . . . E V N - - W K K I S T A 214
d 169L L M V N E A T R F Q T V . . . Q V N G - W Q D L S A A 218
e 167V T V T A E A L R F R Q I . . . T L N - - W G R L S S V 209

```

Fig. 5. Alignment of homologous amino acids in the polypeptide chains of trichosanthin (a), ricin A chain (b), SO-6 (c), barley protein-synthesis inhibitor (d) and Shiga-like toxin (e). Conserved amino acids in the cleft of the ricin A-chain crystal structure are indicated by asterisks. Numbers refer to the positions of residues in the mature protein. Dashes indicate gaps introduced into the sequences to maximize alignments. Alignments are derived from those of [34] and [32].

tively charged antibody, thus protecting the conjugate's chemical linkage from degradation [36]. This, coupled to the RIP's remarkable resistance to proteases and stability, results in immunotoxins with excellent pharmacokinetic characteristics [37] and powerful activity *in vitro* and *in vivo* [38–40]. Recombinant chimaeras between genes coding for bacterial toxins and ligands are now becoming available to kill selectively receptor-bearing cells [41–44]. Thus, the availability of the gene encoding SO-6 should allow the design of powerful biochemical and genetic conjugates for specific cellular targeting.

REFERENCES

- Endo, Y., Mitsui, K., Motizuki, M. & Tsurugi, K. (1987) *J. Biol. Chem.* **262**, 5908–5912.
- Barbieri, L. & Stirpe, F. (1982) *Cancer Surv.* **1**, 489–520.
- Lamb, F. J., Roberts, L. M. & Lord, J. M. (1985) *Eur. J. Biochem.* **148**, 265–270.
- Halling, K. C., Halling, A. C., Murray, E. E., Ladin, B. F., Houston, L. L. & Weaver, R. F. (1985) *Nucleic Acids Res.* **13**, 8019–8033.
- O'Hare, M., Roberts, L. M., Thorpe, P. E., Watson, G. J., Prior, B. & Lord, J. M. (1987) *FEBS Lett.* **216**, 73–78.
- Kim, J. & Weaver, R. F. (1988) *Gene* **68**, 315–321.
- Stirpe, F. & Barbieri, L. (1986) *FEBS Lett.* **195**, 1–8.
- Houston, L. L., Ramakrishnan, S. & Hermodson, M. A. (1983) *J. Biol. Chem.* **258**, 9601–9604.
- Pastan, I., Willingham, M. C. & FitzGerald, D. J. (1986) *Cell* **47**, 641–648.
- Viretta, E. S., Fulton, R. J., May, R. D., Till, M. & Uhr, J. W. (1987) *Science* **238**, 1098–1104.
- Frankel, A. (1988) *Immunotoxins*, Kluwer Academic Publishers, Boston.
- Stirpe, F., Gasperi-Campani, A., Barbieri, L., Falasca, A., Abbondanza, A. & Stevens, W. A. (1983) *Biochem. J.* **216**, 617–625.
- Lappi, D. A., Esch, F. S., Barbieri, L., Stirpe, F. & Soria, M. (1985) *Biochem. Biophys. Res. Commun.* **129**, 934–942.
- Lappi, D. A., Montecucchi, P. C., Lazzarini, A. M., Martineau, D., Cadeddu, T. & Soria, M. (1986) *J. Cell Biochem.* **66**, G49.
- Montecucchi, P. C., Lazzarini, A. M., Barbieri, L., Stirpe, F., Soria, M. & Lappi, D. A. (1989) *Int. J. Pept. Protein Res.* **33**, 263–267.
- Chirgwin, J. M., Przybyla, A. E., MacDonald, R. J. & Rutter, W. J. (1979) *Biochemistry* **18**, 5294–5299.
- Aviv, H. & Leder, P. (1972) *Proc. Natl Acad. Sci. USA* **69**, 1408–1412.
- Maniatis, T., Fritsch, E. F. & Sambrook, J. (1982) *Molecular cloning: a laboratory manual*, Cold Spring Harbor Laboratory, Cold Spring Harbor, NY.
- Sanger, F., Nicklen, S. & Coulson, A. R. (1977) *Proc. Natl Acad. Sci. USA* **74**, 5463–5467.